Particle emissions and exposure to hazardous chemical agents during binder jetting utilising a silica sand

L. Meiring

orcid.org/0000-0002-8563-3012

Dissertation submitted in fulfilment of the requirements for the degree Master of Health Sciences in Occupational Hygiene at the North-West University

Supervisor: Dr S du Preez
Co-supervisor: Prof JL du Plessis

Examination: November 2023
Student number: 28850467

ABSTRACT

Title: Particle emissions and exposure to hazardous chemical agents during binder jetting utilising a silica sand

Background: There are research gaps in additive manufacturing (AM) concerning particle number concentrations, particle emission rates, area concentrations, and personal respiratory exposure in real-world workplaces. Binder jetting (BJ) machines, have the potential to release particles, including ultrafine particles, into the air. AM operators might be exposed to particle emissions and hazardous chemical agents (HCAs) namely, respirable crystalline silica, and respirable particulates not otherwise specified (PNOS) during the pre-processing phase, processing phase, and post-processing phase when using silica sand. More research is needed regarding particle number concentrations, particle emissions, area concentrations and respiratory exposure of AM operators to respirable crystalline silica and respirable PNOS during BJ utilising a silica sand.

Aims and objectives: The research aim of this dissertation was to determine the powder characteristics and chemical composition of uncoated, coated and used silica sand and to quantify particle number concentrations, particle emission rates, area concentrations, and personal respiratory exposure of the AM operator to respirable crystalline silica and respirable PNOS during the three AM phases at a South African AM research facility. The research objectives were: (i) To determine the powder characteristics and chemical composition of uncoated, coated, and used silica sands during BJ; (ii) To quantify particle number concentrations and to determine emission rates (ERs) of particles released during BJ, and (iii) to assess area concentrations and personal respiratory exposure of the AM operator to respirable crystalline silica and respirable PNOS during BJ.

Methodology: Powder characterisation of uncoated, coated, and used silica sand was determined through particle size distribution (PSD) and shape analysis using a Malvern Morphologi particle analyser and scanning electron microscopy (SEM), while the and wavelength dispersive X-ray fluorescence (WD-XRF) was used to determine chemical composition. Direct-reading instruments including, a Grimm-Portable Laser Aerosol Spectrometer model 11-A and a Nanozen DustCount® 9000 Z1 optical particle counter, were used to quantify particle number concentrations and emission rates of particles released during the three AM phases. Both area

monitoring and personal exposure monitoring were conducted during the AM operator's full shift to determine area concentrations and personal respiratory exposure to respirable crystalline silica and respirable PNOS in the AM research facility. This was conducted by means of time-integrated sampling (GilAir Plus pump with a 2-piece cassette and aluminium cyclone) and real-time monitoring (DustCount® used to obtain real-time data and filter analysis results). This study was conducted over six days: four days were allocated for printing parts, while two days were allocated for the carbon dioxide (CO_2) decay method (as part of the air exchange rate (AER) and ER calculations).

Results: The PSD and SEM results could not be compared to the safety data sheet (SDS) since the particle size distribution and shape of silica sand were not stated in the SDS. PSD results indicated that uncoated, coated and used silica sand fell into the inhalable size fraction (< 100 µm). PSD analysis indicated that 10% of particles [d(0.1)] in uncoated (0.58 ± 0.03 µm), coated0.61 ± 0.08 µm), and used silica sand (0.58 ± 0.04 µm) were respirable sized particles. PSD analysis indicated that 50% [d(0.5)] of uncoated, coated, and used silica sand particles were smaller than 1.29 ± 0.36 µm, 4.27 ± 0.08 µm and 2.42 ± 0.04 µm respectively. Statistically significant differences was found for particles [d(0.5)]. PSD analysis indicated that 90% [d(0.9)] of uncoated, coated, and used silica sand particles were smaller than 42.21 ± 29.96, 104.7 ± 23.33 µm and 54.9 ± 49.93 µm respectively.SEM images and PSD results supported these findings since particles < 100 µm in size were detected. PSD analysis and SEM images confirmed that silica sand particles were smooth and non-spherical in shape. All three silica sand samples contained high crystalline silica content, ranging from 96.83 to 98.20%, which corresponded with the >90% stated in the SDS. The highest peak particle number concentration and particle ER were 680.51 p/cm^3 and 3.06 × 10^5 p/min respectively for particles < 1 µm in size. Real-time monitoring using the DustCount® indicated that particles sized 0.375 µm in size were the most prevalent during the AM process with detectable respirable crystalline silica and respirable PNOS during the AM phases. Personal exposure 8-hour Time Weighted Average (TWA) concentrations were measured at 0.01 ± 0.00 mg/m^3 for respirable crystalline silica and 0.04 ± 0.03 mg/m^3 for respirable PNOS. It was found that respirable crystalline silica measured during printing was equal to 10% of the Time-weighted Average-Occupational Exposure Limit-Maximum limit (TWA-OEL-ML) of 0.1 mg/m^3.

Conclusion: PSD analysis and SEM images of uncoated, coated and used silica sand indicated particles in the inhalable fraction (< 100 µm). Particles < 1 µm in size were emitted during the three AM phases, indicating that BJ using silica sand are a high emitter of submicron particles. A

statistically significant difference was found between the uncoated, coated, and used silica sand particle according to the d(0.5) PSD results. There was a notable difference in the particle number concentrations and particle ERs measured by the direct-reading instruments, with the DustCount® yielding much lower particle number concentrations and particle ERs. When comparing the particle number concentrations measured by the DustCount® in area one (in front of AM machine) and area two (back of AM machine), higher particle number concentrations were measured in area two. Time-integrated sampling and real-time monitoring of respirable crystalline silica and respirable PNOS indicated that all 8-hour TWA personal exposures complied with their respective TWA-OELs. However. It's important to note that the respirable crystalline silica concentrations during personal monitoring was equal 10% of the TWA-OEL-ML.

PREFACE

This dissertation was written in article format and written according to the requirements of the North-West University's Manual for Postgraduate Studies (2020). Chapter 3 is the manuscript that is to be submitted for publication to an accredited journal and conforms to the requirements preferred by the journal *Annals of Work Exposures and Health*. The literature in Chapter 3 is referenced according to the style required by *Annals of Work Exposures and Health*. The dissertation is written according to the United Kingdom English spelling, except for direct quotes, titles of articles or journals, and names of organisations that use United States spelling. For a detailed description, of the guidelines for authors and referencing style, see Chapter 3.

The outline of this dissertation is as follows:

- Chapter 1: Introduction proposing the study and the problem statement, research aim, objectives, and hypotheses.
- Chapter 2: A literature study on topics relevant to this dissertation.
- Chapter 3: A manuscript entitled: *"Particle emissions and exposure to hazardous chemical agents during binder jetting utilising a silica sand",* written in a format that meets specifications of the journal *Annals of Work Exposure and Health*.
- Chapter 4: Concluding chapter providing the main findings, recommendations, study limitations, and future research suggestions.
- Annexure A: Ethics approval letter.
- Annexure B: Declaration of language editing.

AUTHORS' CONTRIBUTION

The study was planned and executed by a team of researchers. The contribution of each researcher is outlined in Table 1 below.

Table 1: Contributions of the different authors

Name	Contributions
Ms L Meiring	• Student researcher. • Study design and planning. • Conducting literature research. • Execution of monitoring, data collection, statistical analyses, interpretation of results, writing of the article, and formulating recommendations. • Writing of the dissertation.
Dr S du Preez	• Supervisor. • Assisted with the study planning and design. • Assisted with scientific and ethics approval of the study. • Assisted with communication with the participating university. • Provided feedback and recommendations. • Review of the dissertation.
Prof JL du Plessis	• Co-supervisor. • Assisted with the study planning and design. • Assisted with scientific and ethics approval of the study. • Provided feedback and recommendations. • Review of the dissertation.

The following is a statement from the co-authors that confirms each individual's role in this study (Meiring, 2024):

By signing below, I declare that I have approved the dissertation and article and that my role in the study as indicated above is representative of my actual contribution and that I hereby give my consent that it may be published as part of L Meiring's MHSc (Occupational Hygiene) dissertation.

Ms L Meiring (Student researcher)

Dr S du Preez (Supervisor)

Prof JL du Plessis (Co-supervisor)

ACKNOWLEDGEMENTS

I would like to thank those who contributed to the completion of this study:

- Special thanks to the Department of Science and Innovation under the Collaborative Program in Additive Manufacturing for funding this study.
- I would like to express my deepest appreciation to Dr Sonette du Preez and Prof Johan du Plessis who provided guidance throughout this project.
- My parents and brother for their unconditional love and support.
- A special thanks to Dr Malan van Tonder, David Mauchline, Conrad Beukes, Lucky Mokone and George Fumba at the Vaal University of Technology who assisted and participated in this study (Meiring, 2024).
- Miss Marelize van Ree, for her helpful advice and assistance with the Malvern Morphologi G3 microscope.
- Mr Corné van der Merwe, for setting up access to the GraphPad prism license.
- Mr Willie Landman and Dr Anine Jordaan for the Scanning Electron Microscopy analysis.
- Mr Willem Wepener and his laboratory team for their assistance and competence in analysing the samples.
- Ms Desdemona Kruger for handling the car booking arrangements and finances of the study.
- Mrs Venita de Kock for language editing of the dissertation.

“You can only run your own race. Stay in your lane. Don’t look at what others are doing. Those that look back in the race usually fall off.”

Oprah Winfrey

CONTENTS TABLE OF CONTENTS

LIST OF ABBREVIATIONS

3D	Three dimensional
ACGIH	American Conference of Governmental Industrial Hygienists, United States of America
AER	Air exchange rate
$\overline{\mathrm{AER}+\mathrm{k}}$	Average particle removal rate
AM	Additive manufacturing
ANOVA	Analysis of variance
ASTM	American Society for Testing and Materials
BC	Before Christ
BCE	Before Common Era
BJ	Binder jetting
C_0	Initial carbon dioxide concentration which was measured at the start of the decay period
C_1	Carbon dioxide concentration measured at the end of the decay period
CAD	Computer Aided Design
CARC	Carcinogen
$C_{(in)}$	Mean particle concentration
$C_{(in0)}$	Initial indoor particle concentration at time zero
$C_{(int)}$	Peak particle concentration
CO_2	Carbon dioxide

COPD	Chronic Obstructive Pulmonary Disease
CR	Carbon dioxide concentration measured in the outdoor air
BDL	Below the detection limit
DED	Directed energy deposition
DL	Detection limit
DoD	Drop-on-demand
ER	Emission Rate
FDM	Fused deposition modelling
FFP	Filtering Face Piece
GHS	Globally Harmonised System
HCA	Hazardous Chemical Agent
I	Inhalable
IARC	International Agency for Research on Cancer
ISO	International Organisation for Standardisation
k	Contaminant loss due to surface deposition
LEV	Local exhaust ventilation
ME	Material extrusion
NIOSH	National Institute for Occupational Safety and Health, United States of America
NWU-HREC	North-West University Health Research Ethics Committee
OEL	Occupational Exposure Limit

OEL-CL	Occupational Exposure Limit - Control Limit (Regulations for Hazardous Chemical Substances)
OEL-ML	Occupational Exposure Limit - Maximum limit (Regulations for Hazardous Chemical Agents)
OEL-RL	Occupational Exposure Limit - Recommended Limit (Regulations for Hazardous Chemical Substances) or Occupational Exposure Limit - Restricted Limit (Regulations for Hazardous Chemical Agents)
OPC	Optical particle counter
OSHA	Occupational Safety and Health Administration, United States of America
PBF	Powder bed fusion
PBF-SLS	Powder bed fusion - selective laser sintering
PM_4	Particulate matter with particle aerodynamic diameter of equal to or less than 4 micrometres
PNOS	Particulates not otherwise specified
PPE	Personal protective equipment
ppm	Parts per million
PSD	Particle Size Distribution
PVC	Polyvinyl chloride
R	Respirable
RHCA	Regulations for Hazardous Chemical Agents
RHCS	Regulations for Hazardous Chemical Substances
RPE	Respiratory protective equipment
SANS	South African National Standard

SANAS	South African National Accreditation System
SD	Standard deviation
SDS	Safety Data Sheet
SEM	Scanning Electron Microscopy
SiO_2	Silicon dioxide
STL	Standard Tessellation Language
TWA	Time-Weighted Average
TWA-OEL	Time-Weighted Average Occupational Exposure Limit
TWA-OEL-CL	Time Weighted Average Occupational Exposure Limit - Control Limit
UFP	Ultrafine Particle
V	Volume
VOCs	Volatile Organic Compounds
W	Width
WD-XRF	Wavelength Dispersive X-ray Fluorescence
XRD	X-ray Diffraction

LIST OF SYMBOLS

~	Approximately equal to
%	Percentage
°C	Degrees Celsius
<	Less than
>	Greater than
≤	Less or equal than
≥	Greater or equal than
±	Plus, minus
Δt	Change in time
h	Height or hour
µg/m^3	Microgram per cubic metre
µm	Micrometre
g/ml	Grams per millilitre
l	Length
ℓ/min	Litres per minute
m	Metre
m^2	Square metre
m^3	Cubic metre
min	Minute
mg	Milligram

mg/m^3	Milligram per cubic metre
ml	Millilitre
ml/min	Millilitre per minute
mm	Millimetre
mm^3	Cubic millimetre
MV12	Dust mask mandatory sign
nm	Nanometre
p	P-value
p/cm^3	Particles per cubic centimetre
p/m^3	Particle per cubic metre
®	Registered Trademark
™	Trademark

CHAPTER 1 INTRODUCTION

1.1 Introduction

Additive manufacturing (AM) processes and materials emerged in the early 1980s (Sun and Shang, 2021:194). During the process of AM, layers of materials are joined together to produce physical objects utilising three-dimensional (3D) model data (ISO/ASTM 52900:2022). Hence AM entails geometric shapes made of lines and points to produce physical objects utilising 3D computer aided design (CAD) (Gibson *et al*., 2015:16). AM enables designers and engineers to fabricate complex geometric parts not attainable using traditional methods of subtractive manufacturing (Caiazzo *et al*., 2017: 4023-4031; Gibson *et al*., 2015:2). AM is being applied in a broad range of industries such as automobile manufacturing, medical devices, and aerospace, to name a few (Sun and Shang, 2021:194).

The two main techniques for producing sand moulds are binder jetting (BJ) and powder bed fusion selective laser sintering (PBF-SLS) (Le Néel *et al*., 2018:1325-1336). This study focused on BJ, which is a process where a print head is used to deposit a liquid bonding agent onto the surface of the powder bed to selectively join powder particles together (Afshar-Mohajer *et al*., 2015:293-301).

BJ of sand moulds consists of coating the uncoated (virgin) silica sand particles followed by the three AM phases (Nyembwe *et al*., 2016:230-237). During the coating process, the uncoated silica sand particles are treated with liquid sulphonic acid, prior to the pre-processing phase, thereafter a furan binder is applied to the silica sand particles. The sulphonic acid acts as an acid catalyst. When the furan binder is catalysed, it forms a cross-linked polymer structure. As a result, the resin's ability to bind particles together to form a sand mould is enhanced (Zhang *et al*., 2014:373-381). It should be noted that the coating process of uncoated silica sand particles was not investigated during this study.

The three AM phases differ depending on the AM technology being utilised and the part design (Gibson *et al*., 2015:66). The three AM phases of BJ were investigated in this study (Meiring, 2024), namely the pre-processing phase, followed by the processing phase, and the post-processing phase. The pre-processing phase involves the use of CAD software to generate a 3D surface presentation. The data describing the part geometries is stored in standard tessellation

language (STL) file format and transferred to an AM machine. Thereafter the AM machine is programmed to fabricate a part and the powder is loaded into the feedstock bin of the AM machine. The processing phase involves the printing of the desired part. During the post-processing phase, the part is brushed to remove the loose powder, and the AM machine is cleaned with a vacuum cleaner (Elliot *et al*., 2016:1890-1899; Zhang and LeBlanc, 2018:89-118). Following the post-processing phase, the unfused powder can be disposed of or reused (Meera *et al*., 2017:86-91).

The powder characteristics of AM feedstock material are of significance when considering the respiratory health of AM operators (Du Preez *et al*., 2018). The size of the particle determines where the particle settles in the respiratory tract (Thomas, 2013:847-858). Particles are categorised in size fractions depending on the place of deposition in the respiratory system namely, inhalable (< 100 µm, 50% cut-point), thoracic (< 10 µm, 50% cut-point), and respirable (< 4 µm, 50% cut-point) particles (Brown *et al*., 2013:1-12). Ultrafine particles (UFPs) are defined as particles with a particle diameter of less than 100 nm (U.S. EPA, 2009). BJ machines can release particles, including UFPs into the workplace air during the three AM phases (Afshar-Mohajer *et al*., 2015:293-301; Lewinski *et al*., 2019:1-7; Matlhatsi, 2021:1-133).

A hazardous chemical agent (HCA) is defined as a Globally Harmonized System (GHS) aligned chemical agent as listed in Annexure 1 of the Regulations for Hazardous Chemical Agents (RHCA), where an HCA is considered as a physical, health and/or environmental hazard (DoEL, 2021:1-98). The AM operators are at risk of exposure to HCAs namely, respirable crystalline silica and respirable particulates not otherwise specified (PNOS) during the three AM phases, which may pose a risk to human health (Adams, 2016:1-84; Matlhatsi, 2021:1-133).

Silica or silicon dioxide is present as amorphous silica or in crystalline form (such as quarts, tridymite, and cristobalite). Amorphous silica does not cause fibrosis and is not classified as carcinogenic to humans (IARC, 2023; Merget *et al*., 2002:625-635). The most common natural form of silica is found in crystalline silica (quarts) which is the most well-known and one of the most abundant minerals in the earth's crust (NIOSH, 2002:1-145). Inhalation of respirable crystalline silica, otherwise known as silica dust, in the form of cristobalite or quarts, impairs the clearance of particles, activates macrophages, and results in continuous inflammation and irritation of the lungs (Guha *et al*., 2011:310-320). Respiratory adverse health effects from exposure to respirable crystalline silica include silicosis, chronic obstructive pulmonary disease

including bronchitis and emphysema as well as lung cancer (IARC, 2023; NIOSH, 2004; OSHA, 2021).

PNOS are also known as particulates not otherwise regulated, particulates not otherwise classified, nuisance dust, and biologically inert dust (DoEL, 2021:1-98; Hearl, 2011:608-612; NIOSH, 2019; NIOSH method 0600, 1998:1-6;). PNOS are dust particles (< 100 µm) generated from solid materials without component-specific occupational exposure limits (Hearl, 2011:608-612). PNOS contains < 1% quarts and any reaction that occurs from exposure to PNOS is reversible (Cherrie *et al*., 2013:685-691; NIOSH method 0600, 1998:1-6).

1.2 Problem statement

In 1999, it was stated that safe working practices were necessary in AM laboratories to safeguard the health and welfare of the employees (Deak, 1999:161-166). The author found that prolonged chemical exposure in AM laboratories is likely to lead to chemical sensitivity, which might result in allergic reactions (Deak, 1999:161-166). Twenty years later Petretta *et al*. (2019:891-912) developed a risk evaluation framework for all AM process categories excluding sheet lamination. AM could potentiality pose a risk to the AM operator due to the presence of particles (including UFPs) and chemical substances either used or released during the AM process (Dobrzyńska *et al*., 2022:40273-40278). According to Stephens *et al*. (2013:334-339) exposure to UFPs during the three AM phases has become both an environmental and occupational health concern (Stephens *et al*., 2013:334-339).

Two unpublished studies investigated particle emissions and/or respiratory exposure to HCAs during AM of sand moulds, namely Adams (2016:1-84) and Matlhatsi (2021:1-133). Adams (2016:1-84) and Matlhatsi (2021:1-133) determined both the powder characterisations and chemical composition of silica sand during PBF-SLS and BJ, respectively. Adams (2016:1-84) stated that the AM sand casting process did not change the size of the uncoated, coated, and used silica sand particles. Matlhatsi (2021:1-133) found that the coated silica sand contained larger particles when compared to uncoated and used silica sand when using particle size distribution (PSD). In this study (Meiring, 2024), the results of the size, shape, and chemical composition were determined, similar to Adams (2016:1-84) and Matlhatsi (2021:1-133) to verify their results. This study builds on that of Adams (2016:1-84) and Matlhatsi (2021:1-133) to assess area concentrations and personal respiratory exposure to HCAs (respirable crystalline silica and respirable PNOS). In this study (Meiring, 2024), a window period of 24-hours (one day) was

allocated between sampling to prevent particle build-up in the AM research facility and to ensure that background airborne particle concentrations were as low as possible. Matlhatsi (2021:1-133) calculated emission rates (ERs) of particles released during the three AM phases by using a provided air exchange rate (AER) of 0.22. The author found that the pre-processing phase 3.14×10^6 p/cm^3 (3.14×10^{12} p/m^3) had a mean particle number concentration that was significantly higher than the processing phase 2.17×10^6 p/cm^3 (2.17×10^{12} p/m^3) and the post-processing phase 1.98 × 106 p/cm^3 (1.98×10^{12} p/m^3) for particles 0.01 to 1.0 µm in size. In this study (Meiring, 2024), AER was calculated in the same AM research facility using a carbon dioxide decay method, and the ERs of the particles were calculated using the calculated AER. In this study (Meiring, 2024), particle number concentrations were assessed for particles > 1.0 µm in size, which was not investigated by Matlhatsi (2021:1-133). Time-integrated sampling is a gravimetric filter analysis method that provides data on the elements that were collected on filters (Stefaniak *et al*., 2021:1-51). Adams (2016:1-84) and Matlhatsi (2021:1-133) assessed personal respiratory exposure to respirable crystalline silica and PNOS of sand moulds utilising time-integrated sampling and stated that the AM operators were exposed to respirable crystalline silica and respirable PNOS at concentrations below the respective South African TWA-OELs in the Regulations for Hazardous Chemical Agents (RHCA). In this study (Meiring, 2024) personal exposure monitoring was conducted using real-time monitoring and time-integrated sampling. This study differs from Adams (2016:1-84) and Matlhatsi (2021:1-133), because the full shift of the AM operator was monitored in real-time at 1-minute intervals for direct reading of particulate matter with particle aerodynamic diameter of equal to or less than 4 micrometres (PM 4) using Nanozen Dustcount 9000 (Nanozen Industries Inc., British Columbia Canada).

Stefaniak *et al*. (2021:1-51) conducted a review of emissions and exposures for all AM process categories. A total of forty-six publications matched the inclusion criteria, but only two of the publications applied to BJ (Stefaniak *et al*., 2021:1-51). Afshar-Mohajer *et al*. (2015:293-301) utilised gypsum (calcium sulphate) as AM feedstock material and stated that particles with a size between 205 and 255 nm were found to have the highest particle number concentration throughout the printing process (0.9 to 1.16×10^4 p/cm^3). The authors stated that the ER peaked at 4.4×10^4 p/min for particles 352 to 407 nm in size during the post-processing phase (Afshar-Mohajer *et al*., 2015:293-301). Lewinski *et al*. (2019:1-7) reported the highest mean particle number concentration during the processing phase (3.8×10^4 p/cm^3), then the pre-processing phase (3.5×10^4 p/cm^3) and post-processing phase (3.3×10^4 p/cm^3) for particles 0.3 to 10 µm in

size. Despite measuring peak particle number concentrations, the authors reported no statistically significant differences between the three AM phases (Lewinski *et al*. 2019:1-7).

Du Plessis *et al*. (2022:1-40) conducted a review study on the efficacy of the hierarchy of controls for all AM process categories. Only one of the forty-two publications included by the authors that matched the inclusion criteria focused on BJ, namely Lewinski *et al*., (2019:1-7). Lewinski *et al*., (2019:1-7) provided administrative controls relevant to the specifications of the workplace. The authors stated that data on the effectiveness of controls for particle emissions for all AM process categories are required. There are limited publications on particle emissions during BJ (Lewinski *et al*., 2019:1-7).

According to Dobrzyńska *et al*. (2021:1733-1758) research in AM is needed to promote awareness and understanding of particle emissions and exposures to HCAs related to the AM process. To protect worker health and safety, occupational hygienists (as well as AM operators and management at AM facilities) must have a clear understanding of the particle emissions and HCA exposures related to the AM process. Toxicologists must also have this knowledge to develop experimental protocols that mimic the conditions of the real-world workplace environment (Stefaniak *et al*., 2021:1-51).

The lack of information about the health risk posed to the AM operator necessitates a study evaluating AM operator particle exposure and emissions during BJ in order to establish the urgency of implementing control measures.

1.3 Research aim and objectives

1.3.1 Research aim

To determine the powder characteristics and chemical composition of uncoated, coated, and used silica sand and to assess particle number concentrations, particle ERs, area concentrations, and personal respiratory exposure of AM operators to HCAs (respirable crystalline silica and respirable PNOS) during the three AM phases of BJ at a South African AM research facility.

1.3.2 Research objectives

1. To determine the powder characteristics and chemical composition of uncoated, coated, and used silica sand during BJ. These were evaluated through PSD and shape analysis, scanning electron microscopy (SEM), and wavelength dispersive X-ray fluorescence (WD-XRF).

2. To quantify particle number concentrations and to determine ERs of particles released during BJ by means of direct-reading instruments during the pre-processing phase, processing phase, and post-processing phase of AM.
3. To assess area concentrations and personal respiratory exposure of the AM operators to HCAs (respirable crystalline silica and respirable PNOS) during BJ utilising silica sand by means of area monitoring and personal exposure monitoring during the full duration of the shift. This was done through real-time monitoring and time-integrated sampling.

1.4 Hypothesis

Afshar-Mohajer *et al*. (2015:293-301) and Lewinski *et al*., (2019:1-7) investigated particle emissions during BJ (not during sand moulding). According to Afshar-Mohajer *et al*. (2015:293-301) particles with a size between 205 and 255 nm were found to have the highest particle number concentration throughout the printing process (0.9 to 1.16 × 10^4 p/cm^3). The authors stated that ER peaked at 4.4 x 10^4 p/min for particle sizes of 352 to 407 nm when the BJ machine was switched off and the printed part was ejected (Afshar-Mohajer *et al*., 2015:293-301). Lewinski *et al*. (2019:1-7) did not observe statistically significant differences in mean particle number concentrations between the pre-processing (3.5 × 10^4 p/cm^3), processing (3.8 × 10^4 p/cm^3), and post-processing (3.3 × 10^4 p/cm^3) for particles 0.3 to 10 µm in size when compared to the background particle number concentration (3.3 × 10^4 p/cm^3). Matlhatsi (2021:1-133), used an AER (0.22) provided by the AM research facility to calculate the ERs of particles. He found that with each printing day, the background airborne particle number concentration increased, on day one of printing the background airborne concentration was 7.62 × 10^5 p/cm^3 (7.62 × 10^{11} p/m^3) and on day five of printing the background airborne concentration was 4.74 × 10^6 p/cm^3 (4.74 × 10^{12} p/m^3). In some instances, the background airborne concentrations were higher than those during the AM phases, causing the calculated ERs to be negative. However, since negative ERs are not possible, these results were excluded in the study (Afshar-Mohajer *et al*., 2015:293-301).

The author stated that the mean ERs were the highest for particle sizes 0.01 to 1.0 µm during the pre-processing phase (1.2 × 10^9 p/min), followed by the post-processing phase (7.74 × 10^8 p/min) and processing phase (5.27 × 10^8 p/min).

1. The correct AER is crucial for calculating an accurate ER. Matlhatsi (2021:1-133) did not calculate the AER but used a provided AER. It is hypothesised that the calculated AER is higher than that provided by Matlhatsi (2021:1-133).

Adams (2016:1-84) and Matlhatsi (2021:1-133) investigated the personal respiratory exposure of AM operators to respirable crystalline silica and PNOS and stated that the respirable crystalline silica (≤ 0.07 mg/m^3) complied with the South African TWA-OEL-CL of 0.1 mg/m^3 and respirable PNOS concentrations (≤ 0.60 mg/m^3) complied with the South African TWA-OEL-RL of 5 mg/m^3 in the RHCS, 1995.

2. It is hypothesised that the AM operator is exposed to respirable crystalline silica and respirable PNOS at concentrations below the respective South African TWA-OELs in the RHCA for time-integrated sampling.

1.5 References

Adams, G.E.M. 2016. *Respiratory exposure during the additive manufacturing of sand casting moulds*. Potchefstroom: North-West University (Dissertation – Masters).

Afshar-Mohajer, N., Wu, C. Y., Ladun, T., Rajon, D. A. & Huang. Y. 2015. Characterization of particulate matters and total VOC emissions from a binder jetting 3D printer. *Building and Environment,* 93:293-301.

Brown, J.S., Gordon, T., Price, O. & Asgharian, B. 2013. Thoracic and respirable particle definitions for human health risk assessment. *Particle and Fibre Toxicology*, 10(12):1-12.

Caiazzo, F., Alfieri, V., Corrado, G. & Argenio, P. 2017. Laser powder-bed fusion of Inconel 718 to manufacture turbine blades. *The International Journal of Advanced Manufacturing Technology*, 93:4023-4031.

Cherrie, J.W., Brosseau, L.M., Hay, A. & Donaldson, K. 2013. Low-toxicity dusts: current exposure guidelines are not sufficiently protective. The *Annals of Occupational Hygiene*, 57(6):685-691.

Deak, S.M. 1999. Safe work practices for rapid prototyping. *Rapid Prototyping Journal*, 5(4):161-63.

Department of Employment and Labour (DoEL). *South Africa. Hazardous Chemical Substances Regulations, 1995*. Available from http://www.acts.co.za/occupational-health-and-safety-act 1993/index.html Date of access: 2 July 2021.

Department of Employment and Labour (DoEL). 2021. Regulations for hazardous chemical agents (RHCA), 2021. (Notice 280). *Government Gazette*, 44348: 6-28, 29 Mar.

Du Plessis, J.L., Du Preez, S. & Stefaniak, A.B. 2022. Identification of effective control technologies for additive manufacturing. *Journal of Toxicology and Environmental Health,* Part *B*:1-40.

Du Preez, S., de Beer, D.J. & Du Plessis, J.L. 2018. Titanium powders used in powder bed fusion: The relevance to respiratory health. *South African Journal of Industrial Engineering*, 29(4):94-102.

Dobrzyńska, E., Kondej, D., Kowalska, J. & Szewczyńska, M. 2022. Exposure to chemical substances and particles emitted during additive manufacturing. Environmental Science and Pollution Research, 29, 40273:40273-40278.

Elliot, A.M. & Love, L.J. Operator burden in metal additive manufacturing. In Solid Freeform Fabrication 2016, Proceedings of the 26th Annual International Solid Freeform Fabrication Symposium – An Additive Manufacturing Conference, 2016. pp. 1890-1899.

Gibson, I., Rosen, I.D.W. & Stucker, B. 2015. Additive manufacturing technologies: rapid prototyping to direct digital manufacturing. Cham, Switzerland: Springer. pp. 1-484. Available from Springer eBook Collection: 2010_Book_AdditiveManufacturingTechnolog.pdf (ethernet.edu.et) - Search (bing.com) Date of access: 27 Feb. 2021.

Guha, N., Straif, K. & Tallaa, L. 2011. The IARC Monographs on the carcinogenicity of crystalline silica. *La Medicina del lavoro*, 102(4):310-320.

Hearl, J.R. 1998. Current exposure guidelines for particulates not otherwise classified or regulated: History and Rationale. Applied *Occupational and Environmental Hygiene*, (8):608-612.

International Agency for Research on Cancer (IARC). 2023. Agents classified by the IARC monographs, volumes 1-134 Agents Classified by the IARC Monographs, Volumes 1–134.pdf Date of access: 24 November 2023.

International Organization for Standardizations/American Society of Testing Materials (ISO/ASTM): Additive Manufacturing - General principles – Fundamentals and Vocabulary (ISO/ASTM 52900) [Standard] Geneva, Switzerland: ISO/ASTM, 2022.

Le Néel T.A., Mognol, P. & Hascoet, J.Y. 2018. A review on additive manufacturing of sand molds by binder jetting and selective laser sintering. *Rapid Prototyping Journal*, 24(8):1325-1336.

Lewinski, N.A., Seconda, L.E. & Ferri, J.K. 2019. On-site three-dimensional printer aerosol hazard assessment: pilot study of a portable in vitro exposure cassette. *Process Safety Progress*, 38(3):1-7.

Matlhatsi, N.L. 2021. *Particulate emissions and respiratory exposure to hazardous chemical substances during additive manufacturing of sand moulds.* Potchefstroom: North-West University. (Masters – Dissertation).

Meera, K.J., Banganayi, F. and Oyombo, D. 2017. Moulding sand recycling and reuse in small foundries. *Procedia Manufacturing*, 7:86-91.

Merget, R., Bauer, T., Küpper, H.U., Philippou, S., Bauer, H.D., Breitstadt, R. & Bruening, T. 2002. Health hazards due to the inhalation of amorphous silica. *Archives of Toxicology*, 75(11):625-34.

National Institute for Occupational Safety and Health (NIOSH). 1998. *Particulates not otherwise regulated, respirable 0600* NMAM 0600: PARTICULATES NOT OTHERWISE REGULATED, RESPIRABLE (cdc.gov) Date of access: 20 Oct. 2021.

National Institute of Occupational Safety and Health (NIOSH). 2002. *Health effects of occupational exposure to respirable crystalline silica.* https://www.cdc.gov/niosh/docs/2002-129/pdfs/2002-129.pdf Date of access: 12 June 2021.

National Institute for Occupational Safety and Health (NIOSH). 2004. Silicosis: *Learn the facts!* Silicosis: Learn the facts. nomas80404 (cdc.gov) Date of access: 8 Aug. 2021.

National Institute for Occupational Safety and Health (NIOSH). 2019. *Particulates not otherwise regulated.* CDC - NIOSH Pocket Guide to Chemical Hazards - Particulates not otherwise regulated Date of access: 12 Aug. 2021.

Nyembwe, K., Motadi, M. & Gonya, E.M. 2005. Descriptive statistical analysis of foundry properties of sand parts produced by three-dimensional printing. https://ujcontent.uj.ac.za/vital/access/services/Download/uj:31586/SOURCE1?view=true Date of access: 29 Apr. 2022.

Occupational Safety and Health Administration (OSHA). 2021. Silica, Crystalline. Silica, Crystalline - Overview | Occupational Safety and Health Administration (osha.gov) Date of access: 20 Mar. 2022.

Petretta, M., Desando, G., Grigolo, B. & Roseti, L. 2019. 3D printing of musculoskeletal tissues: Impact on safety and health at work. *Journal of Toxicology and Environmental*, 82(16):891-912.

Stefaniak, A.B., Du Preez, S. & Du Plessis, J.L. 2021. Additive Manufacturing for Occupational Hygiene: A Comprehensive Review of Processes, Emissions, & Exposures. *Journal of Toxicology and Environmental Health, Part B* 24(5):1-51.

Stephens, B., Azimi, P. & Orch, Z.E. 2013. Ultrafine particle emissions from desktop 3D printers. *Atmospheric Environment*, 79:334-339.

Sun, C. & Shang, G. 2021. On application of metal Additive manufacturing. *World Journal of Engineering and Technology*, 9(1):194.

Thomas, R.J. 2013. Particle size and pathogenicity in the respiratory tract. *Virulence*, 4(8): 847-858.

United States Environmental Protection Agency (U.S. EPA). 2009*. Integrated Science Assessm ent for Particulate Matter* file:///C:/Users/27676/Downloads/PM_ISA_without_annexes.pdf Date of access: 27 July 2022.

Zhang, H. & LeBlanc, S. 2018. Processing parameters for selective laser sintering or melting of oxide ceramics. In: Zhang, H. & LeBlanc, S. *Additive Manufacturing of High-performance Metals and Alloys - Modeling and Optimization*. Washington: intechopen. pp. 89-118.

Zhang, H., Zhao, H., Zheng, K., Liu G. & Wang Y. 2014. Diminishing hazardous air pollutant emissions from pyrolysis of furan no-bake binders using methane sulfonic acid as the binder catalyst. *Journal of Thermal Analysis and Calorimetry*, 116:373-381.

CHAPTER 2 LITERATURE STUDY

2.1 Introduction

The chapter discusses sand moulding, additive manufacturing (AM), AM phases, AM process categories used in sand moulding, binder jetting (BJ), silica sand as AM feedstock material, and the furan binder system. In addition, the respiratory system and the health effects associated with silica sand are discussed. Finally, occupational exposure in AM and casting foundries and relevant occupational exposure limits (OELs) of hazardous chemical agents (HCAs) are shortly discussed.

2.2 Sand moulding (sand casting)

Casting is one of the oldest techniques of producing metal components in the machine industry and automobile industry (Pandey, 2015:477-483; Sahoo *et al*., 2019:9805-9835). The first evidence of casting dates as far back as 3200 before Common Era (BCE) when a copper frog was fabricated in Mesopotamia. Other castings such as cult artifacts and weapons dating back to 3000 BCE have been discovered in India and the Middle East. The earliest evidence of a sand mould dates from 645 BCE in China (Pandey, 2015:477-483).

Vannoccio Biringuccio was the author of *De la Pirotechnia* (first edition Venice, 1540). His comprehensive work was dedicated to the traditional sand moulding process (Biringuccio, 1540; Stefanescu, 2017:1-745). Traditional sand moulding is used in various industries to produce metal parts. The manufacturing of sand moulds through traditional sand moulding involves three fundamental steps. The first step in traditional sand moulding is to design a pattern out of a material such as metal, wood, or plastic. The pattern is used to create a cavity (out of the sand) surrounded by sand (Le Néel *et al*., 2018:1325-1336). The mould cavity is a replica of the shape of the desired part (Hawaldar and Zhang, 2018:1037-1045). The second step is to pour molten material into the cavity of the mould. After the molten material has solidified, the part is removed from the mould. Lastly, the excess material is removed from the part and the surface is cleaned (Le Néel *et al*., 2018:1325-1336).

The foundry industry contributes significantly to global economic growth (Shi *et al*., 2021:286-295). Foundries worldwide have found AM to be advantageous and have implemented this method into their foundry processes. In sand moulding foundries, AM is used to create sand moulds or sand moulding patterns (Adefuye *et al*., 2020:55-63). The process of manufacturing

sand moulds using AM is referred to as an indirect AM process (Le Néel *et al*., 2018:1325-1336). The absence of sand compaction and wet-mixing steps distinguishes indirect AM from traditional sand moulding and core-making procedures (Nyembwe *et al*., 2016:230-237).

The process of manufacturing sand moulds using AM has advantages over traditional sand moulding in terms of cost, production rate, surface roughness, defect control, part consolidation, weight reduction, reduced material waste, functional performance, geometry, and process complexity (Adefuye *et al*., 2020:55-63; Blakey-Milner *et al*., 2021:1-33; ExOne, 2016; Gebhardt and Hötter, 2016; Gibson *et al*., 2021:9; Shah *et al*. 2021:1-5; Yang and Zhao, 2015:444-449). Some of the limitations and challenges of manufacturing sand moulds using AM include the initial cost of an AM machine, the requirement for qualified AM operators to design sand moulds, and the identification and implementation of binders that are not environmentally harmful (Sivarupan *et al*., 2021:1-17).

A variety of AM feedstock sands (such as plaster-ceramic composites, ceramic beads, chromite, olivine, zircon, or silica) and binder systems (phenol or furan) in BJ. Collectively these materials are used to create three-dimensional (3D) printed sand moulds with the required characteristics (Nyembwe *et al.,* 2016:230-237; Upadhyay *et al*., 2017:211-220). The fabrication of manifolds is an example of a sand mould application utilising silica sand (Sivarupan *et al*., 2021:1-17).

2.3 AM overview

AM processes and materials emerged in the early 1980s (Sun and Shang, 2021:194). The terms habitually used in conjunction with AM are additive processes, additive layer manufacturing, 3D printing, freeform fabrication, additive processes, rapid prototyping, direct digital manufacturing, additive fabrication, additive techniques, and generative manufacturing (Cozmei and Caloian, 2012:457-462; ISO/ASTM 52900:2021). AM is defined as a process in which AM feedstock material is joined in a layered manner to create parts from 3D model data (ISO/ASTM 52900:2021).

The International Organisation for Standardisation and the American Society for Testing and Materials (ISO/ASTM) devised a set of standards that categorise AM into seven distinctive process categories, namely, binder jetting (BJ), directed energy deposition (DED), material extrusion (MEX) material jetting (MJT), powder bed fusion (PBF), sheet lamination (SHL) and vat photopolymerisation (VPP) (ISO/ASTM 52900:2021). Each AM process category can further be categorised into the machine technologies and AM feedstock materials used (ASTM

F2792:2013). A variety of AM feedstock materials are available on the market. The general material types include metals, sand, composites, ceramics, and polymers (Anderson *et al*., 2018:8-15; Le Néel *et al*., 2018:1325-1336).

2.3.1 AM process categories used in sand moulding

Two main AM process categories are adopted to manufacture sand moulds and cores in compliance with the computer aided design (CAD) data, namely BJ and PBF-selective laser sintering (PBF-SLS) (Le Néel *et al*., 2018:1325-1336; Shi *et al*., 2021: 286-295; Snelling *et al.*, 2013: 827-845). In the following section both BJ and PBF-SLS are discussed in further detail. The primary focus of this study, however, is on BJ as the facility which was investigated during this study uses the process of BJ.

2.3.2 Binder Jetting

BJ is based on an ink-jet printing technology and was originally referred to as the 3D printing technique or ProMetal3D technique or 3D printing (Mostafaei *et al.*, 2021:1-138; Sen *et al.*, 2021:1-12). Sachs *et al* (1993:1-14) received the first patent for BJ at the Massachusetts Institute of Technology, Thereafter, Z-Corporation (Burlington, Massachusetts) obtained its license to use BJ in 1995 (Gibson *et al*., 2021:239). BJ is compatible with a wide range of powdered materials such as sand, polymers, ceramics, and metals (Le Néel *et al*., 2018:1325-1336). The applications of BJ are dependent upon the part being manufactured and its purpose (Chua and Leong, 2017:247; Gibson *et al*., 2021:247). BJ is particularly used in applications including, cores and moulds, cosmetics industry, electro-chemical, bone scaffolds, plastic surgery and electronic components (Ziaee and Crane, 2019:781-801; Zhou *et al*., 2014:1-10). Examples of 3D sand moulding machines that use foundry or silica sand include Voxeljet (Augsburg, Germany) and ExOne (Irwin, Pennsylvania) (ExOne, 2020; Voxeljet, 2020). BJ utilises a drop-on-demand printing process in which individual drops are generated on demand using drop-on-demand (DoD) printheads through thermal or piezoelectric action. Piezoelectric printheads contain piezoelectric (quasi-adiabatic) elements. The physical dimension of the piezoelectric element changes when an electrical current is received. As a result, a certain amount of binder droplets is ejected through the printhead onto the powder bed. The thermal printhead consists of heating elements. The heating elements cause evaporation and bubble formation of the binder. The binder droplets are ejected through the printhead due to a pressure difference formed inside and outside the printhead (Sen *et al.*, 2021:1-12). Continuous-jet printheads produce liquid droplets continuously

and can print at higher speeds than DoD printheads (Utela *et al*., 2008:96-104). The formation of drops is caused by the fluid's jet breakup behaviour, which was first investigated by Leonardo da Vinci in the Codex Leicester (Maccurdy, 1955). The jet breakup behaviour of fluid is not affected by perturbation and nozzle length acting on the jet, whereas the breakup behaviour is affected by viscosity, surface tension, and droplet velocity. A stable drop is created when the satellite droplets and main droplets merge before they reach the powder bed, hence increasing the print resolution (Eggers and Villermaux, 2008:1-78).

BJ consists of three main manufacturing phases, namely a pre-processing phase, followed by a processing phase, and then a post-processing phase (Gibson *et al.*, 2021:53-60). The pre-processing phase requires the use of a hopper dispensing system to supply the job box of the AM machine with the AM feedstock material (Wei *et al*., 2021:106-112). The pre-processing phase also makes use of CAD software to produce a digital model (Sarvankar and Yewale, 2019:1-10). After the model has been designed, the next step is to export the files to stereolithography or standard tessellation language (STL) file format and transfer them to the AM machine. STL file format describes an object's surfaces using polygons or triangles (Sarvankar and Yewale, 2019:1-10). Even though the conversion from CAD programs to STL file format is automated, there is a risk for errors to occur during this phase. As a result, a variety of software tools have been created to identify and, if possible, correct such issues (Gibson *et al*., 2021:56). The STL file format is converted to a G-code file by the slicing software. A G-code file consists of commands in G-code, a programming language used to describe how an AM machine should print a part. The AM operator can also control the process parameters like part orientation and layer thickness using the slicer software (Sarvankar and Yewale, 2019:1-10). The software parameters of the AM machine are then programmed to fabricate a part. The drawback of AM is that each part has its own set of specifications; therefore, it is challenging to choose optimal process parameters for instance layer thickness, scanning speed, and hatch spacing (Yakout *et al.*, 2017:2081-2098). Thereafter the powder is sifted, loaded, and levelled in the AM machine. A build plate must be fitted and levelled in relation to the axes of the AM machine for AM processes that use them. These setup processes can either be done automatically or manually by skilled AM operators (Gibson *et al*., 2021:58).

The AM machines operate automatically once the printing process has started. The automated printing process of BJ includes dispensing powder, powder spreading, and binder dispensing (Sen *et al.*, 2021:1-12). The powder is discharged from the powder reservoir onto the build platform. A counter-rotating roller is used to disperse a thin layer of powder evenly throughout a

build platform. A print head contains one or multiple ejection nozzles that move along the x- and y-directions and deposits binder droplets (5 to 80 µm in size) at designated places on the powder bed (Adefuye *et al*., 2020:55-63; Afshar-Mohajer *et al*., 2015:293-301; Sachs *et al.*, 1993:1-14). The powder particles interact with the binder droplets to generate primitives, which bind together to form a cross-sectional layer. The parts in the powder bed are self-supporting, thus no support structures are required (Gibson *et al*., 2021:249). The build platform moves down (z-direction) as soon as a layer has been completed. The distance that the build platform moves down is equivalent to a layer thickness (100 to 200 µm) to guarantee that the working plane remains the same. This process is repeated until a complete part is built (Afshar-Mohajer *et al*., 2015:293-301; Sachs *et al.*, 1993:1-14).

After the part has been successfully printed it will go through the post-processing phase (Ziaee and Crane, 2019:781-801). The post-processing phase is the process of finalising a part for specific use (Gibson *et al*., 2021:59). The BJ's post-processing phase can be divided into three steps namely, curing (drying), de-powdering, and densification (sintering and infiltration) (Mostafaei, 2021:1-138). Curing is a process in which a printed part is cured in an oven for 2 to 4 °hours at 180°C to allow a binder to dry completely and to prevent the formation of irregular cracks, especially at sharp edges (Hackney and Wooldridge, 2017a:7-15; Mostafaei, 2021:1-138; Ziaee and Crane, 2019:781-801). When using furan resin and sulphonic acid, the part can be cured without the use of heat (Sivarupan *et al*., 2021:1-17, Ziaee and Crane, 2019:781-801). Once curing and de-powdering are completed, the final part's relative density is between 50 to 60% (Mostafaei *et al.*, 2021:1-138). Near full densification of the part can be achieved through sintering and infiltration in a furnace (Mostafaei, 2021:1-138; Nandwana *et al*., 2017:207-218). The porosity of the binder jetted part is removed due to sintering and infiltration which results in the part shrinking (Lucas, 2017: 233-255; Mostafaei, 2021:1-138). When a part is sintered, its shrinks as a result of material diffusing from grain boundaries or bulk particles into pore openings, whereas infiltration causes less shrinkage of the part because the pore openings are filled with more infiltrated material (such as polyurethane, molten wax, and cyanoacrylate) by capillary action, resulting in less distortion than sintering. In this study (Meiring, 2024) curing using heat, de-powdering, and densification activities were not conducted during the post-processing phase.

2.3.3 PBF-SLS

PBF was one of the first commercially available AM processes and it is suitable for a variety of materials, including sand, polymers, ceramics, metals, and composites (Gibson *et al*., 2021:125-

126). PBF consists of four distinct technologies namely, direct metal laser sintering (DMLS), electron beam melting (EBM), selective laser melting (SLM), and SLS. Although PBF is divided into separate technologies, they all share the same printing process, whereby a high-energy source such as a laser or electron beam is used as a heating source to selectively bind a thin layer of deposited powder particles together layer-by-layer in compliance with the CAD data (ASTM: F2792:2013). PBF can further be divided into four mechanisms of fusion, namely chemically induced binding, full melting, liquid-phase sintering, and solid-state sintering (Gibson *et al*., 2021:130).

SLS was the first PBF process to be commercialised (Gibson *et al*., 2021:125). PBF-SLS technology sinters specific regions of the top layer of the powder bed by means of a laser beam that adheres to the digital 3D design pattern (ASTM F2792:2013; Kruth *et al*., 2003:357). In PBF-SLS, a carbon dioxide laser or a neodymium-doped yttrium aluminium garnet can be utilised as a heat source, either separately or in a dual-beam technique (Abe *et al*., 2001:210-213; Birmingham *et al*., 1992:147-153). Diode lasers can also be used to sinter metals, polymers, and sand (Casalino *et al*., 2002:100-106; Gueche *et al*., 2021:1-26).

The pre-processing phase of PBF involves the use of CAD software or reverse-engineering apparatus to generate a 3D surface presentation. The data describing a part is stored in STL and transferred to an AM machine to be programmed to manufacture the desired part. Thereafter, the powder is loaded into the AM feedstock bin of the AM machine. The processing phase requires the use of a counter-rotating roller to disperse a layer of powder evenly across a build platform within an enclosed chamber. Nitrogen gas is present in the build chamber to reduce the decay and oxidation of the powder. The powder must first be heated to prevent thermal distortion and allow fusion in the previous layer before being sintered by a laser beam. Infrared radiation preheats powder inside the build platform to a uniform temperature slightly lower than the melting (sintering) point before the powder is spread over the build area (Gibson *et al.*, 2021, 126). Two mirrors are used to selectively melt the powder by reflecting the laser onto the powder (Stefaniak *et al*., 2021:173-222). The unfused powder gives support for successive layers, thereby eliminating the necessity for a secondary support structure (Chua and Leong, 2017:141; Zhang and LeBlanc, 2018:869-870). The lack of support structures allows for the printing of extremely complicated geometries, including moving and interlocking parts (Zhang and Jung, 2018:8). As soon as a layer has been completed, the build platform lowers, and a new powder layer is deposited. This procedure is repeated from the bottom to the top until a complete part is built.

Following the completion of the final layer, the fully formed part remains in the AM machine until the part is cooled down completely, where after the part is taken out of the powder.

The post-processing involves brushing off loose powder and applying supplementary treatment if necessary to create a final product (Chua and Leong, 2017:141; Gibson *et al.*, 2021:59; Zhang and LeBlanc, 2018:869-870). The powder that has not been fused after the AM process can be reused (Zhang and Jung, 2018:81).

2.4 Silica sand as AM feedstock material

AM feedstock material refers to the raw material utilised in the building process of AM (ISO/ASTM 52900:2021). During this study, silica sand was used as the AM feedstock material. Silica is a mineral often found in crystalline form and seldom in amorphous form. Silica occurs in nine different crystalline or polymorphic forms. However, quarts, cristobalite, and tridymite are the most prevalent polymorphic forms. Sand is composed of fine particles of rock fragments and minerals. However, the dominant mineral in the sand is quarts (NIOSH: 2002:1-145). Silica sand is used as an AM feedstock material due to its low cost and global availability (Svidró *et al*., 2020:1-6). Silica sand is odourless and yellowish, and it has a density of 1.32 to 1.37 g/ml. Silica sand is insoluble in aqueous solutions and it is stable at normal ambient temperatures (Voxeljet, 2014b:1-7). Silica is inert and is a hard mineral listed as seven out of ten on the Mohs scale of hardness (Ahmed, 2013:1-38). Pure silica has a high melting point of 1760°C. However, silica-containing impurities have a lower melting point. Silica's drawbacks include low thermal conductivity and high thermal expansion. Foundry workers are also at risk of developing silicosis due to the cumulative inhalation of silica particle (Rosenman *et al*., 1996:1-12).

2.4.1 Characteristics of an AM feedstock material

The particle size of the AM feedstock material is one of the most important control parameters in the AM process. The density and flowability of the AM feedstock material are both affected by particle size distribution. This has an impact on the quantity of energy required to process the powder and the surface finish (Micromeritics, 2017:1-5). Lu *et al.* (2008:178-183) observed that smaller particles (< 20 µm) promoted a lower porosity bed and a higher packing density resulted in a part with a smoother surface and higher mechanical strength. However, smaller particles displayed poor flowability and a greater propensity to agglomerate due to their larger surface area, ability to rapidly absorb moisture, and higher Van der Waals interaction forces. The density and flow properties of the AM feedstock are influenced by the particles' shape. Spherical shape

particles promote flowability and packing density. Particles with an irregular shape reduce the density and increase the porosity of the final part (Micromeritics, 2017:1-5).

2.5 Furan binder system

The furan no-bake binder system was established in 1958 and gained popularity in the 1980s (Carey and Lott, 2022:1-10). The furan no-bake binder system is a popular binder system due to its ease of use, sand reusability, and high mechanical strength (Hackney and Wooldridge, 2017b:457-465). The furan binder system is compatible with chromite, silica, and zircon sand (Carey and Lott, 2022:1-10).

In the furan no-bake binder system, a catalyst catalyses the polymerisation of furan resin, which results in a remarkable colour shift, turning green and then black as it polymerises (Carey and Lott, 2022:1-10). During the process of curing, chromophoric chemicals develop, which causes the colour shift. The chromophoric conjugation is broken down by ultraviolet light, allowing the pigment to revert to its brownish colour. The colour shift does not affect the properties of coated sand (Carey and Lott, 2022:1-10).

The furan resin-to-catalyst ratio and the sequence in which the catalyst is added, are important. The mixing ratio of furan resin is dependent on the mass of the sand, and it typically ranges from 0.9 to 2.0%. The quantity of catalyst ranges between 20 to 50% and it is determined by the mass of the furan resin (Carey and Lott, 2022:1-10). With regard to the sequence of catalyst addition, the sand should be treated with an acid catalyst first followed by furan binder. If the sand is coated with furan resin first, it will be over-catalysed, resulting in a considerable loss of mechanical strength. Under no circumstances can the catalyst and furan resin be added at the same time or mixed beforehand. An explosion can happen as a result of an uncontrolled exothermic poly-condensation chemical reaction that occurs once the liquids are mixed (Carey and Lott, 2022:1-10).

Furan resin is a polymer that contains furfuryl alcohol (> 80%) (Voxeljet, 2014a:1-13; Xuhai *et al*, 2022:1-15). The part's strength increases as the binder content increases, but this can cause the part's precision to diminish (Hu and Du, 2018:1-6). During the casting process, a substantial amount of gas is created as the binder content is increased (Sivarupan *et al*., 2021:1-17). The resin's viscosity decreases as the contained amount of furfuryl alcohol increases (Holtzer *et al*., 2013:1-9). Chemical compounds such as phenol, urea, furfuryl, formaldehyde, and their

derivatives can also be found in furan resin (Xuhai *et al*, 2022:1-15). The commercial classification of furan resins relies on their water and nitrogen content.

The water content varies from 0 to 30%, while the nitrogen content ranges from 0 to 11%. A high furan binder grade can be obtained by utilising a low content of water and nitrogen (Carey and Lott, 2022:1-10).

Furan resin must meet certain requirements to be utilised in/as a furan binder system. The viscosity and surface tension of the furan resin must be tailored to fit within a particular range, and it must have sufficient stability and rheology to be deposited by an inkjet printhead. The furan resin needs to be stable to preclude solidifying in the printhead. The powder bed must be wetted adequately by the furan resin for optimal diffusion. On the other hand, the powder bed must not be wetted to the point that the furan resin migrates far beyond the impact site. The binding strength must be sufficient to ensure that the part maintains its structural integrity. Lastly, the burning of the furan resin must be conducted in such a way that minimizes hazardous chemical traces (Utela *et al*., 2008:96-104).

Furan resins are a potential human carcinogen, posing a health concern to AM operators (Bakhiya and Appel, 2010:84:563-578; Voxeljet, 2014a:1-13). Furthermore, it has been found that furan resin is not environmentally friendly and must be substituted with less hazardous binders (Sivarupan *et al*., 2021:1-17). Many AM companies, including Voxeljet, are still in search for more environmentally friendly binders, such as acrylic-epoxy/SO_2 (Carey, 2012:1-10; Sivarupan *et al*., 2021:1-17).

2.6 Respiratory tract anatomy

The respiratory tract is anatomically divided into two compartments based on function. Compartment one consists of the upper respiratory tract and tracheobronchial tree, which conducts air from the surrounding environment to the gas exchange sites. The second compartment consists of the pulmonary regions (bronchiole and alveoli), which engage in gas exchange (Hall and Guyton, 2016:497-557).

2.6.1 Particle deposition in the respiratory tract

The main route of particle exposure is inhalation through the mouth and/or nose (Geraets *et al*., 2014:54-64). The respiratory tract of adult humans is exposed to inhaled air of more than

10 000 litres daily, which may contain hazardous chemical agents (HCAs) (Tsuda *et al*., 2013:1437-1471). Particles are categorised in size fractions depending on the place of deposition in the respiratory tract (Klaassen and Watkins, 2015:228-229). Inhalable particles (50% penetration of particles with an aerodynamic diameter of < 100 µm) are breathed in through the mouth and nose and can access the nasopharyngeal region. Extra thoracic particles are inhaled but cannot deposit further than the larynx. Thoracic particles (< 10 µm, 50% cut-point) can deposit past the larynx, while respirable particles (< 4 µm, 50% cut-point) can penetrate the alveolar region of the lungs (Brown *et al*., 2013:1-12).

The deposition of particles in the respiratory tract determines the respiratory defence (clearance) mechanism and the toxicity of the inhaled particles. The deposition of particles in the respiratory tract is influenced by factors such as the powder characteristics and chemical composition of the particle, the anatomy of the respiratory tract, and the physiological characteristics (such as breathing and airflow patterns) of the respiratory tract (Yeh *et al*., 1976:147-156).

Particles that are inhaled follow a complicated route through the respiratory system, where they are deposited by different mechanisms (Darquenne, 2020:181-185). According to Scheckman and McMurry (2011:508-516) particle deposition in the respiratory tract can occur through five mechanisms, namely diffusion, impaction, interception, electrostatic deposition, and sedimentation. Diffusion is the random movement of particles (0.5 to 1 µm) caused by collisions with surrounding molecules (CCOHS, 2022; Fröhlich and Salar-Behzadi, 2014:4795-4822). As the particle size decreases, the movement becomes more vigorous. The deposition of particles in the bronchiole and the alveoli is primarily caused by diffusion (CCOHS, 2022a). Another mechanism is impaction, and it is governed by Newton's first law of motion also known as inertia. This law states that once an object begins moving, it will resist changing its direction or velocity unless it is acted upon by an external force (Wijesuriya, 2015:2723-2732). As a result, when the airway system suddenly curves, particles (> 2 µm) collide or stick to the airway system's surface (Salar-Behzadi, 2014:4795-4822). These particles deposit in the upper respiratory tract (CCOHS, 2022a; Heyder, 2004:315-320). Deposition by interception occurs when a particle moves close to the wall of the airway passages, it can intercept or deposit onto the wall of the airways (CCOHS, 2022a). Elongated particles (for example fibres) with a large length-to-diameter ratio are subjected to interception (Darquenne, 2020:181-185). The particle's length influences where it will intercept. For example, a particle with a length of 200 µm and a diameter of 1 µm will intercept within the bronchial tree (CCOHS, 2022a). Electrostatic deposition occurs when particles deposit

on the walls of the airway passages due to their electrostatic charge. Electrostatic deposition contributes the least to particle deposition in the respiratory tract (Darquenne, 2020: 181–185). Sedimentation occurs when particles (> 1 µm) settle on the lung's surface (CCOHS, 2022a; Fröhlich and Salar-Behzadi, 2014:4795-4822). This happens when the particle's buoyancy is exceeded by air resistance and gravitational forces. The bronchi and bronchioles are the most prevalent sites for this sort of deposition (CCOHS, 2022a).

In an experimental study, it was found that particles that are spherical-shaped and rod-shaped resulted in less cytotoxicity compared to needle-shaped and plate-shaped particles (Zhao *et al*., 2013:87:1037-1052). Particle size should be considered because larger particles have a greater settling rate in still air than smaller particles and are less likely to be inhaled. However, in turbulent air, as is common in the foundry environment, small particles may remain suspended for days (Scholz *et al*., 2007:1-82; Wang *et al*., 2017:100-108).

2.6.2 Clearance mechanisms

Particles larger than 5 µm that enter the nose (upper respiratory tract) are cleared by blowing, wiping, or sneezing. The upper respiratory tract and tracheobronchial tree are lined by cilia and epithelial cells are protected by mucus (Fröhlich and Salar-Behzadi, 2014:4795-4822). Dust and other particles captured in mucus are transported to the pharynx, where they can be swallowed into the gastrointestinal tract (mucociliary escalator) or expectorated. To execute this role, cilia beat in synchronised metachronal waves at a fixed frequency (Bustamante-Marin and Ostrowski, 2017:1-17). Both ultrafine particles (UFP) and respirable particles (< 4 µm, 50% cut-point) can penetrate the lung's alveolar region and come into touch with the air-blood barrier (Brown *et al*., 2013:1-12; Fröhlich and Salar-Behzadi, 2014:4795-4822). The lung alveoli are not protected by cilia or mucus due to the need for gas exchange. In the alveoli of the lungs, macrophages are found. The primary function of macrophages is the detection and phagocytosis of harmful or foreign substances (Saldana, 2022). The macrophage system does not work effectively for quarts. The enzymes released by macrophages are unable to clear quarts, and as a result, macrophages are eventually destroyed, causing damage to the lung's surface and the formation of scar tissue. The area available for gas exchange reduces as more of the surface of the lung is scarred over time (Scholz *et al*., 2007:1-82).

2.7 Health effects associated with respirable crystalline silica

Silica or silicon dioxide is present as amorphous silica or as crystalline silica. Amorphous silica has a random orientation, while crystalline silica has a definite repeating pattern of silicon-oxygen tetrahedra (Technology Planning and Management Corporation, 1998:1-54). Natural amorphous silica is generally contaminated with crystalline silica, but synthetic amorphous silica is free of crystalline silica contamination. The health effects of amorphous silica are difficult to determine since it might be contaminated with crystalline silica (Merget *et al*., 2002). The toxicity of amorphous silica is lower than that of crystalline silica. However, there is a paucity of data that indicates negative health effects, especially with regard to amorphous silica UFPs. In terms of overall lung cytotoxicity, the cytotoxic events seen with respirable crystalline silica, which led to permanent fibrotic alterations, are not apparent with the amorphous silica (McLaughlin *et al*., 1997: 553-566).

The accumulation of respirable crystalline silica in the alveoli is associated with adverse health effects. The health effects are silicosis, bacterial infections (non-tuberculosis and tuberculosis), fungal infections, autoimmune diseases, chronic obstructive pulmonary disease (COPD), renal diseases, and lung cancer (NIOSH: 2002:1-145). Only silicosis, COPD, and lung cancer will be discussed in further detail because the study's focus is on respiratory health effects.

The primary concern of inhaling respirable crystalline silica is silicosis (Rosental, 2017:106). Silicosis is a lung disease first described by Hippocrates in the year 430 before Christ (BC). In 1713, Bernadino Ramazani observed silicotic nodules in post-mortems of stone cutters with respiratory symptoms. The advent of machine tools in the mining industry in the 1800s raised silica concentrations in the workplace, leading to a rise in cases and a better understanding of silicosis (Barnes *et al*., 2019:1165-1175). Workers in a wide range of industries around the world are now affected by silicosis. In the early twentieth century, South Africa became the pioneering country for silicosis in institutional, medical, and legislative aspects. Many countries throughout the world had implemented a compensation system to deal with work-related injuries by the end of the nineteenth century. Occupational diseases like silicosis were added to these systems later (Rosental, 2017:5;108;207). Respirable silica settles in the alveoli of the lungs, causing inflammation, formation of silicotic nodules, and scarring of the lung’s alveoli. As a result, the gas exchange (oxygen and carbon dioxide) between the bloodstream and the air is inhibited. Prolonged inhalation of silica particles can cause nodules to develop and grow, making breathing difficult (Scholz *et al*., 2007:1-82).

Other symptoms of silicosis may include fever, fatigue, chest pain, severe cough, and loss of appetite (Scholz *et al*., 2007:1-82). However, in the early stages of silicosis, there are no symptoms (Workplace Health and Safety Queensland, 2020:1-4). The respirable crystalline concentration, particle size, and cumulative exposure to respirable crystalline silica are the principal factors that determine the severity of silicosis (Scholz *et al*., 2007:1-82). Chronic, accelerated, and acute silicosis (silicolipoproteinosis, silicoproteinosis) are the three kinds of silicosis classified by the National Institute for Occupational Safety and Health (NIOSH) (NIOSH: 2002:1-145). The most common classification of this disease is chronic silicosis (Wisconsin Department of Health Services: 2008:1-2). After 10 years or more of low-moderate exposure, chronic silicosis develops (NIOSH: 2002:1-145). Chronic silicosis can have a wide range of symptoms, from mild to fatal (Scholz *et al*., 2007:1-82). Accelerated silicosis develops within 5 to 10 years of moderate-high level exposure (NIOSH: 2002:1-145). The symptoms of accelerated silicosis are similar to symptoms of chronic silicosis; however, they occur sooner and progress more rapidly. After a few years of onset, accelerated silicosis can result in death (Scholz *et al*., 2007:1-82). A rare classification of this disease is acute silicosis (Wisconsin Department of Health Services: 2008:1-2). This disease is caused by high concentration exposure (about 100 mg/m^3) and can develop anywhere from weeks to 5 years after the first exposure (NIOSH: 2002:1-145; Scholz *et al*., 2007:1-82). Again, the symptoms are similar to chronic silicosis; however, they occur sooner, progress more rapidly, and always result in death (Scholz *et al*., 2007:1-82). When silicotic nodules develop in organs other than the lungs (spleen, bone marrow, liver, pancreas, or bone marrow), it is referred to as systemic silicosis. These changes can be caused by respirable crystalline silica being transferred outside the respiratory system via the lymph and/or bloodstream. Other contributing factors, like immune responses, could also play a role in these changes (Slavin *et al*., 1985:393-412; Papachristou *et al*., 2006: 170-172).

Inhaling respirable crystalline silica increases the incidence of COPD (NIOSH, 2002:1-145). COPD refers to a treatable group of non-cancerous respiratory diseases, which are characterised by the narrowing of the lungs' airways, leading to airflow limitation. Chronic bronchitis and emphysema contribute to COPD. Chronic bronchitis is a condition characterised by a chronic cough sputum production caused by inflammation of the lining of the airways. Emphysema is a lung condition in which the alveoli at the end of the bronchioles are destroyed. The symptoms of COPD may include chest tightness, shortness of breath, tiredness, chronic cough, and sputum production, (WHO, 2021).

The International Agency for Research on Cancer (IARC) (2021) classified respirable crystalline silica exposure as a Group 1 confirmed human carcinogen. Crystalline silica's mechanism of carcinogenicity is not well explained in the literature (ATSDR, 2019:183). Borm *et al*. (2011:756-70) completed a review on crystalline silica's mechanism of carcinogenicity and concluded that crystalline silica's carcinogenicity is likely owed to the secondary genotoxic effect caused by silica-induced inflammation. Lung cancers such as adenocarcinoma, small-cell carcinoma, and squamous cell carcinoma may occur as a result of exposure to respirable crystalline silica (Cassidy *et al*., 2007:36-43).

2.7.1 Health effects associated with particulates not otherwise specified (PNOS)

PNOS are defined as particles that do not typically cause adverse health effects (CCOHS, 2015). However, significantly high concentrations of PNOS can impair vision, cause unpleasant deposits in nasal passages, ears, and eyes, and irritate the mucous membranes and skin (Cherrie *et al*., 2013:685-691). Furthermore, the results from three studies showed a correlation between the inhalation of PNOS and respiratory disorders and lung function impairment among foundry workers (Kayhan *et al*., 2013:1-5; Kuo *et al*., 2018:1-15; Saraei *et al*., 2018:285-290). In addition, even minor increases in PNOS concentrations can aggravate the symptoms of those with pre-existing respiratory disorders such as chronic obstructive pulmonary disease (Department of Health, 2022).

2.7.2 Health effects associated with UFPs

UFPs emitted from 3D machines are potentially harmful to human health due to their small size and large surface area (Bharti and Singh, 2017, 94:879-885). The toxicity of UFPs is significantly higher when compared to larger particles consisting of the same elements in the same ratio or proportion (Da *et al*., 2019:73-81; Cena *et al*., 2011; HEI, 2013; Kittelson, 1998:575-588; Oberdörster *et al.,* 1992:193-199; Seaton *et al.,* 1995:176-178). UFPs deposit effectively in both the alveolar and pulmonary regions of the lung (Deng *et al*., 2016:11:1-18). UFPs are retained in the lung for a longer period compared to larger particles and can efficiently move from the lungs into the bloodstream and to organs such as the brain and heart (Cena *et al*., 2011; HEI, 2013; Schraufnagel, 2020:311-317). They can translocate from the nasal regions through the olfactory neurons and into the brain tissue, causing neurodegenerative disorders (Oberdörster *et al*., 2005:823-839). UFPs can also be transported from the respiratory epithelium to the circulation system causing toxicity in the vascular endothelium, which leads to an inflammatory response

and cardiovascular diseases (Du *et al*., 2016:8-19). It is challenging to compare and interpret the health effects across UFP health studies since the definition of UFPs is not standardised (Kittelson *et al*., 2022:1-31).

2.8 Occupational exposure in AM

Adams (2016:1-84) investigated the respiratory exposure of AM operators during the casting of moulds with PBF-SLS utilising silica sand. The particle size distribution and shape analysis and scanning electron microscopy (SEM) images of the uncoated, coated and used sand were similar, indicating that the particle size did not change during PBF-SLS. The author stated that the chemical composition of respirable crystalline silica (98.6 to 100%) of uncoated, coated silica sand was very similar. Adams (2016:1-84) stated that the area concentration and the personal respiratory exposure of the AM operators to respirable crystalline silica ($\leq$ 0.06 mg/m^3) and respirable PNOS ($\leq$ 0.06 mg/m^3) did not exceed their respective South African time-weighted average occupational exposure limit - control limit (TWA-OEL-CL) (0.1 mg/m^3) and time-weighted average occupational exposure limit - recommended limit (TWA-OEL-RL) (5 mg/m^3).

Matlhatsi (2021:1-133) investigated particle emissions and respiratory exposure during the BJ printing of sand moulds. The SEM images illustrated that the coated sand contained larger particles than the uncoated and used silica sand. He stated that uncoated and used silica sand contained mainly respirable particles, while coated silica sand predominantly contained inhalable particles. The peak particle number concentrations during the pre-processing (1.43×10^1 p/cm^3 to 5.98×10^6 p/cm^3), processing phase (1.45×10^1 p/cm^3 to 7.76×10^6 p/cm^3) and post-processing phase (1.19×10^1 to 3.74×10^6 p/cm^3) for particles 0.3, 0.5, 1.0 and 0.01 to 1.0 µm in size. Matlhatsi (2021:1-133) reported statistically significant differences in the particle number concentrations among the three repetitions of the same AM phase. He stated that it is not possible to confirm if the particle emissions were mostly due to the pre-processing due to the phases being performed successively. Therefore, it is possible that particle emissions during the pre-processing phase can result in high particle number concentrations during the next phase. The author stated that the mean ERs for particles 0.3 µm and 0.01 to 1.0 µm in size were higher during the pre-processing phase (1.62×10^4 and 1.2×10^9 p/min) compared to the processing phase (1.53×10^4 and 5.27×10^8 p/min) and post-processing phase (1.13×10^4 and 7.74×10^8 p/min). Matlhatsi (2021:1-133) stated that there were no statistically significant differences between the particle AM phases. The respirable crystalline silica concentrations ($\leq$ 0.07 mg/m^3) and respirable PNOS concentrations ($\leq$ 0.266 mg/m^3) during cleaning and printing complied with the South African

TWA-OEL-CL. Matlhatsi (2021:1-133) used a provided air exchange rate (AER) to calculate particle ERs. In this study (Meiring, 2024), the AER was calculated using a carbon dioxide decay method.

Adams (2016:1-84) and Matlhatsi (2021:1-133) both determined the size, shape, and chemical composition of silica sand and assessed area concentrations and personal respiratory exposure of the AM operators to HCAs (respirable crystalline silica and respirable PNOS) during the AM process by means of time-integrated sampling. Matlhatsi (2021:1-133) quantified particle number concentrations and used a provided air exchange rate (AER) to calculate particle ERs for particles 0.01 to 1.0 µm in size during the three AM phases. Adams (2016:1-84) did not investigate particle number concentrations emitted and did not calculate ERs. In this study (Meiring, 2024), the size, shape, and chemical composition of silica sand were determined to verify the results of Adams (2016:1-84) and Matlhatsi (2021:1-133). In this study (Meiring, 2024) the AER was calculated, a window period of 24-hours was allocated between sampling and particle number concentrations, and ERs were determined for particles > 1 µm, < 1 to > 4 µm, > 4 to < 10 µm and > 10 µm in size at different locations in the AM research facility (area one and area two) and for the operator during the three AM phases. In this study (Meiring, 2024), particle number concentrations of particulate matter with aerodynamic diameters of ≤ 4 µm (real-time monitoring) versus TWA data (time-integrated sampling) were used to assess area concentrations and personal respiratory exposure of the AM operators to HCAs (respirable crystalline silica and respirable PNOS) during BJ utilising silica sand and to determine the dominant particle size fraction.

Two published studies investigated particle emissions during BJ, although, not during sand moulding. The first study by Afshar-Mohajer *et al*. (2015:293-301) used gypsum as AM feedstock material and Lewinski et al. (2019:1-7) utilised stainless-steel powder as AM feedstock material during BJ. According to Afshar-Mohajer *et al.* (2015:293-301) BJ machines utilising gypsum powder as AM feedstock material are a possible source of volatile organic compounds and fine particulate matter because of the constant movement of AM feedstock material within BJ machine chambers and injection of resin binder. According to Afshar-Mohajer *et al*. (2015: 293-301) background airborne particle number concentrations for particles 10.4 nm to 407 nm in size, ranged between 1.0×10^2 and 1.2×10^3 p/cm^3 and reached a peak of 8.0×10^1 p/cm^3 for particles 0.45 µm to 8.75 µm in size. They detected the highest particle number concentrations of 0.9 to 1.16×10^4 p/cm^3, during the printing period for particles 205 and 255 nm in size. However, from the start of printing, the particle number concentration for particles 54.3 nm in size was higher than other particle sizes and reached a steady state after 70 min (9.0×10^3 p/cm^3). They reported

the peak ER during the post-processing phase (4.4×10^4 p/min) when the BJ machine lid was opened and the unfused powder around the printed part was brushed off. Lewinski *et al*. (2019:1-7) reported a mean background airborne particle number concentration of 3.3×10^4 p/cm^3 for particles 0.3 to 10 µm in size and a mean background airborne particle number concentration of 5.9×10^3 p/cm^3 for particles 10 to 400 nm in size. They found that the mean particle number concentration was the highest during the processing phase (3.8×10^4 p/cm^3), then the pre-processing phase (3.5×10^4 p/cm^3) and post-processing phase (3.3×10^4 p/cm^3) for particles 0.3 to 10 µm in size. Lewinski *et al*. (2019:1-7) did not calculate the particle ERs.

2.8.1 Occupational exposure in sand moulding foundries

There are similarities between AM of sand moulds and sand moulding foundries. These similarities include the presence of heat, exposure to respirable crystalline silica, PNOS, and resins (Adefuye *et al*., 2020:55-63; Envirocare, 2021). PNOS are released during most casting process stages, such as when dry sands are mixed and shaken for mould production (Vu, 2020). These activities can be extrapolated to the loading of the AM machine during the pre-processing phase. According to studies performed by NIOSH, high concentrations of respirable crystalline silica are generated when sand mould castings are cleaned (NIOSH, 1998). Therefore, the concentration of crystalline silica is expected to be higher during the post-processing phase than during the pre-processing phase and processing phase of AM.

2.9 Relevant occupational exposure limits

OELs play a vital role in regulating exposure to HCA at work to protect workers' health and safety (Adkins *et al*., 2009:1-11). A country's OELs are influenced by its health and socioeconomic aspects. As a result, an OEL can differ from one country to the next (Deveau, 2015: S127-S144). Respirable crystalline silica is listed under the RHCA with a TWA-OEL-ML of 0.1 mg/m^3, while international organisations such as the NIOSH, the American Conference of Governmental Industrial Hygienists (ACGIH), and the Occupational Safety and Health Administration (OSHA) list it with a TWA-OELs of 0.05 mg/m^3, 0.025 mg/m^3 and 0.05 mg/m^3 respectively (CCOHS, 2022b; DoEL, 2021:1-98; NIOSH, 2014; OSHA, 2022). Respirable PNOS have an OEL-RL of 5 mg/m^3 under the RHCA, and international organisations such as the NIOSH, the ACGIH, and the OSHA have TWA-OELs of 5 mg/m^3, 3 mg/m^3, and 5 mg/m^3 respectively (CCOHS, 2018; DoEL, 2021:1-98; NIOSH, 2019).

2.10 Conclusion

The application of AM technologies in various industries is constantly increasing. However, the occupational hazards associated with all AM processes are still not well-understood for all AM process categories, including the BJ of sand moulds. According to Stefaniak *et al*. (2021:1-51) there is a total of forty-six publications related to particle emissions and exposure for all AM process categories; but only two of the studies (Afshar-Mohajer *et al*., 2015:293-301 and Lewinski *et al*., 2019:1-7) applied to BJ. Publications on foundry sand are available, however, the only study that uses silica sand during BJ is unpublished (mini-dissertations) (Matlhatsi, 2016:1-84).

2.11 References

Abe, F., Osakada, K., Shiomi, M., Uematsu, K. & Matsumoto, M. 2001. The Manufacturing of Hard Tools from Metallic Powders by Selective Laser Melting. *Journal of Materials Processing Technology*, 111(1-3):210-213.

Adams, G.E.M. 2016. *Respiratory exposure during the additive manufacturing of sand casting moulds*. Potchefstroom: North-West University (Dissertation – Masters).

Adefuye, O. A., Raji, N.A., Adedeji, K.A., Fadipe, O.L. & Olowu, B. 2020. Additive manufacturing and sand casting foundries practices in Nigeria. *Engineering & Technology Research Journal*, 4(1):55-63.

Adkins, C., Booher, L., Culver, D., *et al*. 2009. Occupational Exposure Limits - Do they have a future? Microsoft Word - MASTER OEL Green Paper 09.18.09.doc (cdc.gov) Date of access: 15 Mar. 2022.

Afshar-Mohajer, N., Wu, C. Y., Ladun, T., Rajon, D. A. & Huang. Y. 2015. Characterization of particulate matters and total VOC emissions from a binder jetting 3D printer. *Building and Environment*, 93:293-301.

Ahmed, A. 2013. Geological Overview of White silica Sands. https://www.researchgate.net/publication/282354067_Geological_Overview_of_White_silica_Sands Date of access: 14 Mar. 2022.

American Society for Testing and Materials (ASTM) F2792. 2013. Standard terminology for additive manufacturing technologies.

Anderson, I.E., White, E.M. & Dehoff, R. 2018. Feedstock powder processing research needs for additive manufacturing development. *Current Opinion in Solid State and Materials Science*, 22(1), 8-15.

Bakhiya, N. & Appel, K.E. 2010. Toxicity and carcinogenicity of furan in human diet. *Archives of Toxicology*, 2010:84:563-578.

Barnes, H., Goh, N.S.L., Leong, T.I. & Hoy, R. 2019. Silica-associated lung disease: An old-world exposure in modern industries. *Respirology*, 24:1165-1175.

Bharti, N. & Singh, S. 2017. Three-dimensional (3D) printers in libraries: perspective and preliminary safety analysis. *Journal of Chemical Education*, 94:879-885.

Biringucci, B. *De la Pirotechnia.* Available from Science History Institute Museum and Library e-books: https://digital.sciencehistory.org/works/n888ils Date of access: 10 Feb. 2024.

Birmingham, B.R., Tompkins, J.V., Zong, G. & Marcus, H.L. 1992. *Development of a Selective Laser Reaction Sintering Workstation.* Available from the University of Texas Libraries: Development of a Selective Laser Reaction Sintering Workstation (utexas.edu) Date of access: 27 Feb. 2022.

Blakey-Milner, B., Gradl, P., Snedden, G., Brooks, M., Pitot, J., Lopez, E., Leary, M., Berto. F.& Plessis, A. Metal additive manufacturing in aerospace: A review *Materials &Design*, 209(1)'1-133.

Borm, P.J.A., Tran, L. & Donaldson, K. 2011. The carcinogenic action of crystalline silica: a review of the evidence supporting secondary inflammation-driven genotoxicity as a principal mechanism. *Critical Reviews in Toxicology*, 41(9):756-70.

Brown, J.S., Gordon, T., Price, O. & Asgharian, B. 2013. Thoracic and respirable particle definitions for human health risk assessment. *Particle and Fibre Toxicology*, 10(12):1-12.

Bustamante-Marin, X.M. & Ostrowski, L.E. 2017. Cilia and Mucociliary Clearance. *Cold Spring Harbor Perspectives in Biology*, 9(4):1-17.

Canadian Centre for Occupational Health and Safety (CCOHS). 2015. *WHMIS 2015 - Glossary – N-Z* WHMIS 2015 - Glossary - N-Z: OSH Answers (ccohs.ca) Date of access: 4 Mar. 2022.

Canadian Centre for Occupational Health and Safety (CCOHS). 2018. *Flavorings-Related Lung Disease: Occupational Exposure Limits* Flavorings-Related Lung Disease: Occupational Exposure Limits | NIOSH | CDC Date of access: 15 Mar. 2022.

Canadian Centre for Occupational Health and Safety (CCOHS). 2022a. *How Do Particulates Enter the Respiratory* System? How Do Particulates Enter the Respiratory System?: OSH Answers (ccohs.ca) Date of access: 12 Mar. 2022.

Canadian Centre for Occupational Health and Safety (CCOHS). 2022b. *Silica, quartz*. Silica, quartz: OSH Answers (ccohs.ca)

Carey, P.R. J. 2012. *Sand binder systems*. https://www.ask.chemicals.com/fileadmin/user_upload/Download_page/professional_articles/EN/FMT_Article_part1.pdf Date of access: 15 Mar. 2022.

Carey, P.R. & Lott, M. 2022. *Sand Binder Systems*. FMT_Article_part5.pdf (ask-chemicals.com) Date of access: 2 Feb. 2022.

Casalino, G., De Filippis, L.A.C., Ludovico, A.D. & Tricarico, L. 2002. An Investigation of Rapid Prototyping of Sand Casting Molds by Selective Laser Sintering. *Journal of Laser Applications*, 14(2):100-106.

Cassidy, A., Mannetje, A., van Tongeren, M., Field, J. K., Zaridze, D., Szeszenia-Dabrowska, N., Rudnai, P., Lissowska, J., Fabianova, E., Mates, D., Bencko, V., Foretova, L., Janout, V., Fevotte, J., Fletcher, T., Brennan, P. & Boffetta, P. 2007. Occupational Exposure to Crystalline Silica and Risk of Lung Cancer: A Multicenter Case-Control Study in Europe. *Epidemiology*, 18(1), 36-43.

Cena, L.G., Anthony, T.R. & Peters, T.M. 2011. A personal nanoparticle respiratory deposition (NRD) sampler. *Environmental Science & Technology*, 45:6483-6490.

Chua, C.K. & Leong, K.F. 2017. *3D printing and additive manufacturing principles and applications technologies.* 5th ed. USA: World Scientific.

Cherrie, J.W., Brosseau, L.M., Hay, A. & Donaldson, K. 2013. Low-toxicity dusts: current exposure guidelines are not sufficiently protective. The *Annals of Occupational Hygiene*, 57(6):685-691.

China Investment Casting Manufacturer. 2015. *The history of sand casting*. https://www.simiscasting.com/the-history-of-sand-casting-171.html Date of access: 12 May 2022.

Cozmei, C. & Caloian, F. 2012. Additive manufacturing flickering at the beginning of existence. *Procedia Economics and Finance*, 3 (1):57-462.

Darquenne, C. 2020. Deposition Mechanisms. *Journal of aerosol medicine and pulmonary drug delivery*, 33(4):181-185.

Deng, Y., Cao, S., Chen, A. & Guo, Y. 2016. The impact of manufacturing parameters on submicron particle emissions from a desktop 3D printer in the perspective of emission reduction. *Building and Environment*, 11:1-18.

Department of Health. 2022. Health effects of dust Health effects of dust (healthywa.wa.gov.au)

Department of Labour. 2005. *National programme for the elimination of silicosis*. National Silicosis (ilo.org) Date of access: 4 Mar. 2022.

Deveau, M., Chen, C.P., Johanson, G., Krewski, D., Maier, A., Niven, K. J., Ripple., Schulte, P. A., Silk, J., Urbanus, J. H., Zalk, D. M. & Niemeier, R. W. 2015. The Global Landscape of Occupational Exposure Limits – Implementation of Harmonization Principles to Guide Limit Selection. *Journal of Occupational and Environmental Hygiene*, 12: S127-S144.

Du, Y., Xu, X., Chu, M., Guo, Y. & Wang, J. 2016. Air particulate matter and cardiovascular disease: the epidemiological, biomedical and clinical evidence. *Journal of Thoracic Disease*, 8(1):8-19.

Eggers, J. & Villermaux, E. 2008. Physics of liquid jets. *Reports on progress in physics*, 71(3):1-79.

Envirocare. 2021. *Foundry health risks*. Foundry Health Risks & Hazards | Envirocare Date of access: 15 Mar. 2022.

ExOne. 2016. *A Case Study in Optimizing Casting Design Using 3D Printing,* http://www.afsinc.org/multimedia/MCTVDetail.cfm?ItemNumber=19145 Date of access: 15 May 2022.

ExOne. 2020. *S-Max*. https://www.exone.com/en-US/3d-printing-materials-and-binders/sand Date of access: 2 Feb. 2022.

Fröhlich, E. & Salar-Behzadi, S. 2014. Toxicological assessment of inhaled nanoparticles: role of in vivo, ex vivo, in vitro, and in silico studies. *International Journal of Molecular Sciences,* 15:4795-4822.

Gebhardt, A. & Hötter, J.S. 2016. *Additive Manufacturing: 3D Printing for Prototyping and Manufacturing, Carl Hanser Verlag*. ISBN 9783446452367.

Geraets, L., Bessems, J.G.M., Zeilmaker, M.J. & Bos, P.M.J. 2014. Human risk assessment of dermal and inhalation exposures to chemicals assessed by route-to-route extrapolation: The necessity of kinetic data. *Regulatory Toxicology and Pharmacology*, 70(1):54-64.

Gibson, I., Rosen, I.D.W., Stucker, B. & Khorasani, M. 2021. *Additive manufacturing technologies: rapid prototyping to direct digital manufacturing*. 3rd ed. Cham, Switzerland: Springer.

Gueche, Y.A., Sanchez-Ballester N.M., Cailleaux, S., Bataille, B. & Soulairol, I. 2021. Selective Laser Sintering (SLS), a New Chapter in the Production of Solid Oral Forms (SOFs) by 3D Printing. *Pharmaceutics*, 13(8):1-26.

Hall J.E. & Guyton, A.C. 2016. *Guyton and Hall Textbook of Medical Physiology.* 13th ed. Philadelphia, Pennsylvania: Elsevier.

Hackney P.M. & Wooldridge R. 2017a. Characterisation of the direct 3D sand printing process for the production of sand cast mould tools. *Rapid Prototyping Journal*, 23(1):7-15.

Hackney, P. & Wooldridge, R. 2017b. Optimisation of Additive Manufactured Sand Printed Mould Material for Aluminium Castings. *Procedia Manufacturing*, 11:457-465.

Hawaldar, N. & Zhang, J. 2018. A comparative study of fabrication of sand casting mold using additive manufacturing and conventional process. The I*nternational Journal of Advanced Manufacturing Technology*, 97:1037-1045.

Health Effects Institute (HEI). 2013. Understanding the health effects of ambient ultrafine particles. https://www.healtheffects.org/publication/understanding-health-effects-ambient-ultrafine-particles Date of access: 3 June 2022.

Heyder, J. 2004. Deposition of inhaled particles in the human respiratory tract and consequences for regional targeting in respiratory drug delivery. *Proceedings of the American Thoracic Society*, 1(4):315-320.

Holtzer, M., Kubecki, M., Dańko, R. & Żymankowska-Kumon, S. 2013. *Research on the influence of moulding sand with furan resin on the environment.* (PDF) Research on the Influence of Moulding Sand with Furan Resin on the Environment (researchgate.net) Date of access: 14 Feb. 2022.

Hu, C. & Du, W. 2018. Research on the method for improving mechanical properties of sand mold based on 3D printing process. *Institute of Physics Conference Series: Materials Science and Engineering*, 394(3):1-7.

Institution of Occupational Safety and Health (IOSH). 2018. *Respirable crystalline silica: the facts 2018.* Factsheet_Respirable_crystalline_silica_the_facts_MKT2730.pdf (notimetolose.org.uk) Date of access: 4 Mar. 2022.

International Agency for Research on Cancer (IARC). 2021*. Agents classified by the IARC monographs, volumes 1-129*. Agents Classified by IARC Monographs, Volume 1-29 - Search (bing.com) pdf Date of access: 4 Mar. 2022.

International Organization for Standardizations/American Society of Testing Materials (ISO/ASTM): Additive Manufacturing - General principles – Fundamentals and Vocabulary (ISO/ASTM 52900) [Standard] Geneva, Switzerland: ISO/ASTM, 2021.

Kayhan, S., Tutar, U., Cinarka, H., Gumus, A., Koksal, N. 2013. Prevalence of occupational asthma and respiratory symptoms in foundry workers. Pulmonary Medicine, 2013:1-5.

Kittelson, D.B. 1998. Engines and nanoparticles: a review. *Journal of Aerosol Science*, 29(56): 575-588.

Kittelson, D., Khalek, I., McDonald, J., Stevens, J., Giannelli, R. 2022. Particle emissions from mobile sources: Discussion of ultrafine particle emissions and definition. *Journal of Aerosol Science*, 159:1-31.

Klaassen, C.D & Watkins III, J.B. 2015. *Casarett & Doull's Essentials of Toxicology*. 3rd ed. New York, NY: McGraw-Hill Education.

Kruth, J.P., Wang, X., Laoui, T. & Froyen, L. 2003. Lasers and materials in selective laser sintering. *Assembly Automation*, 23(4):357-371.

Kuo, C.T., Chiu, F.F., Bao, B.Y. & Chang, T.Y. 2018. Determination and prediction of respirable dust and crystalline-free silica in the Taiwanese foundry industry. *International Journal of Environmental Research and Public Health*, 15(10):1-15.

Le Néel T.A., Mognol, P., Hascoet, J.Y. 2018. A review on additive manufacturing of sand moulds by binder jetting and selective laser sintering. *Rapid Prototyping Journal*, 24(8):1325-1336.

Lewinski, N.A., Seconda, L.E & Ferri, J.K. 2019. On-site three-dimensional printer aerosol hazard assessment: pilot study of a portable in vitro exposure cassette. *Process Safety Progress*, 38(3):1-7.

Lu, K., Hiser, M., Wu, W. 2009. Effect of particle size on three-dimensional printed mesh structures. *Powder Technology*, 192(2):178-183.

Lucas F.M. da Silva. 2017. *Materials Design and Applications.* Available from Springer: https://link.springer.com/book/10.1007/978-3-319-50784-2 Date of access: 14 Feb. 2022.

Maccurdy, E. *The Notebooks of Leonardo da Vinci.* Available from Internet Archive e-books: https://archive.org/details/noteboo00leon/page/n7/mode/2up Date of access: 11 Feb. 2024.

Matlhatsi, N.L. 2021. *Particulate emissions and respiratory exposure to hazardous chemical substances during additive manufacturing of sand moulds.* Potchefstroom: North-West University. (Masters – Dissertation).

McLaughlin, J.K., Chow, W. & Levy, L.S. 1997. Amorphous silica: A review of health effects from inhalation exposure with particular reference to cancer. *Journal of Toxicology and Environmental Health*, 50(6):553-566.

Merget, R., Bauer, T., Küpper, H., Philippou, S., Bauer, H.D., Breitstadt, R. & Bruening, T. 2002. Health hazards due to the inhalation of amorphous silica. *Archives of Toxicology*, 75:625-634.

Micrometrics. 2017. *Additive Manufacturing Characterization of powder-bed based manufacturing* https://www.micromeritics.com/Repository/Files/additive-manufacturing_brochure_2016_v2.pdf Date of access: 15 Mar. 2022.

Mostafaei., A., Elliott, A.M., Barnes, J.E., Li, F., Tan, W., Cramer, C.L., Nandwana, P. & Chmielus, M. 2021. Binder jet 3D printing – Process parameters, materials, properties, modelling, and challenges. *Progress in Materials Science*, 119:1-138.

Nandwana, P., Elliott, A.M., Siddel, D., Merriman, A., Peter, W.H. & Babu, S.S. 2017. Powder bed binder jet 3D printing of Inconel 718: Densification, microstructural evolution, and challenges. *Current Opinion in Solid State and Materials Science*, 21(4):207-218.

National Institute for Occupational Safety and Health (NIOSH). 1998. *Controlling Silica Dust from Foundry Casting-Cleaning Operation* Controlling Silica Dust from Foundry Casting-Cleaning Operations | NIOSH | CDC Date of access: 15 Mar. 2022.

National Institute for Occupational Safety and Health (NIOSH). 2002. *Health effects of occupational exposure to respirable crystalline silica.* Silica_prelim 1-17-02. vp (cdc.gov) Date of access: 4 Mar. 2022.

National Institute for Occupational Safety and Health (NIOSH). 2014. *Preventing Silicosis and Deaths in Construction Workers*. Preventing Silicosis & Deaths in Construction Workers | NIOSH | CDC Date of access: 12 Mar. 2022.

National Institute for Occupational Safety and Health (NIOSH). 2019. *Particulates not otherwise regulated* CDC - NIOSH Pocket Guide to Chemical Hazards - Particulates not otherwise regulated Date of access: 14 Mar. 2022.

Nyembwe, K., Motadi, M. & Gonya, E.M. 2005. Descriptive statistical analysis of foundry properties of sand parts produced by three dimensional printing. https://ujcontent.uj.ac.za/vital/access/services/Download/uj:31586/SOURCE1?view=true Date of access: 29 Apr. 2022.

Nyembwe, k., Oyombo, D., de Beer, D.J. van Tonder, & P.J.M. 2016. Suitability of a South African silica sand for three-dimensional printing of foundry moulds and cores. *South African Journal of Industrial Engineering*, 27(3): 230-237.

Oberdörster, G., Ferin, J., Gelein, l.R., Soderholm, S.C. & Finkelstein, J. 1992 Role of the Alveolar Macrophage in Lung Injury: Studies with Ultrafine Particles. *Environmental Health Perspectives*, 97:193-199.

Oberdörster, G., Oberdörster, E. & Oberdörster, J. 2005. Nanotoxicology: an emerging discipline evolving from studies of ultrafine particles. *Environmental Health Perspectives*, 113(7): 823-839.

Occupational Safety and Health Administration (OSHA). 2022. *Respirable crystalline silica*. 1910.1053 - Respirable crystalline silica. Occupational Safety and Health Administration (osha.gov) Date of access: 16 Mar. 2022.

Pandey, L.N. 2015. Sand casting – a basic review. *International Journal of Innovative Research in Technology*, 2(7):477-483.

Papachristou, G.I., Papachristou, D.J., Schoedel, K., McGrath, K. & Slivka A. 2006. Systemic silicosis that involves the pancreas. *Gastrointestinal Endoscopy*, 63(1):170-172.

Rosenman, K.D., Mary J.R., Rice, C., Hertzberg, V., Tseng, C. & Anderson, H.A. 1996. Silicosis among foundry workers: Implication for the need to revise the OSHA. *Standard American Journal of Epidemiology*, 144(9):1-12.

Rosental, P. 2017. *Silicosis: a world history.* 1st USA: John Hopkins University Press.

Scheckman, J. H. & McMurry, P. H. 2011. Deposition of silica agglomerates in a cast of human lung airways: Enhancement relative to spheres of equal mobility and aerodynamic diameter. *Journal of Aerosol Science*, 42(8), 508-516.

Sachs, E.M, Haggerty, J.S. & Williams P.A. 1993. *Three-dimensional printing techniques*. (Patient: US Patent 5204055). https://patentimages.storage.googleapis.com/9e/92/4c/16485de942a672/US5204055.pdf Date of access: 28 Apr. 2022.

Sahoo, P.K., Sarojrani, S. & Sutar, M. 2019. A State-of-the-Art Review on Manufacturing and Additive Influences on Sand-Cast Components. *Arabian Journal for Science and Engineering*, 44(3):9805-9835.

Saldana, J.I. 2022. *Macrophages*. Macrophages | British Society for Immunology Date of access: 9 Mar. 2022.

Saraei, M., Masaoudi, H., Aminian, O. & Izadi, N. 2018. Respiratory health and cross-shift changes of foundry workers in Iran. *Tanaffos*, 17(4): 285-290.

Savarkar, S.G. & Yewale, S.N. 2019. Additive Manufacturing in Automobile Industry. *International journal of research in aeronautical and mechanical engineering,* 7(4):1-10.

Sivarupan, T., Balasubramani, N., Saxena, P., Nagarajan, D., Mansori, M.E.I., Salonitis, K., Jolly, M., Dargusch, M.S. 2021. A review on the progress and challenges of binder jet 3D printing of sand moulds for advanced casting. *Additive Manufacturing,* 40:1-17.

Scholz, R.C., Slavin, T.J. & Rowntree, K. 2007. *Control of silica exposure in foundries*. https://afsinc.s3.amazonaws.com/Documents/EHS/silica_book_no%20copyright.pdf Date of access: 26 Apr. 2022.

Schraunfnagel, D.E. 2020. The health effects of ultrafine particles. *Experimental & Molecular Medicine*, 52:311-317.

Seaton, A., Godden, D., MacNee, W. & Donaldson, K. 1995. Particulate air pollution and acute health effects. *The Lancet*, 345(8943):176-178.

Sen, K., Mehta, T., Sansare, S., Sharifi, L., Ma, A.W.K. & Chaudhuri, B. 2021. Pharmaceutical applications of powder-based binder jet 3D printing process – A review. *Advanced Drug Delivery Reviews*, 177.

Shah, M., Patel, D.R. & Pande, S. 2021. Additive manufacturing integrated Casting - A review. *Materials Today: Proceedings*, 1:1-5.

Shi, Y., Zhang, J., Wen., S., Song, B., Yan, C., Wei, Q., Wu, J., Yin, Y., Zhou, J., Chen, R., Zhou, W., Jia, H., Yang, H. & Nan, H. 2021. Additive manufacturing and foundry innovation. *Special Review*, 18(4):286-295.

Sivarupan, T., Balasubramani, N., Saxena, P., Nagarajan, D., Mansori, M.E., Salonitis, K., Jolly, M. & Dargusch, M.S. 2021. A review on the progress and challenges of binder jet 3D printing of sand moulds for advanced casting. *Additive Manufacturing*, 40:1-17.

Slavin, R.E., Swedo, J.L., Brandes, D., Gonzales Vitale, J.C. & Osornio Vargas, A. 1985. Extrapulmonary silicosis: A clinical, morphologic and ultrastructural study. *Human Pathology*, 16(4):393-412.

Snelling, D., Williams, C.B. & Druschitz, A.P. 2014. *A comparison of binder burnout and mechanical characteristics of printed and chemically bonded sand molds.* 2013-66-Snelling.pdf (utexas.edu) Date of access: 2 Feb. 2022.

Stefanescu, D.M. 2017. *Cast Iron Science and Technology*. 1st ed. Ohio: ASM International.

Stefaniak, A.B., Johnson, A.R., Du Preez, S., Hammond, D.R., Wells, J.R., Ham, J.E., LeBouf, R.F., Martin Jr, S.B., Duling, M.G., Bowers, L.N., Knepp, A.K., De Beer, D.J. & Du Plessis J.L. 2019a. Insights into Emissions and Exposures from Use of Industrial-Scale Additive Manufacturing Machines *Safety and Health at Work*, 10(2):229-236.

Stefaniak, A.B., Du Preez, S. & Du Plessis, J.L. 2021b. Additive Manufacturing for Occupational Hygiene: A comprehensive review of processes, emissions, & exposures. *Journal of Toxicology and Environmental Health, Part B*, 24(5):173-222.

Sun, C. and Shang, G. 2021. On application of metal Additive manufacturing. *World Journal of Engineering and Technology*, 9(1):194.

Svidró, J., Svidró, J.T. & Diószegi, A. 2020. The role of purity level in foundry silica sand on its thermal properties. *Journal of physics*, 1527:1-7.

Technology Planning and Management Corporation. 1998. *Report on carcinogens background document for silica, crystalline (respirable size).* RoC Background Document: Silica, Crystalline (Respirable Size); Dec. 2-3, 1998 (nih.gov) Date of access: 4 Mar. 2022.

Tsuda, A., Henry, F.S., Butler, J.P. 2013. Particle transport and deposition: basic physics of particle kinetics. Comprehensive Physiology, 3(4):1437-1471.

Upadhyay, M., Sivarupan., T. & El Mansori, M. 2017. 3D printing for rapid sand casting - A review. *Journal of Manufacturing Processes,* 29:211-220.

Utela, B., Stortia, D., Anderson, R. & Ganter, M. 2008. A review of process development steps for new material systems in three dimensional printing (3DP). *Journal of Manufacturing Processes*, 10(2):96-104.

Voxeljet. 2014a. Safety data sheet. Voxeljet – Binder VX-2C Type B. voxeljet - Binder VX-2C Type B_GB.pdf Date of access: 22 Mar. 2022.

Voxeljet. 2014b. Safety data sheet. Voxeljet – premixed quartz-sand type GS14/GS19. voxeljet - Premixed Quartz-Sand Type GS14, GS19_GB.pdf Date of access: 22 Mar. 2022.

Voxeljet. 2020. *Material data sheet Voxeljet 3D printers*. 2020-06-18_frs_material data sheet 3D printer. (voxeljet.de) Date of access: 8 Feb. 2022.

Vu, D.T. 2020. *Foundry safety precaution in casting workshop.* Foundry safety & foundry health hazards in metal casting workshop (vietnamcastiron.com) Date of access: 15 Mar. 2022.

Wang, Y., Chen, L., Chen, R., Tian, G., Li, D., Chen, C., Ge, X. & Ge, G. 2017. Effect of relative humidity on the deposition and coagulation of aerosolized SiO2 nanoparticles. *Atmospheric Research*, 194(1):100-108.

Wei, X., Moghadasi, M., Du, W., Ma, C. & Pei, Z. Experimental investigation on ultrasonic hopper dispensing system in powder bed additive manufacturing. *Journal of Manufacturing Processes*, 71: 106-112,

Wijesuriya, K.H.K.G. 2015. Newton's First Law of motion is not real. *Journal of advances in physics*, 10(2):2723-2732.

Wisconsin Department of Health Services. 2018. *Environmental and occupational disease case reporting and investigation protocol.* https://www.dhs.wisconsin.gov/publications/p02190.pdf Date of access: 26 Apr. 2022.

World Health Organization (WHO). 2021. *Chronic obstructive pulmonary disease (COPD).* https://www.who.int/news-room/fact-sheets/detail/chronic-obstructive-pulmonary-disease-(COPD) Date of access: 28 Apr. 2022.

Workplace Health and Safety Queensland. 2020 *Silica and the lung.* https://www.worksafe.qld.gov.au/__data/assets/pdf_file/0021/17238/silica-lung-factsheet.pdf Date of access: 27 Apr. 2022.

Xuhai, Z., Bruijnaers, B.J., Lourençon, T. & Balakshin, M. 2022. Structural Analysis of Lignin-Based Furan Resins. *Materials*, 15(1):1-15.

Yakout, M., Cadamuro, A., Elbestawi, M.A., & Veldhuis, S.C. 2017. The selection of process parameters in additive manufacturing for aerospace alloys. *International Journal of Advanced Manufacturing Technology*, 92:2081-2098.

Yang, S., Tang, Y. & Zhao, Y. F. 2015. A new part consolidation method to embrace the design freedom of additive manufacturing. *Journal of Manufacturing Processes*. 20(3):444-449.

Yeh, H.C., Phalen, R.F. & Raabe. 1976. *Factors Influencing the Deposition of Inhaled Particles Environmental Health Perspectives*, 15:147-156.

Zhang, J. & Jung, Y. 2018. *Additive manufacturing: materials, processes, quantifications and applications*. 1st ed. UK: Butterworth-Heinemann.

Zhao, X., Ng, S., Heng, B.C., Guo, J., Ma, L., Tan, T.T.Y., Ng, K.W. & Loo, S.C.J. 2013. Cytotoxicity of hydroxyapatite nanoparticles is shape and cell-dependent. *Archives of Toxicology*, 87:1037-1052.

Zhou, Z., Buchanan, F., Mitchell, C. & Dunne, N. 2014. Printability of calcium phosphate: Calcium sulfate powders for the application of tissue-engineered bone scaffolds using the 3D printing technique. *Materials Science and Engineering*, 38(1):1-10.

Ziaeea, M. & Craneb, N.B. 2019. Binder jetting: A review of process, materials, and methods. *Additive Manufacturing*, 28:781-801.

CHAPTER 3 ARTICLE

Introductions to authors

The format of this article follows the guidelines set forth by the *Annals of Work Exposure and Health*.

Note to reader: The length of this manuscript submitted as part of this dissertation for examination exceeds 5000 words. This was done to convey some aspects more comprehensively (such as the Methods and Discussion sections). The manuscript will however be shortened prior to submission to the journal.

Annals of Work Exposures and Health

Annals of Work Exposures and Health publishes original research and development material that helps reduce the risk of ill health resulting from work and welcomes submissions in these areas.

Submitted material must be original, and not under consideration elsewhere. If the findings have been published elsewhere in part, or if the submission is part of a closely related series, this must be clearly stated in the letter accompanying the manuscript, and the submitted manuscript must be accompanied by a copy of the other publications.

Language: Manuscripts must be in English and authors should try to write in a way that is simple and clear. British or American styles and spelling may be used but should be used consistently, and words or phrases that might be unclear in other parts of the world should be avoided or clearly explained. It is the author's responsibility to provide a text in good English, and authors whose first language is not English should seek help from a native speaker or competent translator. If English is not your first language, you may wish to have your manuscript edited for language before submission.

Brevity: The necessary length of a paper depends on the subject, but any submission must be as brief as possible and consistent with clarity. The number of words, excluding the abstract, references, tables, and figures, must be stated as a message to the Editor at the time of submission. If this length is more than 5000 words, a statement must be included justifying the extra length. Suitable extra material can be included as supplementary material.

Title, abstract, and keywords: Titles should be constructed to succinctly describe the major issue or question examined by the paper and should not assert the research findings as truth. Recognisable, searchable terms and keywords must be included to enable readers to find your paper more. To optimise the visibility of your paper we advise you to make a list of the 10 most likely search terms that your intended readers will use to find your work and to ensure that these appear in your title, the abstract, and the keywords. The 'number one search term from your list should appear somewhere in the paper's title. The 'top 5' search terms (including 'number one') should each appear at least once in the abstract, with the 'top 3' appearing more than once if possible. Your abstract must be written in a naturalistic and engaging style that will encourage readers to follow up by reading the full paper. The 'bottom 5' search terms can then be added as keywords.

Authorship: Persons should only be named as authors if they have made substantial contributions to the conception or design of the work, or the acquisition, analysis, or interpretation of data for the work AND have assisted with the drafting or revising of the paper for important intellectual content AND have final approval of the version to be published and can take responsibility for the accuracy of the work. Other contributions may be recognised by acknowledgment at the end of the submission. All names and affiliations of authors should be clearly stated at the beginning of the paper.

Structure of the paper: Papers should generally conform to the pattern: Introduction, Methods, Results, Discussion, and Conclusions, unless these are inappropriate. A paper must be prefaced with an abstract of the argument and findings, which may also be arranged under the same headings. As with many other journals, we are unable to publish footnotes to the text. Please incorporate this sort of material into the body of the paper, in brackets if appropriate.

Design and analysis: The quality of the data and analysis must always be good enough to justify the inferences and conclusions drawn. Particular attention should be given to the design of sampling surveys, which should be planned using modern statistical principles, and to the treatment of results below the limit of detection.

Units and symbols: SI units must be used, though their equivalent in other systems may be given as well.

Figures: These include photographs, diagrams, and charts. The first submission should include good-quality low-resolution copies of Figures and may be incorporated into the text or at the end of the manuscript.

Tables: Tables should be numbered consecutively and given a suitable caption. As with Figures, it is helpful to incorporate them into the text of the first submission, but in the revised version each table should be presented on a separate page. Footnotes to tables should be provided below the table and should be referred to by superscript lowercase letters.

References: References should only be included which are essential to the development of an argument or hypothesis, or which describe methods for which the original account is too long to be reproduced. References in the text should be in the form of Jones (1995), Jones and Brown (1995), or Jones et al. (1995) if there are more than two authors, and they should be incorporated naturally into the text.

Example:

Jones and Brown (1995) and Hospath et al (2006) observed total breakdown of control, or Total breakdown of control has sometimes been observed (Jones and Brown, 1995; Hospath et al., 2006).

Papers whose references are not properly arranged may be returned for revision without review. At the end of the paper, references should be listed in alphabetical order by name of the first author, using the Harvard Style of abbreviation and punctuation. ISBNs should be given for books and other publications where appropriate. Material unobtainable by readers should not be cited. Personal Communications, if essential, should be cited in the text (e.g., Professor O.H. Poobah, Institute for Dusty Sciences). Internet material can be referred to if it is likely to be permanently available; the date on which it was last accessed should be given. References will not be checked editorially, and their accuracy is the responsibility of the authors.

Examples:

Simpson AT, Groves JA, Unwin J, Piney M. (2000) Mineral oil metal working fluids (MWFs) — Development of practical criteria for mist sampling. Ann Occup Hyg; 44: 165–72.

Vincent JH. (1989) Aerosol sampling: science and practice. Chichester, UK: John Wiley. ISBN 0 471 92175 0.

Swift DL, Cheng Y-S, Su Y-F, Yeh H-C. (1994) Ultrafine aerosol deposition in the human nasal and oral passages. In Dodgson J, McCallum RI, editors. Inhaled Particles VII. Oxford: Elsevier Science. p. 77–81. ISBN 0 08 040841 9 H.

British Standards Institution. (1986). BS 6691: 1986. Fume from welding and allied processes. Part 1. Guide to methods for the sampling and analysis of particulate matter. London: British Standards Institution.

Morse SS. (1995) Factors in the emergence of infectious diseases. Emerg Infect Dis [serial online] 1995 Jan–Mar;1(1). Available from: URL: http://www.cdc.gov/ncidod/ EID/eid.htm (accessed 25 Oct 2010).

Particle emissions and exposure to hazardous chemical agents during binder jetting utilising a silica sand

L MEIRING, S DU PREEZ, JL DU PLESSIS

Occupational Hygiene and Health Research Initiative (OHHRI), North-West University, Potchefstroom Campus, South Africa

Corresponding author:

Dr Sonette du Preez

Occupational Hygiene and Health Research Initiative (OHHRI)

North-West University

Potchefstroom Campus

Private Bag X6001

Potchefstroom

2520

South Africa

Tel: +27 (0)18 285 2689

Fax: +27 (0)18 299 1053

Email: dupreezsonette@nwu.ac.za

Word count: 7133 (excluding the abstract, figures, tables, and references)

Note to the reader: The length of this manuscript submitted as part of this dissertation for examination exceeds 5000 words. This was done to convey some aspects more comprehensively for examination purposes (such as the Methods and Discussion sections). The manuscript will however be shortened prior to submission to the specified journal.

Keywords: Particle emission rates; area monitoring; personal exposure monitoring; additive manufacturing, particle shape; particle size; respirable crystalline silica.

Abstract

Background: Studies on human health risks and exposure associated with additive manufacturing (AM) of sand moulds in real-world workplaces remains limited. An AM operator might be exposed to particle emissions and hazardous chemical agents (HCAs), namely respirable crystalline silica, and respirable particulates not otherwise specified (PNOS) during the pre-processing, processing, and post-processing activities when using silica sand during binder jetting (BJ). More research is needed regarding particle emissions, area concentrations and respiratory exposure of AM operators to respirable crystalline silica and respirable PNOS during BJ utilising silica.

Aims: (i) Firstly to determine the powder characteristics and chemical composition of uncoated, coated, and used silica sand; (ii) secondly, to quantify particle number concentrations and particle emission rates released during the different phases of the AM process; (iii) finally to assess area concentrations and personal respiratory exposure of AM operators to respirable crystalline silica and respirable PNOS during BJ.

Methodology: Particle size distribution (PSD) and shape analysis, as well as scanning electron microscopy (SEM) was performed to determine the physical characteristics of the uncoated, coated, and used silica sand powder, while wavelength dispersive X-ray fluorescence (WD-XRF) was utilised to determine chemical composition of all three powders. Direct-reading instruments were used to quantify particle number concentrations and emission rates of particles released during the AM phases. Area monitoring and personal exposure monitoring using time-integrated sampling and real-time monitoring were conducted during the operator's full shift to determine area concentrations and personal respiratory exposure to respirable crystalline silica and respirable PNOS.

Results: The PSD and SEM results could not be compared to the safety data sheet (SDS) since the physical characteristics (particle size distribution and shape) of silica sand were not declared on the manufacturer's SDS. PSD results indicated that uncoated, coated and used silica sand fell into the inhalable size fraction (< 100 µm), which were supported by SEM images. Silica sand particles were shown to be smooth and non-spherical in shape by PSD analysis and SEM images. Statistically significant differences was only found for particles size [d(0.5)]. PSD analysis indicated that 90% [d(0.9)] of uncoated, coated, and used silica sand particles were smaller than 42.21 ± 29.96, 104.7 ± 23.33 µm and 54.9 ± 49.93 µm respectively.The quartz content of the silica

sand, as determined by WD-XRF, ranged from 96.83 to 98.20%, which corresponded with the manufacturer's SDS. Increased particle number concentrations were observed during specific activities conducted in each AM phase. The Grimm and a DustCount® displayed peak particle number concentrations of 680.51 and 37.10 p/cm^3 (respectively) during the post-processing phase for particle < 1 µm in size. The peak particles ERs in this study (Meiring, 2024) for particles < 1 µm in size was 3.06×10^5 and 12.09×10^0 p/min for a Grimm and a DustCount®. The DustCount® indicated that particles sized 0.375 µm in size were the most prevalent emitted during the AM phases. The personal exposure 8-hour Time Weighted Average (TWA) concentrations were measured at 0.01 ± 0.00 mg/m^3 for respirable crystalline silica and 0.04 ± 0.03 mg/m^3 for respirable PNOS. All 8-hour TWA personal exposures complied with their respective TWA-OELs. However, it was found that respirable crystalline silica measured during BJ was equal to 10% of the TWA-OEL-ML (0.1 mg/m^3).

Conclusion: PSD analysis and SEM images indicated that uncoated, coated and used silica sand fell into the inhalable size fraction (< 100 µm), indicating that the particles are small enough to be inhaled and potentially pose a risk to human health. The d(0.5) result, indicated a statistical significant difference between uncoated, coated, and used silica sand particle. The particle number concentrations and particle ERs obtained by the direct-reading instruments differed significantly, with the DustCount® yielding significantly lower particle number concentrations and particle ERs. When comparing the particle number concentrations measured by the DustCount® in area one (in front of the AM machine) and area two (back of the AM machine), higher particle number concentration was measured in area two at the back of the AM machine. All 8-hour TWA personal exposures were below the respective TWA-OELS. However, during BJ, respirable crystalline silica was equal to 10% of the TWA-OEL-ML indicating a potential health concern to the AM operator.

Introduction

Additive manufacturing (AM) is the process of combining AM feedstock materials to create parts from three dimensional (3D) model data, layer by layer, as opposed to formative and subtractive manufacturing techniques (ISO/ASTM 52900:2021). The term AM encompasses seven distinct process categories, which are used in a wide range of industries such as automotive production, manufacturing of medical devices, and aerospace (ISO/ASTM 52900:2021; Sun and Shang, 2021:194).

AM processes, such as binder jetting (BJ) and powder bed fusion selective laser sintering (PBF-SLS) can successfully make sand moulds and cores (Le Néel et al., 2018). BJ is a process that deposits a liquid bonding agent to selectively bind the AM feedstock material together, whereas PBF-SLS is a process that uses one or more lasers as a heating source to selectively melt or fuse surface particles (ASTM F2792, 2013; ISO/ASTM 52900:2021).

As AM is expanding rapidly, it is crucial to recognize that new approaches could present new health concerns for the AM operator (Manoj et al., 2020; Ljunggren et al., 2021). For this reason, every advancing and evolving AM technology needs to constantly assess the variables related to AM technology that could contribute particle emissions, exposure to hazardous chemicals (HCAs), and potential health hazards (Zisook et al., 2020). BJ consists of three phases, namely the pre-processing, processing, and post-processing phase. In the pre-processing phase, computer aided design (CAD) software is used to create a 3D presentation of the surface. Stratified tessellation language (STL) files are used to describe part geometry and are transferred to an AM machine. (Gibson et al., 2015). Once the AM machine is programmed, the powder is loaded into the feedstock bin. In the processing phase, the desired part is printed. During the post-processing phase, the part is brushed to remove the loose powder, and the AM machine is cleaned with a vacuum cleaner (Elliot and Love, 2016; Zhang and LeBlanc, 2018). After post-processing, the unfused powder can be disposed of or reused (Meera *et al*., 2017:86-91). AM operators handling silica sand and using the BJ machine may be exposed to respirable crystalline silica and respirable particulates not otherwise specified (PNOS). PNOS is defined as dust that contain < 1% quartz (NIOSH method 0600, 1998). Low exposure to PNOS have a negligible harmful impact on the body and any changes to the airways that occur from exposure to PNOS are potentially reversible. However, when PNOS are inhaled in sufficient quantity, PNOS particles accumulate and damage the proximal alveoli and terminal airways, causing inflammation that eventually results in the development of pneumoconiosis and COPD (Cherrie et al., 2013).

Inhalation of respirable crystalline silica, in the form of cristobalite or quartz, impairs particle clearance, activates macrophages, and causes continuous lung inflammation and irritation. The primary concern with inhaling respirable crystalline silica is silicosis, but respirable crystalline silica is also classified as a Group 1 confirmed human lung carcinogen (IARC, 2021; Rosental, 2017).

The powder characteristics and chemical composition of particles should be considered when investigating the potential health effects of AM. The physical characteristics refer to the size and shape of particles, while the chemical composition refer to its elemental composition. The site of deposition of particles within the respiratory tract is determined by the physical characteristics and chemical composition of the particles (Thomas, 2013; McClellan, 2002). Particles are categorised in three size fractions depending on the place of deposition in the respiratory system namely an inhalable fraction (< 100 µm, 50% cut-point) representing particles reaching the nasopharyngeal region, a thoracic fraction (< 10 µm, 50% cut-point) representing particles that deposit beyond the larynx, and a respirable fraction (< 4 µm, 50% cut-point) representing particles that reach the alveolar region of the lung (Brown et al., 2013). In addition, ultrafine particles (UFPs) represents particles with a particle diameter of less than 100 nm in size (U.S. EPA, 2009). Inhaled UFPs deposit effectively in the alveolar and pulmonary regions of the lung (Deng et al., 2016). UFPs may be released into the air by BJ machines (Afshar-Mohajer et al., 2015; Lewinski et al., 2019; Oberdörster et al., 2005). In general, inhalation in UFPs is associated with adverse health effects such as respiratory system inflammation, neurodegenerative disorders, and cardiovascular diseases (Du et al., 2016; Oberdörster et al., 2005).

In the South African context, there have been only two postgraduate studies conducted on human health risks and exposure during the AM of sand moulds (Adams, 2016; Matlhatsi, 2021). These studies found that silica sand as AM feedstock contains inhalable sized particles, however, Matlhatsi (2021:1-133) also found that silica sand contains thoracic and respirable sized particles. Particle emissions in the size range of 0.01 to 1 µm peaked at a number concentration of 5.98×10^6 p/cm^3 during the pre-processing phase, 7.76×10^6 p/cm^3 during the processing phase and 3.74×10^6 p/cm^3 during the post-processing phase (Matlhatsi, 2021). Time-integrated sampling indicated the exposure to concentrations of respirable crystalline silica (≤ 0.07 mg/m^3) and respirable PNOS (≤ 0.60 mg/m^3) that complied with their respective South African occupational exposure limits (OELs) (Adams, 2016; Matlhatsi, 2021).

Apart from these two postgraduate studies, two other studies have been conducted on human health risks and exposure during BJ. Afshar-Mohajer et al. (2015) utilised gypsum as AM feedstock, while the other study used stainless-steel powder as AM feedstock material (Afshar-Mohajer et al., 2015; Lewinski et al., 2019). Afshar-Mohajer et al. (2015), detected the highest particle number concentrations (0.9 to 1.16 × 10^4 p/cm^3) during the printing phase (processing phase) for particles 205 and 255 nm in size. Lewinski et al. (2019), reported a peak number concentration during the processing phase (1.2 × 10^4 p/cm^3) for particles 10 to 400 nm in size and an approximate peak particle number concentration of 6 × 10^4 p/cm^3 during the pre-processing phase for particles 0.3 to 10 µm in size.

Firstly, our study aimed to determine the physical characteristics and chemical composition of uncoated, coated, and used silica sand powder. Secondly, it quantified the particle number concentrations released and particle emission rates of particles released during the different phases of the AM process using direct-reading instruments. Finally, area monitoring and personal exposure monitoring were conducted by means of time-integrated sampling and real-time monitoring to establish area concentrations and personal respiratory exposure to respirable crystalline silica and respirable PNOS.

Methodology

This quantitative study was conducted at an AM research facility located at a tertiary education institution in South Africa.

Facility description

The AM process was conducted in an AM research facility with the following dimensions: length = 11.50 m, width = 5.90 m, height (sloped ceiling) = 2.50 m (lower sloped side), and 4.60 m (higher inclined side) with a calculated room volume of 240.87 m^3. The layout of the AM research facility was as follows: one door in the front, a large roll-up door at the back that was kept closed, and no windows that were opened. The AM machine was situated in the centre of the AM research facility (Supplementary material: Figure S1). There was an unpacking station with a local extraction ventilation system (not in a working condition), however, the AM operator did not make use of the unpacking station. There was a hopper located at the back of the room. Area monitoring was conducted at two areas in the AM research facility. Area one was in front of the AM machine and area two was behind the AM machine and in front of the hopper (Supplementary material: Figure S1). The door was left open on the first day of printing and kept closed on the second,

third, and fourth days of printing. There was an extraction ventilation system directly connected to the AM machine, which ventilated the AM machine's build envelope. The AM research facility had an air conditioner both in the front and at the back. However, the air conditioner in the front was not switched on or not operational at the time of the study and therefore not used to regulate indoor air conditions. The split-level air conditioner at the back of the AM research facility was set to a constant temperature of 22°C on each sampling day (Supplementary material: Figure S1)

The facility used an industrial scale BJ machine, namely a Voxeljet VX1000 (Voxeljet, Germany), Premixed quartz sand Type GS14/GS14/GS19 was used (Voxeljet - Pre-mixed quartz-sand type, 2014:1-7). Prior to the pre-processing phase, uncoated silica sand was coated with liquid sulphonic acid and furan binder in the coating room by coating operators (Voxeljet - Activator VX-2C/8, 2014:1-9; Voxeljet - Binder VX-2C Type B, 2014: 1-13). Emissions and exposure associated with coating are described by Matlhatsi (2021). A detailed description of the activities performed during the AM process is provided in Supplementary Material Table S1. In short, the pre-processing phase was initiated by the AM operator by setting up the software for producing the part. The AM operator would leave the AM research facility during the processing phase and periodically return to check on the part. In addition to performing BJ tasks, the operator also engaged in office work and operated other AM machines outside the room, potentially exposing him to HCAs. During both the pre-processing and processing phases, the AM operator manually loaded coated silica sand in the hopper and used a rod to level the loaded silica sand. For this study, parts with dimensions of height (h) 20 mm, width (w) 20 mm, and length (l) 200 mm under the same manufacturing conditions were produced. Upon completion of the processing phase, the part was kept inside the job box of the AM machine for 24 hours to cure (without the use of heat) at room temperature. Therefore, a one-day window was implemented between the processing and post-processing phases to allow particle number concentrations to recover to background concentrations. The post-processing phase entailed removing the job box of the AM machine using a hydraulic trolley jack, cleaning the printed parts, and vacuuming the AM machine. Only one AM operator conducted the printing of sand moulds at the AM machine during a full shift.

Powder characteristics and chemical composition of silica sand

Bulk samples of uncoated, coated, and used silica sand samples were collected from the AM research facility to establish the physical characteristics and chemical composition of the powders. Particle size distribution (PSD) and shape analysis were based on the methodology

described by Du Preez et al. (2018). PSD and shape analysis were performed using an automated Malvern Morphologi G3 microscope (Malvern Instruments Ltd, United Kingdom). Samples (10 mm^3) were placed in the dispersion chamber of the instrument, where after each sample was dispersed and scanned. The magnification scale was set at 20x (1.8 µm to 100 µm) and 2.5x (13 µm to 1000 µm). An image of the individual particles was captured for all three powders and the analysis was repeated three times for each sample of uncoated, coated, and used silica sand.

The scanning electron microscopy (SEM) (Phenom-World B., Eindhoven, Netherlands) was used for further analysis of particle shape and size. The samples (5 mm^3) were placed separately on double-sided adhesive carbon strips. The samples were placed in a sputter holder and covered with an SPI module sputter coater (SPI-Module™. Sputter Coater, SPI Supplies, United States) equipped with a source of gold-palladium alloy. Each sample of uncoated, coated, and used silica sand was examined by placing the sample in the sampling chamber of the SEM microscope at a power of 5 kV and magnification scale at approximately 3000x to observe respirable particles. PSD and SEM analyses were conducted at the North-West University Potchefstroom Campus, South Africa.

The chemical composition of uncoated, coated, and used silica sand was determined using an Applied Research Laboratories 9800XP Sequential X-ray fluorescence (Thermo Scientific™, United States). The test of major and minor elements (16 elements) by wavelength dispersive X-ray fluorescence (WD-XRF) was conducted by a South African National Accreditation System (SANAS) accredited laboratory using an in-house method in accordance with the following procedures: Sample preparation for X-ray fluorescence analysis and procedure for X-ray fluorescence analysis (TWS-ESS-DP-52, R2, 1989; TWS-ESS-DP-111 R1,1989).

Particle emissions

A Grimm-Portable Laser Aerosol Spectrometer model 11-A (GRIMM, Aerosol Technik GmbH & Co., Germany) was used to measure real-time particle emissions ranging from 0.25 µm to 32 µm in 31 size channels and two Nanozen DustCount® 9000 Z1 optical particle counters (Nanozen Industries Inc., Vancouver, Canada) were utilised to measure particles 0.30 µm to 20.82 µm in size. Grimm and DustCount® measured the particle number concentrations in respectively 31 and 20 size channels and data were grouped into size four fractions (< 1 µm, > 1 to < 4 µm, > 4 to < 10 µm and ≥ 10 µm), which were calculated by summing the data from the different

channels. The direct-reading instruments were placed at a height of 1.5 m and as near as possible to the AM machine, within 1.5 m. The direct-reading instruments collects particles and reports the particle number concentration (p/cm^3) emitted during BJ. The Grimm and a DustCount® were placed in front of the AM machine on the workbench in area one. A DustCount® was also placed directly behind the AM machine in front of the hopper in area two (Supplementary material: Figure S1). Prior to conducting any sampling, the indoor background particle number concentration was monitored on each sampling day for at least 10 minutes in the AM research facility before any activity was performed (Van der Walt et al., 2022). The background particle number concentrations were required to calculate the particle emission rate (ER) (He et al., 2004). Particle number concentration of each AM phase was monitored at intervals of one minute.

Air exchange rate calculations

The air exchange rate (AER) was calculated using a carbon dioxide decay method, based on the American Society for Testing and Materials (ASTM) Standard 62.2 (2016), ASTM E741-11 (2017) method, and ASTM D6245-07 (2012) method (ASTM Standard 62.2, 2016, Batterman, 2017; Haung et al., 2021). Four Onset Hobo mx1102A (Cape Cod, Massachusetts) indoor air quality data loggers were placed in various representative areas in the AM research facility to measure the CO_2 concentrations (ppm) inside the AM research facility. A data logger was placed outside the AM research facility to measure the outdoor CO_2 concentration. Four portable fans were utilised throughout the decay method to mix the indoor air. CO_2 was released from a CO_2 cylinder into the vacated AM research facility and left to increase and stabilise at 1000 ppm above ambient CO_2 concentration for 10 minutes, thereafter the CO_2 decay method commenced. The decay of CO_2 was measured at intervals of one minute until the ambient concentration was reached. The AER was measured with the door both open and closed and repeated three times for both scenarios.

The AER (1/h) was calculated using the following equation (Batterman, 2017):

$$AER = 1/\Delta t \ln \{(C_1 - C_R)/(C_0 - C_R)\} \quad \text{Equation 1}$$

Where Δt represents the time (h) between the measurements, C_0 was the initial CO_2 concentration (ppm) at the start of the decay period, C_1 was the CO_2 concentration (ppm) at the end of the decay period, and C_R the CO_2 concentration (ppm) in the outdoor air (Batterman, 2017:1-22).

Particle emissions rate calculations

The particle ER was calculated by making use of the methodology specified in He *et al*. (2004: 3405-3415).

$$\mathrm{ER} = \mathrm{V} \times [\frac{\mathrm{C_{peak}} - \mathrm{C_{out}}}{\Delta \mathrm{t}} + (\overline{\mathrm{AER} + \mathrm{k}}) \times \overline{\mathrm{C_{in}}} - \mathrm{AER} \times \mathrm{C_{out}}] \quad \text{Equation 2}$$

Where V is the volume of the AM research facility (m^3), C_{peak} the peak particle concentration (p/cm^3), C_{out} is the initial indoor particle concentration at time zero (background particle concentration) (p/cm^3) which is assumed to be equal to the outdoor particle concentration, C_{in} the mean particle concentration (p/cm^3), and Δt the time (min) between the C_{peak} and C_{out}. The average particle removal rate was represented by $(\overline{\mathrm{AER} + \mathrm{k}})$, where the AER was calculated using Equation 1 and k was the contaminant loss due to surface deposition and taken as 1/h in an indoor environment (Stefaniak *et al.*, 2019:19-30). The equation does not account for the impact of particle dynamics including evaporation, condensation, and coagulation. (Stabile *et al*., 2017; Stefaniak *et al*., 2019).

Area monitoring and personal exposure monitoring

A GilAir Plus pump (Gilian GilAir Plus Sensidyne, Inc., LP, United States) with a 2-piece cassette and aluminium cyclone (SKC, Inc., PA, United States) was used for time-integrated sampling to establish exposure to respirable crystalline silica and respirable PNOS. The 2-piece cassette containing a support pad and a 37 mm polyvinyl chloride (PVC) filter with a 5.0 µm pore size were used. The flow rate was set at 2.5 ℓ/min in accordance with the National Institute for Occupational Safety and Health (NIOSH) method 7602 and NIOSH method 0600 (NIOSH method 0600, 1998; NIOSH method 7602, 2017). Field calibration was conducted before and after use with a Gillian Gilibrator-2 (Gillian Gilibrator-2, Sensidyne Inc. United States). The flow rate deviation of the samples was less than 5%, therefore none of the samples were discarded (Sensidyne, 2011).

a Nanozen DustCount® 9000 Z1 optical particle counters (Nanozen Industries Inc., Vancouver, Canada) was used as a gravimetric sampling pump (time-integrated sampling) to establish exposure to respirable crystalline silica and respirable PNOS. For the DustCount®, a prepared DustCount® cassette was used that contained a support pad and a 25 mm PVC filter with of 5.0 µm pore size. The DustCount® was and fitted with a < 4 µm particle aerodynamic diameter impactor (PM_4). The flow rate of the DustCount® was kept within 5% of the factory setting of 1.0 ℓ/min. The flow rate deviation of the DustCount® samples was less than 5%, therefore none

of the samples were discarded (Sensidyne, 2011). a DustCount® was also used for real-time monitoring. DustCount® monitored particle number concentrations at intervals of one minute throughout the AM phases.

For personal exposure monitoring both samplers (GilAir Plus pump with a 2-piece cassette and aluminium cyclone as well as DustCount®) were attached to the collar in the breathing zone of the AM operator.

Area monitoring was conducted by placing the GilAir Plus pump with a 2-piece cassette and aluminium cyclone as well as the DustCount® at a height of 1.5 m and as close as possible to the AM machine. A GilAir Plus pump with a 2-piece cassette and aluminium cyclone along with the DustCount® were both placed in area one and area two (Supplementary Figure S1).

A field blank was collected for every sample of each sampling day. The field blanks were loaded and handled in a similar way as samplers used for personal exposure monitoring and area monitoring. However, the air was not drawn through the field blanks. Field blanks are unused sample media that are opened at the sampling site in an area that is not anticipated to be contaminated. Field blanks are analysed together with the samples to determine whether contamination occurred during the handling of samples (OSHA, 2023).

The mean (± standard deviation, SD) sampling time for the entire shift over four days was 150.25 ± 75.59 minutes. The mass collected on the filters during the AM phases was utilised to calculate the 8-hour time-weighted average (TWA) exposure concentrations for respirable crystalline silica and respirable PNOS by using Equation 3. For calculating the mean TWA exposure, the measured mass below the analytical limit of detection (LOD) was substituted by using the analytical LOD divided by the square root of two (LOD/$\sqrt{2}$) substitution method (Glass and Gray, 2001; Made and Utembe: 2019; Hornung and Reed, 1990). The small number of samples prevented the use of other substitution methods. The 8-hour TWAs were calculated from the measured concentrations (for each HCA measured in (mg/m^3) and the time duration of exposure (hours) for the entire AM process.

$$\mathrm{TWA} = \frac{[(C_1 \times t_1) + (C_2 \times t_2) + (C_n \times t_n)]}{t_8} \qquad \text{Equation 3}$$

Where, C = concentration (mg/m^3) of HCA measuring during the AM phase, t = time (hours) of the exposure period, and t_8 = hours in the workday (8 hours) (Schoeman and van den Heever, 2015).

Analyses of the area monitoring and personal exposure monitoring samples collected were performed by a SANAS-accredited laboratory. The 37 mm PVC filters of the 2-piece cassette and aluminium cyclone, as well as the 25 mm PVC filters of the DustCount® were analysed for respirable crystalline silica in accordance with NIOSH Method 7602 (NIOSH method 7602, 2017) and respirable PNOS were based on MDHS 14/4 and analysed in accordance with NIOSH method 0600 (MDHS 14/4, 2016; NIOSH method 0600, 1998). The LOD for gravimetric weighing was < 0.030 mg for respirable PNOS and < 0.010 mg for respirable crystalline silica.

Data analysis of results

Statistical analyses were performed using GraphPad version 9.01 (GraphPad Software, Inc., USA). Basic descriptive statistics were used to calculate the mean and SD of the PSD of the uncoated, coated, and used silica sand. Statistically significant difference of the uncoated, coated, and used silica sand was performed in using a t-test. The mean, SD and peak for the measured particle number concentrations, and the mean and peak for particle ERs during BJ were obtained using descriptive statistics. GraphPad version 9.01 was also used to provide graphical representations of the particle number concentrations and particle emission rates during BJ.

Legal exposure compliance was determined by comparing the 8-Hour TWA exposure of the respirable crystalline silica and respirable PNOS of the AM operator to the respective South African TWA-OELs stated in the Regulations for HCAs (2021).

Ethical considerations

All AM operators at the facility were invited to take part in this study (Meiring, 2024), participation was therefore voluntary and participants provided informed consent. This study was approved by the Health Research Ethics Committee of North-West University (approval number: NWU-00027-22-A1).

Results

Physical characteristics and chemical composition of silica sand

PSD analysis indicated that 50% [d(0.5)] of uncoated, coated, and used silica sand particles were smaller than 1.29 ± 0.36 µm, 4.27 ± 0.08 µm and 2.42 ± 0.04 µm respectively. Additionally, a statistically significant difference in d(0.5), was observed between uncoated, coated, and used silica sand particle sizes (Table 1). PSD analysis indicated that 90% [d(0.9)] of uncoated, coated,

and used silica sand particles were smaller than 42.21 ± 29.96 µm, 104.7 ± 23.33 µm and 54.9 ± 49.93 µm respectively. The measured powder particle sizes could not be compared to the safety data sheet (SDS) for silica sand since it was not stated in the obtainable SDS (Voxeljet, 2014). SEM images of uncoated, coated and used silica sand indicated particles in the inhalable fraction (< 100 µm). The PSD results confirmed the presence of respirable sized particles and indicated that silica sand particles were smooth surfaced (convexity) and non-spherical in shape (circularity) (Table 1), which was confirmed by SEM images (Figure 1). Furthermore, the WD-XRF analysis revealed the presence of quartz in the uncoated, coated, and used silica sand from the AM research facility, with crystalline silica content ranging from 96.83 to 98.20% which corresponded with the manufacturer's SDS (> 90%) (Table 1).

Table 1: PSD (mean ± SD), shape, and chemical composition of silica sand compared to the SDS

Sand type	n	SDS (µm)	Particle size distribution (µm)			Particle shape		Chemical Composition (quartz)	
			d(0.1)	d(0.5)	d(0.9)	Circularity	Convexity	SDS (%)	WD-XRD (%)
Uncoated	**3**	n.s	0.58 ± 0.03	1.29 ± 0.36[a]	42.21 ± 29.96	0.70 ± 0.07	0.97 ± 0.01	> 90%	98.20
Coated	**3**	n.s	0.61 ± 0.08	4.27 ± 0.08[a]	104.7 ± 23.33	0.65 ± 0.03	0.95 ± 0.01	n.a	96.83
Used	**3**	n.s	0.58 ± 0.04	2.42 ± 0.04[a]	54.9 ± 49.93	0.64 ± 0.03	0.96 ± 0.01	n.a	97.28

Legend: Uncoated silica sand: collected from the AM feedstock provided by the manufacturer; Coated silica sand: collected after the coating process; Used silica sand: reused sand gathered during the post-processing phase; mean : measure central tendency of a probability distribution along median and mode ; SD: standard deviation is a measure of how dispersed data is in relation to the mean; peak: peak(maximum) is the largest value in the data set; n: number of repeated measurements; n.s: not stated; d(0.1): 10% of the particles are smaller than the stated diameter; d(0.5): 50% of the particles are smaller than the stated diameter; d(0.9): 90% of the particles are smaller than the stated diameter; a: Statistically significant differences ($p \leq 0.05$); Circularity: The ratio of the perimeter of a circle with the same area as the particle divided by the perimeter of the actual particle image. Circularity values range from 0 - 1, a perfect circle will have a circularity of 1; Convexity: The measurement of the edge roughness of a particle. A smooth particle will have a convexity value of 1 and an irregular particle will have a convexity value of 0 (Malvern Instruments Ltd, 2007).n.a: not applicable.

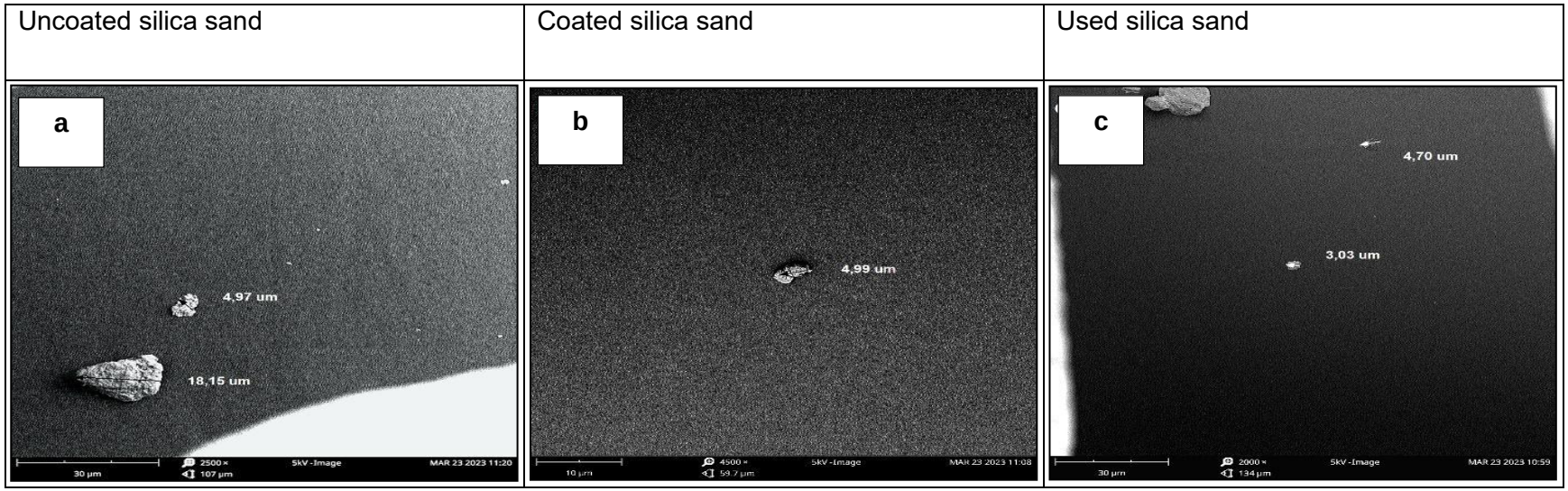

Figure 1: SEM images of (a) uncoated, (b) coated and (c) used silica sand

Particle emissions

The particle number concentrations measured using Grimm and DustCount® were predominately < 1 µm in size (Table 2). There was a notable difference in the particle number concentrations in the particle size ranges measured by the two direct-reading instruments, with the DustCount® yielding much lower particle number concentrations. The Grimm and DustCount® displayed peak particle number concentrations of 680.51 and 37.10 p/cm^3 during the post-processing phase for particle < 1 µm in size. The mean particle number concentrations for particles sizes > 1 µm were in most instances only slightly above the background particle number concentration. The peak particle number concentration for particles > 1 µm in size was 16.31 p/cm^3 during the processing phase when using a Grimm, while DustCount® measured a peak particle number concentration of 6.80 p/cm^3 during the pre-processing phase (Table 2).

Table 2: **Mean particle number concentration as measured with Grimm and DustCount® over four printing days**

Phase		**Particle Size Rage**											
		< 1 µm			**> 1 to < 4 µm**			**> 4 to < 10 µm**			**≥ 10 µm**		
		Grimm (A1)	Dustcount (A1)	DustCount (A2)	Grimm (A1)	Dustcount (A1)	DustCount (A2)	Grimm (A1)	Dustcount (A1)	DustCount (A2)	Grimm (A1)	Dustcount (A1)	DustCount (A2)
Background	Mean	332.92	1.32	18.67	1.05	0.03	1.37	0.05	< 0.01	0.02	< 0.01	< 0.01	< 0.01
	SD	4.00	0.84	0.27	0.11	0.01	0.04	0.01	< 0.01	< 0.01	< 0.01	< 0.01	< 0.01
	Peak	640.92	10.03	35.22	1.78	0.18	2.23	0.12	< 0.01	0.06	0.03	< 0.01	0.01
Pre-processing	Mean	403.15	0.02	23.27	3.18	0.02	2.17	0.16	< 0.01	0.04	< 0.01	< 0.01	< 0.01
	SD	15.79	2.2	1.96	1.02	0.04	0.51	0.08	< 0.01	0.01	< 0.01	< 0.01	< 0.01
	Peak	590.85	12.93	33.24	11.34	0.27	6.80	0.75	< 0.01	0.11	0.07	< 0.01	< 0.01
Processing	Mean	366.96	0.01	21.29	3.76	< 0.01	1.97	0.18	< 0.01	0.04	< 0.01	< 0.01	< 0.01
	SD	8.79	< 0.01	0.62	1.83	< 0.01	0.34	0.12	< 0.01	0.01	< 0.01	< 0.01	< 0.01
	Peak	590.65	0.09	33.66	16.31	0.14	4.66	0.98	< 0.01	0.12	0.01	< 0.01	0.01
Post-processing	Mean	421.44	0.01	23.48	3.36	< 0.01	1.90	0.20	< 0.01	0.04	0.01	< 0.01	< 0.01
	SD	5.55	0.01	0.22	1.07	0.01	0.21	0.08	< 0.01	0.02	< 0.01	< 0.01	< 0.01
	Peak	680.51	0.07	37.10	13.46	0.07	2.56	0.96	< 0.01	0.12	0.07	< 0.01	< 0.01

Legend: A1: area one (in front of AM machine; A2: area two (back of the AM machine); mean(average): measure central tendency of a probability distribution along median and mode; SD: standard deviation is a measure of how dispersed data is in relation to the mean; peak(maximum): largest value in the data set.

Figure 2a shows two distinct peaks in particle number concentrations occurred during the pre-processing phase in area one for day one of printing which were due to the AM operator that configured the software and levelled silica sand in the hopper. During the processing phase particle number concentration gradually decreased towards the phase's end (Figure 2a). The most prevalent particle fraction size for the DustCount® for day one of printing for area two was predominantly 0.375 µm in size compared to other size fractions throughout the AM process (Supplementary material: Figure S2).

Figure 2b illustrates that the particle number concentration during the post-processing phase in area one for day four of printing, was lower than the background particle number concentrations. The particle number concentrations for particles < 1 µm in size increased during the post-processing phase when the AM operator switched on the AM machine, unlocked the job box, and cleaned the part and AM machine. Particles sizes > 1 µm to < 4 µm were not significant during the post-processing phase.

Several peaks can be observed in Figure 3a during the pre-processing phase in area two on day one of printing. The particle number concentration increased at the start of the pre-processing phase when the AM operator configured the software. The highest peak on day one occurred when the AM operator levelled silica sand in the hopper, followed by two smaller peaks. These smaller peaks likely resulted from particle emissions from the hopper during software configuration. A peak particle concentration occurred at the start of the processing phase when printing commenced and gradually decreased towards the end of the phase.

Figure 3b illustrates the particle number concentrations in area two on day two of printing using a DustCount® to monitor particles of sizes < 1 µm and > 1 µm to < 4 µm. Particle number concentrations during BJ were slightly above the background particle number concentration. Particle number concentrations in these size ranges peaked a few times during the post-processing phase when the AM operator took out the job box and cleaned the part and AM machine. An increase in particle concentration occurred during the pre-processing phase when the software was configured and then AM machine was loaded. The particle number concentration peaked at when silica sand was levelled and loaded in the hopper and decreased towards the end of the phase.

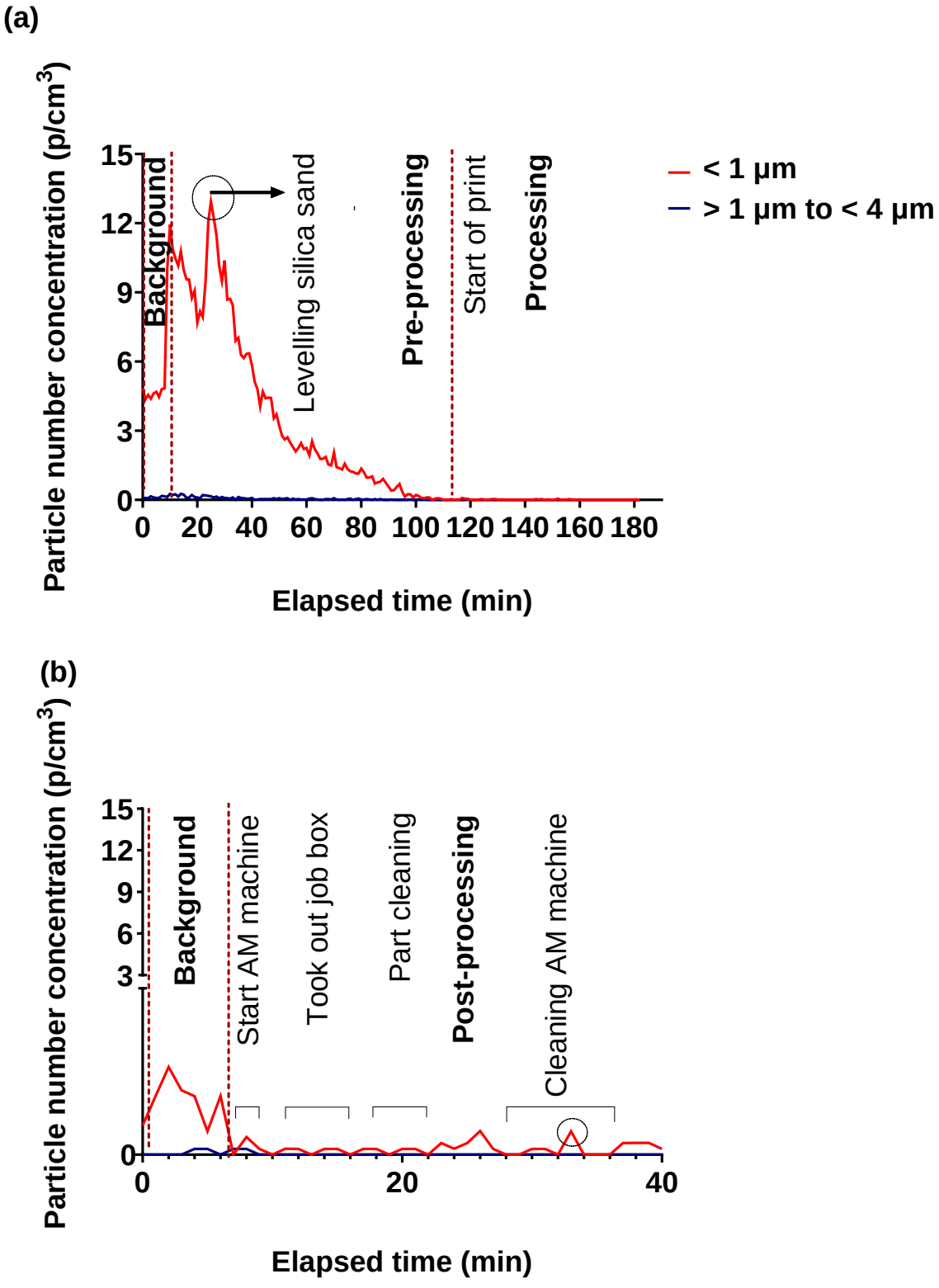

Figure 2: **Total particle number concentrations during the entire BJ process when using a DustCount® in area one for day one (a) and (b) day four of printing.**

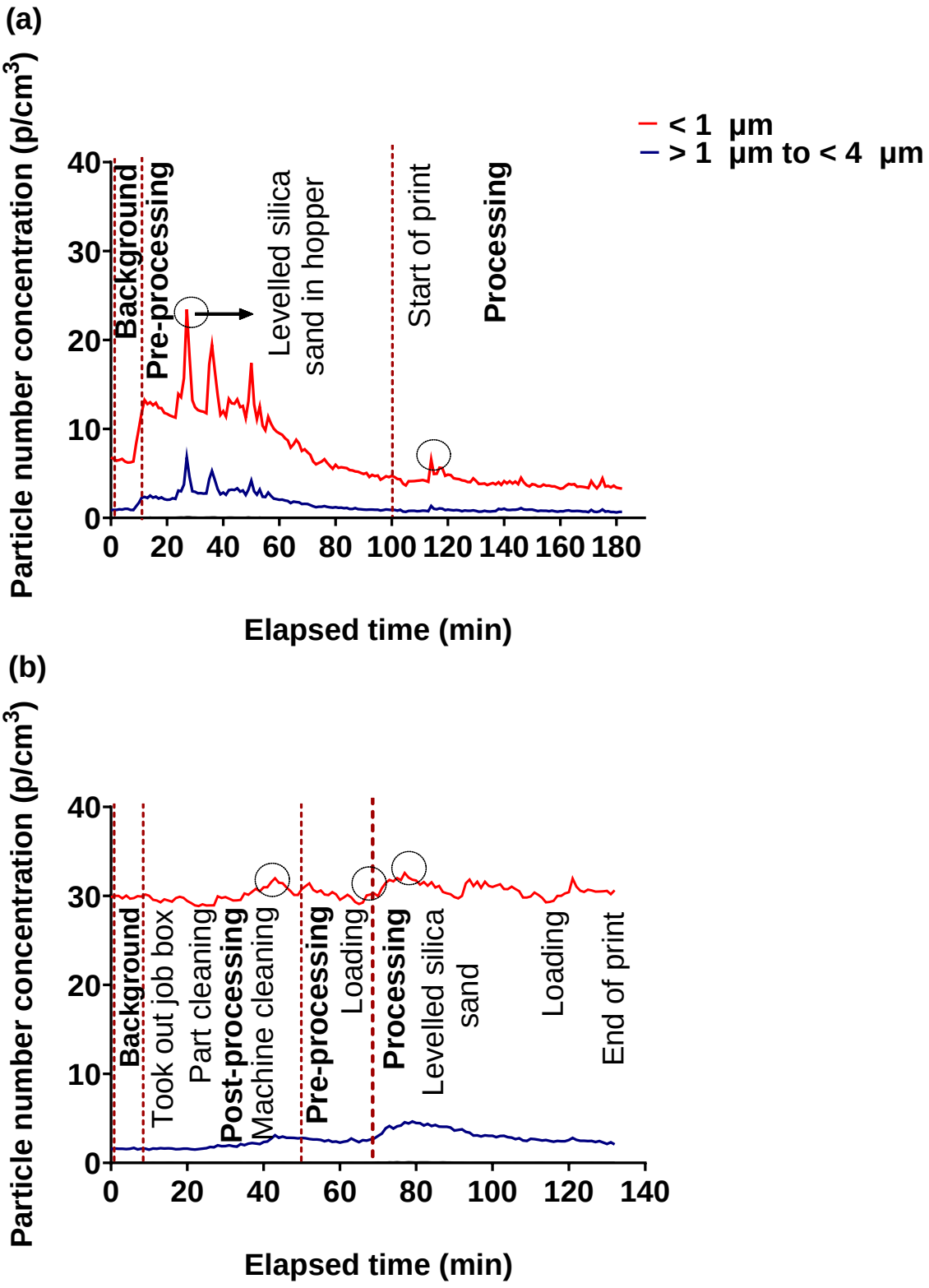

Figure 3: **Total particle number concentrations during the entire BJ process when using a DustCount® in area two for day one (a) and (b) day two of printing.**

The AER was calculated using a carbon dioxide decay method (Supplementary material: Table S2). The calculated AER in this study (Meiring, 2024) was higher than the AER (0.22) used by Matlhatsi (2021:1-133). The AER in the AM research facility with the door open and air conditioner switched on was 3.58 air changes/hour, while the AER was 2.93 air changes/hour with the door closed (Supplementary material: Table S2). The calculated AER (Supplementary material: Table S2) was used to calculate the mean particle ERSs during the three AM phases of BJ (Figure 4a).

Figure 4a illustrates the mean particle ERs during the three AM phases of BJ with silica sand at area one utilising a Grimm, focusing on particles < 1 µm to < 10 µm in size. On day four of monitoring, high background particle number concentration prevented the calculation of mean particle ER. There was a notable difference in the mean particle ERs between the particle sizes. The mean particle ERs of particles < 1 µm in size were higher across the three AM phases of BJ compared to particles > 1 µm to < 4 µm and > 4 µm to < 10 µm in size. The mean particle ER was the highest during the post-processing phase (2.15×10^5 p/min) for particles < 1 µm in size. For the larger particle range, from > 1 to < 4 µm in size, the overall highest mean particle emission rate was during processing phase (2.47×10^3 p/min) (Supplementary material: Table S3).

In Figure 4b the mean particle ERs were examined across three AM phases of BJ with silica sand for particles < 1 µm and > 1 µm to < 4 µm at area one when utilising a DustCount®. High background particle number concentration prevented the calculation of mean particle ERs of some particle size ranges (Supplementary material: Table S3). The mean particle ER was the highest during the pre-processing phase (10.16 p/min) for particles < 1 µm in size. Particles > 1 µm to < 4 µm in size had mean particle ERs of 1.44 p/min during processing phase and 1.46 p/min during the post-processing phase that were lower compared to particles < 1 µm in size. The mean and peak particle ERs are summarised in supplementary Table S3.

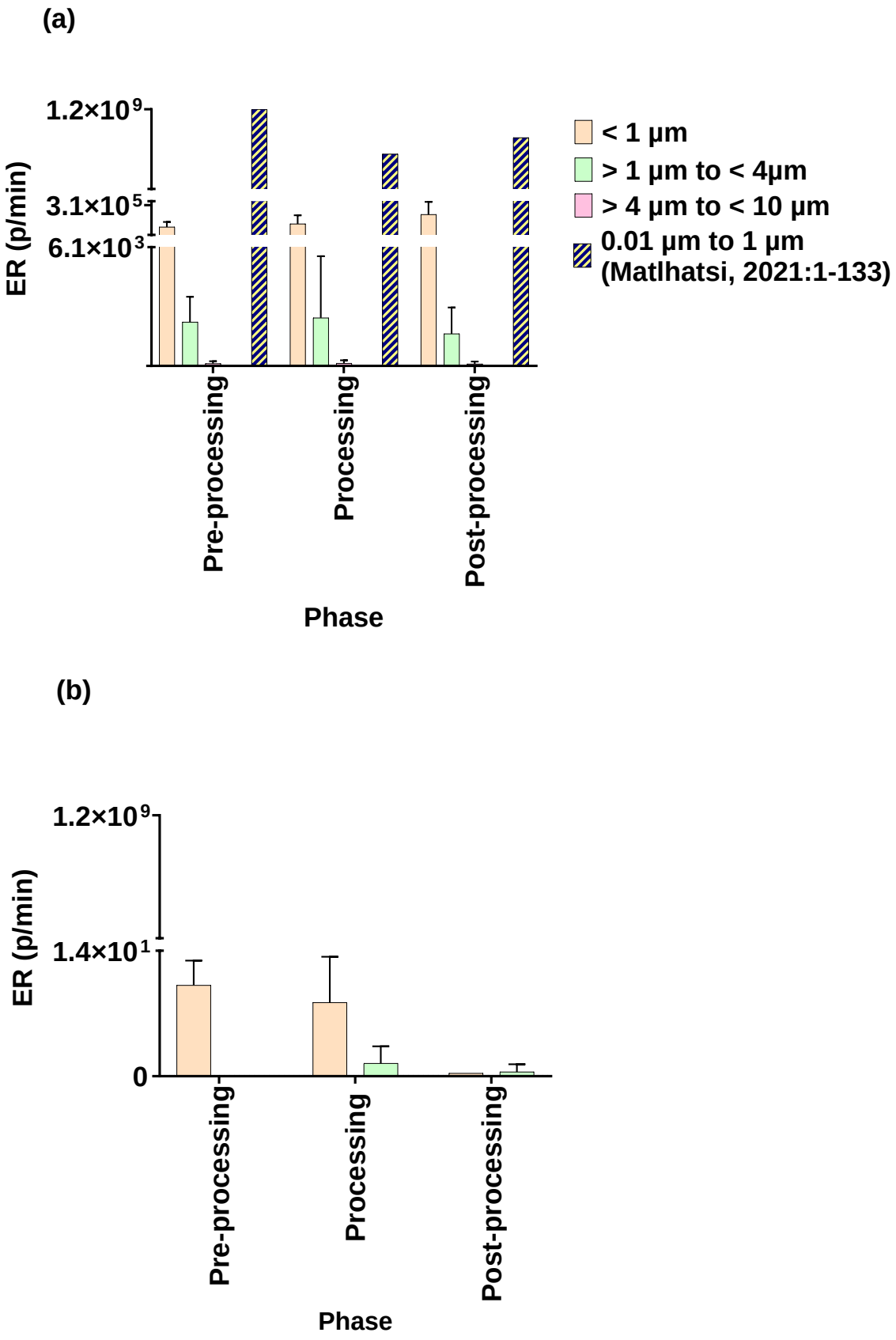

Figure 4: **The mean particle ERs at area one for (a) Grimm and (b) Dustcount® .**

Area monitoring and personal exposure monitoring

Figure 5 displays the particle number concentrations of the AM operator on days one, three, and four of printing using a DustCount®. During the pre-processing phase a few peaks in particle number concentrations can be observed which was likely due to the operator setting up the AM machine, loading and levelling of silica sand in the hopper (Figure 5a and 5b). An increase in particle concentrations occurred at the start of the processing phase as printing commenced. During the processing phase, the AM operator left the AM research facility and returned in between the print to check the progress of the print. Peak particle number concentrations were observed during the processing phase when the AM operator conducted activities outside the AM research facility. (Figure 5a and 5b). The particle number concentrations peaked during the post-processing phase when the AM operator took out the job box, cleaned the part and the AM machine (Figure 5b and 5c). However, on the fourth day of printing peak particle number concentration occurred during the post-processing phase when the AM operator conducted work outside the AM research facility not related to the BJ process (Figure 5c). The most prevalent particle fraction size for the DustCount® for personal exposure monitoring was predominantly 0.375 µm in size compared to other size fractions throughout the AM process (Supplementary material: Figure S2).

Table 3 displays the 8-hour TWA for both area monitoring and personal exposure monitoring over four printing days. The personal exposure monitoring measurements were below the South African respirable crystalline silica Time-Weighted Average-Occupational Exposure Limit-Maximum Limit (TWA-OEL-ML) of 0.1 mg/m^3 and respirable PNOS TWA-OEL-Restricted Limit (TWA-OEL-RL) of 5 mg/m^3. Both time-integrated sampling and real-time monitoring indicated that the 8-hour TWA for area monitoring and personal exposure monitoring to respirable crystalline silica was 0.01 ± 0.00 mg/m^3. The 8-hour TWA for respirable PNOS at areas one and two were $\leq$ 0.04 mg/m^3. The 8-hour TWA of the AM operator to respirable PNOS ranged from 0.01 mg/m^3 to 0.07 mg/m^3 for (time-integrated sampling). The 8-hour TWA for respirable PNOS at area one and area two were $\leq$ 0.11 mg/m^3. The 8-hour TWA of the AM operator to respirable PNOS ranged from 0.07 mg/m^3 to 0.15 mg/m^3 for real-time monitoring (Table 3).

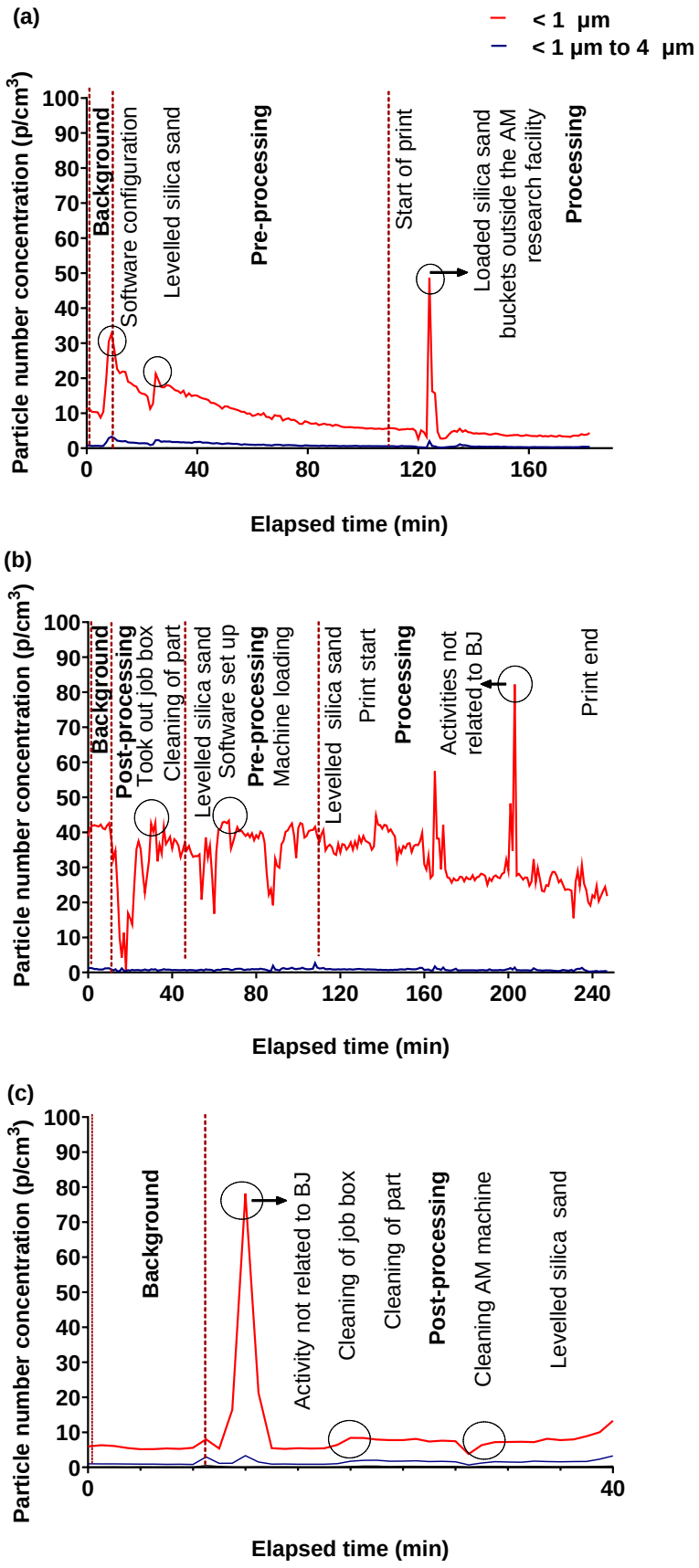

Figure 5: **Particle number concentration for the AM operator on day one (a), three (b), and four (c) of printing using DustCount®.**

Table 3: **Summary of respirable crystalline silica and respirable PNOS TWA results during the entire BJ process using silica sand as AM feedstock material.**

	8-hour TWA (mg/m^3)			
	Time-integrated sampling		Real-time monitoring	
	Respirable crystalline silica	Respirable PNOS	Respirable crystalline silica	Respirable PNOS
Area one (In front of the AM machine)	0.01 ± 0.00	0.01 ± 0.01	0.01 ± 0.00	0.07 ± 0.03
Area two (Back of the AM machine)	0.01 ± 0.00	0.02 ± 0.02	0.01 ± 0.00	0.08 ± 0.03
Personal exposure monitoring	0.01 ± 0.00	0.04 ± 0.03	0.01 ± 0.00	0.11 ± 0.04

Legend: mg/m^3 = milligram per cubic meter; Respirable crystalline silica: TWA-OEL-ML = 0.1 mg/m^3; PNOS TWA-OEL-RL) = 5 mg/m^3.

Discussion

This study investigated the physical characteristics and chemical composition of uncoated, coated, and used silica sand utilised during BJ and particle number concentrations, particle ERs, area concentrations, and personal respiratory exposure of AM operators to HCAs (respirable crystalline silica and respirable PNOS) during the three AM phases of BJ at an AM research facility located at a tertiary education institution in South Africa.

Powder characteristics and chemical composition of silica sand

When assessing the potential health risks associated with the AM process, the characterisation of powder is essential. Powder characteristics includes PSD and particle shape analysis as this has a significant impact on the exposure route and where particles may be deposited in the respiratory tract (Andi et al., 2022; Thomas, 2013).

PSD analysis (Table 1) was in agreement with Matlhatsi's (2021) findings that 10% of particles [d(0.1)] in uncoated, coated, and used silica sand were respirable sized particles. However, Adams (2016) reported significantly larger particles within the inhalable sized fraction. PSD analysis found that 50% of particles [d(0.5)] were in the respirable size fraction (Table 1), which was confirmed by SEM images (Figure 1). The d(0.5) result, indicated a statistically significant difference between uncoated, coated, and used silica sand particle size, as previously reported by Matlhatsi (2021). Statistically significant differences were not found between uncoated, coated, and used silica sand for particles [d(0.1)] and [d(0.9)], which was supported by Adams (2016). The PSD analysis (Table 1), indicated that 90% of particles [d(0.9)] for

uncoated, coated and used silica sand were respectively smaller than 42.21 ± 29.96 µm, 104.7 ± 23.33 µm and 54.9 ± 49.93 µm and fell in the inhalable fraction (Table 1). These findings differed significantly from Adams (2016:1-84) which reported larger particles (> 100 µm). Matlhatsi (2021), found particles smaller than 3.98 ± 0.72 µm, 6.51 ± 2.71 µm, and 115.00 ± 95.15 µm for uncoated, coated, and used silica sand. In this study (Meiring, 2024) both PSD analysis (Table 1) and SEM images (Figure 1) confirmed that silica sand particles were smooth (convexity) and non-spherical in shape (circularity), in agreement with Matlhatsi's findings (2021:1-133). Adams (2016:1-84), did not investigate the convexity and circularity of silica sand particles. This study found no statistically significant differences in edge roughness (convexity) and particle shape (circularity) among uncoated, coated, and used silica sand particles, in line with Matlhatsi's findings (2021). The WD-XRF results (Table 1), confirmed that all collected silica sand samples (uncoated, coated, and used) had a high crystalline silica content, ranging from 96.83 to 98.20%. The uncoated silica sand contained 98.20% crystalline silica content corresponding with the manufacturer's SDS (> 90%) (Table 1). The X-ray Diffraction (XRD) findings of Adams (2016:1-84), showed the presence of crystalline silica for uncoated, coated, and used silica sand respectively with a range of between 3.8 and 4.3% at Facility A and a range of between 98.6 and 100% at Facility B. Matlhatsi (2021:1-133), indicated that uncoated, coated and used silica sand consisted of a high percentage of crystalline silica that ranged between 92.6 and 97.3%. Comparison of this study's findings (Table 1), with that of Adams (2016:1-84), Matlhatsi (2021:1-133), and Afshar-Mohajer et al. (2015:293-301), found that the chemical composition of the AM feedstock was not affected during the BJ process.

Particle emissions

It was found that the particle number concentrations increased to above the background particle mainly for particles < 1 µm and > 1 to < 4 um in size, even with the enclosed BJ machine, as reported in previous studies (Afshar-Mohajer et al., 2015; Lewinski et al., 2019; Matlhatsi, 2021). The mean particle number concentrations measured in the AM facility for particles < 1 µm in size during the BJ process when using a Grimm ranged between 366.96 and 421.44 p/cm^3 (Table 2). The mean particle number concentrations ranged from 0.01 to 0.02 p/cm^3 in area one and 21.29 to 23.48 p/cm^3 when using a DustCount® for particles < 1 µm in size (Table 2). The peak particle number concentration for particles < 1 µm in size was 680.51 p/cm^3 when using a Grimm, while DustCount® measured a peak particle number concentration of 37.10 p/cm^3 during the post-processing phase (Table 2). The mean particle number concentrations measured in the AM facility for particles sizes > 1 µm to ≥ 10 µm ranged from < 0.01 to 3.76 p/cm^3 for Grimm, and ranged between

< 0.01 and 2.17 p/cm^3 for DustCount® (Table 2). When comparing the median particle sizes for uncoated, coated, and used silica sand of 1 29 ± 0.36 µm, 4.27 ± 0.08 µm, and 2.42 ± 0.04 µm (Table 1), the emitted particles throughout the AM process were predominantly 0.375 µm in size based on the Dustcount® (Supplementary material: Figure S2), similar to findings by Matlhatsi (2021), who reported a predominant particle size of 0.3 µm when using an OPC. In contrast, Afshar-Mohajer et al. (2015) and Lewinski et al. (2019) reported smaller particles of 205 to 255 nm and 87 nm in size respectively during the BJ process when gypsum was used as the AM feedstock material. Lewinski et al. (2019), reported higher particle number concentrations of 2.0 × 10^4 p/cm^3 and 6.0 × 10^4 p/cm^3 for particles 0.3 µm to 10 µm in size with the OPS (model 3330; TSI), with stainless-steel powder as AM feedstock material.

The Grimm data indicated an overall higher particle number concentrations during the three AM phases while lower concentrations were observed from the DustCount®, and this is due to the smaller detection sizes of the Grimm. Matlhatsi (2021), reported significantly higher mean particle number concentrations (1.98 × 10^6 p/cm^3 to 3.14 × 10^6 p/cm^3) for particles 0.01 µm to 1 µm during the three AM phases when utilising a Condensation Particle Counter (CPC model 3007 TSI Inc., MN, USA). with a peak particle number concentration of 7.76 × 10^6 p/cm^3 during the processing phase. The DustCount® results of this study cannot be compared to those of Matlhatsi (2021:1–133), as this real-time instrument to measure particle number concentrations was not used in that study. Differences in ventilation, including air conditioning, the regular opening of the front door, and the rear roll-up door could be the cause of the considerable difference in particle number concentrations between these two studies (2021:1-133). The results might have been influenced by the placement of the direct-reading instruments, housekeeping, phase duration, and the regular opening and closing of the AM chamber door. Afshar-Mohajer *et al.* (2015), reported particle number concentrations similar to this study for particles 0.45 µm to 0.90 µm in size using an OPC (TSI Inc., Minnesota). These concentrations ranged between 0.01 p/cm^3 to 500 p/cm^3 (Afshar-Mohajer et al*.,* 2015).

Direct-reading instruments in area one on day one of printing showed increased particle number concentrations during pre-processing tasks such as software configuration and levelling of silica sand in the hopper. Particle number concentrations slightly increased at the start of the processing phase when printing commenced and then decreased towards the phase's end as the part was completed, and no activities took place (Figure 2a). Direct-reading instruments in area one day four showed increased particle number concentrations during specific tasks performed during post-processing phase such as switching on the AM machine, opening the job box, manually cleaning the part with a brush, and cleaning the AM machine.

The highest peak particle number concentration on day four in area one occurred during the vacuum cleaning of the AM machine (Figure 2b).

Direct-reading instruments in area two on day one of printing showed increased particle number concentrations during specific tasks performed during the AM phases such as when the AM operators levelled silica sand in the hopper and when the print started. As the printing process came to an end, the particle number concentrations decreased (Figure 3a). Direct-reading instruments in area two day two of printing showed increased particle number concentrations when the AM operator switched on the AM machine, took out the job box using a hydraulic trolley jack, cleaned the part and AM machine and loaded silica sand in the hopper (Figure 3b). Machine cleaning, loading and levelling of silica sand in the hopper caused the highest particle number concentrations on these printing days (Figure 3a and 3b).

The particle number concentrations measured by the DustCount® was higher in area two (back of the AM machine) (Table 2, Figure 2 and 3). The direct-reading instrument was placed amid the AM machine and hopper, which both emitted particle number concentrations. Lower particle number concentrations in area one possibly occurred due to the direct-reading instrument being positioned farther away from the hopper (Supplementary material: Figure S1). Thus, activities such as loading and levelling silica sand in the hopper were higher in area two. This finding aligns with Matlhatsi, (2021), suggesting that that the hopper might be a source of airborne particles. The particle number concentrations when using a Dustcount® during this BJ activities were low, which could be due to several factors such as particle size range of the direct-reading instrument, ventilation, housekeeping, and phase duration. The mean particle fraction size for the DustCount® was predominantly 0.375 µm in size throughout the AM process (Supplementary material: Figure S2).

Various factors were considered when calculating the particle ERs, such as the volume of the AM facility, the peak particle concentration, background particle concentration, and AER. The ERs were calculated by Matlhatsi (2021) using a provided AER. Since the AM research facility was more effectively ventilated compared to the study of Matlhatsi (2021), and various ER factors were taken into account when calculating the particle ERs, fewer particles may have accumulated in the AM research facility, which could account for this study's low ERs. Furthermore, Matlhatsi (2021) reported that dry sweeping increased ERs. This study did not employ dry sweeping methods, which is an improvement to exposure control. A consistent trend of higher particle ERs was observed for submicron particles, < 1 µm in size compared to larger particles.

The Grimm a peak particle ER of 3.06×10^5 p/min during the post-processing phase, while the DustCount® measured a peak ER of 12.09×10^0 p/min during the processing phase for particles < 1 µm in size (Supplementary material: Table S3). The mean ERs for particles > 1 µm to < 4 µm in size was the highest during the processing phase using Grimm (2.47×10^3 p/min) and DustCount® (1.46×10^0 p/min). Grimm measured low particle ER for particles > 4 µm to ≥ 10 µm in size, whereas high background particle number concentration prevented calculation of the mean and peak particle ERs for particles > 4 µm to ≥ 10 µm in size for DustCount® (Supplementary material: Table S3).

Area monitoring and personal exposure monitoring

Real-time monitoring was used in addition to time-integrated sampling to provide more detail of the exposure of the AM operator during the AM phases. Particle number concentration data shows which activities caused peak exposure within each of the AM phases. Particles > 4 µm in size were excluded from the figure due to their insignificant low particle number concentrations. Figure 5 illustrates the particle number concentrations for the AM operator on days one, three, and four of printing using a DustCount®. Changes in particle number concentrations during BJ were observed during tasks that were performed during each AM phase such as when the software was configured, silica sand was levelled in the hopper, the job box was taken out, and when the printed part and the AM machine were cleaned. Personal exposure monitoring with a Dustcount® during these activities indicated low particle number concentrations. The highest peak particle number concentrations were measured during processing and post-processing phase when the AM operator conducted work outside the AM research facility (Figure 5b and 5c). The particle number concentrations measured by the Dustcount® for personal exposure monitoring was predominately 0.375 µm in size.

Time-integrated sampling was conducted in area one and area two. However, since the OELs given in the RHCA are related to personal exposure to HCA at work, these results could not be compared to South African TWA-OELs. The TWA exposure concentrations to respirable crystalline silica for both areas one and two was 0.01 ± 0.00 mg/m^3. Adams (2016) and Matlhatsi (2021), also reported low TWA exposure concentrations to respirable crystalline silica for area monitoring ranging from < 0.003 to 0.01 mg/m^3. The TWA exposure concentrations for respirable PNOS in areas one and two respectively were 0.01 ± 0.01 mg/m^3 and 0.02 ± 0.02 mg/m^3. Adams (2016:1-84) and Matlhatsi (2021), reported higher TWA exposure concentrations to respirable PNOS for area monitoring ranging from 0 09 to 0.27 mg/m^3. The slightly higher PNOS concentration in area two may be due to the placement of the monitoring equipment amid the AM machine and the hopper. This study

supports the trend that the TWA exposure concentrations for personal exposure monitoring are higher compared to area monitoring (Adams, 2016:1-84; Matlhatsi, 2021).

The TWA exposure indicates exposure experienced over eight-hours; however, the measurement duration was shorter than this time frame. Since the AM operator at this facility mainly conducts work within an office setting and only performs the AM process when required, the personal exposure was anticipated to be zero for the remaining eight hours of this study. The TWA personal exposure concentrations findings of this study found that respirable crystalline silica respirable were 0.01 ± 0.00 mg/m^3 and 0.04 ± 0.03 mg/m^3 for respirable PNOS (Time-integrated sampling). Matlhatsi (2021), reported TWA exposure concentrations for respirable crystalline silica of < 0.003 mg/m^3, whereas Adams (2016:1-84) calculated TWA exposure concentrations ranging between 0.03 and 0.06 mg/m^3. The TWA exposure concentrations of Adams (2016) and Matlhatsi (2021) ranged from 0.08 to 0.60 mg/m^3. This study is aligned with the results of Adams (2016:1-84) and Matlhatsi (2021), who confirmed that none of the personal exposure monitoring measurements exceeded the South African TWA-OEL-ML for respirable crystalline silica (0.1 mg/m^3) and the TWA-OEL-RL for respirable PNOS (5 mg/m^3). However, real-time monitoring and time-integrated sampling of respirable crystalline silica equaled 10% of the TWA-OEL-ML.

Conclusion

This study aimed to determine particle characterisation and chemical composition of silica sand particles while also investigating particle emissions and exposure associated with BJ utilising silica sand. This study was the first to employ personal exposure monitoring through real-time monitoring and time-integrated sampling methods. PSD analysis, supported by SEM images, reveals that the particle sizes of uncoated, coated, and used silica sand are within the inhalable size fraction (< 100 µm). Additionally, there is a statistically significant difference in the median particle sizes d(0.5) among these three types of silica sand. There was a notable difference in the particle number concentrations and particle ERs measured by the direct-reading instruments, with the DustCount® yielding lower particle number concentrations. All 8-hour TWA personal exposures complied with their respective TWA-OELs. However, it's important to note that both time-integrated sampling and real-time monitoring of respirable crystalline silica equaled 10% of the TWA-OEL-ML.

References

American Society of Testing and Materials (ASHRAE). (2016). Ventilation and Acceptable Indoor Air Quality in Residential Buildings. Atlanta: ASHRAE Standing Standard Project Committee 62.2. (ASHRAE Standard 62.2-2016:1-51).

Adams, GEM. (2016). Respiratory exposure during the additive manufacturing of sand casting moulds. Potchefstroom: North-West University (Dissertation – Masters).

Afshar-Mohajer, N, Wu, CY, Ladun, T, Rajon, DA, Huang, Y. (2015). Characterization of particulate matters and total VOC emissions from a binder jetting 3D printer. Building and Environment; 93: 293-301.

American Society for Testing and Materials (ASTM) F2792. (2013). Standard terminology for additive manufacturing technologies.

Alijagic, A., Engwall, M, Särndahl, E, Karlsson, H, Hedbrant, A, Andersson, L, Karlsson, P, Dalemo, M, Scherbak, N., Färnlund, K, Larsson, M, Persson, A. (2022). Particle Safety Assessment in Additive Manufacturing — From Exposure Risks to Advanced Toxicology Testing. Toxicology; 4: 1-22.

Batterman, S. (2017). Review and extension of CO2-based methods to determine ventilation rates with application to school classrooms. International Journal of Environmental Research and Public Health; 14: 1-22.

Brown, JS, Gordon, T, Price, O, Asgharian, B. (2013). Thoracic and respirable particle definitions for human health risk assessment. Particle and Fibre Toxicology; 10(12): 1-12.

Cherrie, JW, Brosseau, LM, Hay, A, Donaldson, K. (2013). Low-toxicity dusts: current exposure guidelines are not sufficiently protective. Annals of Occupational Hygiene; 57: 685-691.

Deng, Y, Cao, SJ, Chen, A, Guo, Y. (2016). The impact of manufacturing parameters on submicron particle emissions from a desktop 3D printer in the perspective of emission reduction. Building and Environment; 104: 311-319.

Department of Employment and Labour (DoEL). (2021). Regulations for hazardous chemical agents (RHCA), 2021. (Notice 280). *Government Gazette*, 44348:1-67, 29 Mar.

Du Preez, S, de Beer, DJ, Du Plessis, JL. (2018). Titanium powders used in powder bed fusion: The relevance to respiratory health. South African Journal of Industrial Engineering; 29: 94-102.

Du Preez, S, Johnson, A, LeBouf, RF, Linde, SJL, Stefaniak, AB, Du Plessis, J. (2017). Exposures during industrial 3-D printing and post-processing tasks. Rapid Prototyping Journal; 1: 865-871.

Du, Y, Xu, X, Chu, M, Guo, Y, Wang, J. (2016). Air particulate matter and cardiovascular disease: the epidemiological, biomedical and clinical evidence. Journal of Thoracic Disease; 8: 8-19.

Elliot, AM, Love, LJ. (2016). Operator burden in metal additive manufacturing. In Solid Freeform Fabrication 2016, Proceedings of the 26th Annual International Solid Freeform Fabrication Symposium – An Additive Manufacturing Conference, 2016. p. 1890-1899.

Geiss, O, Bianchi, I, Barrero-Moreno, J. (2016). Lung-deposited surface area concentration measurements in selected occupational and non-occupational environments. Journal of Aerosol Science*;* 96: 24-37.

Gibson, I, Rosen, IDW, Stucker, B. (2015). Additive manufacturing technologies — Rapid prototyping to z digital manufacturing. Cham, Switzerland: Springer. pp. 1-484. Available from: URL: 2010_Book_AdditiveManufacturingTechnolog.pdf (ethernet.edu.et) - Search (bing.com) (accessed 27 Feb 2021).

Glass, DC, Gray, CN. (2001). Estimating mean exposures from censored data: exposure to benzene in the Australian petroleum industry. The Annals of Occupational; 45: 275-282.

Huang, Q, Marzouk, T, Cirligeanu, R, Malmstrom, H, Eliav, E, Ren, YF. (2021). Ventilation rate assessment by carbon dioxide levels in dental treatment rooms. Journal of Dental Research; 100: 810-816.

He, C, Morawska L, Hitchins, J, Gilbert, D. (2004). Contribution from indoor sources to particle number and mass concentrations in residential houses. Atmospheric Environment; 38: 3405-3415.

Hornung, RW, Reed, LD, (1990). Estimation of average concentration in the presence of nondetectable values. Applied Occupational and Environmental Hygiene; 5: 46-51.

International Agency for Research on Cancer (IARC). (2021). Agents classified by the IARC monographs, volumes 1-129. Available from: URL: Agents Classified by IARC Monographs, Volume 1-29 - Search (bing.com) (accessed 4 Mar 2022).

International Organization for Standardizations/American Society of Testing Materials (ISO/ASTM): Additive Manufacturing – General principles – Fundamentals and Vocabulary (ISO/ASTM 52900) [Standard] Geneva, Switzerland: ISO/ASTM, 2021.

Le Néel TA, Mognol, P, Hascoet, JY. (2018). A review on additive manufacturing of sand molds by binder jetting and selective laser sintering. Rapid Prototyping Journal; 24: 1325-1336.

Lewinski, NA, Seconda, LE, Ferri, JK. (2019). On-site three-dimensional printer aerosol hazard assessment — Pilot study of a portable in vitro exposure cassette. Process Safety Progress; 38: 1-7.

Ljunggren, SA., Ward, LJ, Graff, P, Persson, A, Lind, ML, Karlsson, H. (2021). Metal additive manufacturing and possible clinical markers for the monitoring of exposure-related health effects. PLOS ONE; 16: e0248601.

Made, J, Utembe, W. (2019). Statistical analysis methods used to assess data below the limit of detection in the South African literature, 2010-2017. Occupational Health Southern Africa; 25: 1-5.

Malvern Instruments Limited. (2007). Morphologi G3 Automated Particle Characterization System. Available from: URL: Brochure: Morphologi G3 Automated Microscope System - Malvern.com (labwrench.com) (accessed 29 August 2023).

Malvern Instruments Limited. (2015). A basic guide to particle characterization. Available from: URL: https://www.cif.iastate.edu/sites/default/files/uploads/Other_Inst/Particle%20Size/Particle%20Characterization%20Guide.pdf (accessed 4 Mar 2022).

Manoj, A, Bhuyan, M, Banik, SR, Mamilla, RS. (2020). Review on particle emissions during fused deposition modeling of acrylonitrile butadiene styrene and polylactic acid polymers. Materials Today. Proceedings, 44: 2214-7853.

Matlhatsi, NL. (2021). Particulate emissions and respiratory exposure to hazardous chemical substances during additive manufacturing of sand moulds. Potchefstroom: North-West University (Masters – Dissertation).

McClellan, RO. (2002). Setting ambient air quality standards for particulate matter. Toxicology; 181:329-347.

Meera, KJ, Banganayi, F, Oyombo, D. (2017). Moulding sand recycling and reuse in small foundries. Procedia Manufacturing; 7: 86-91.

Methods for the determination of hazardous substances 14/4. General methods for sampling and gravimetric analysis of respirable, thoracic and inhalable aerosols. Available from: URL: https://www.hse.gov.uk/pubns/mdhs/pdfs/mdhs14-4.pdf (accessed 25 Aug 2022).

National Institute for Occupational Safety and Health (NIOSH). (1998). Particulates not otherwise regulated, respirable 0600 NMAM 0600: PARTICULATES NOT OTHERWISE REGULATED, RESPIRABLE (cdc.gov) (Accessed: 20 Oct. 2021).

National Institute for Occupational Safety and Health (NIOSH). (2017). NIOSH method 7602: Silica, respirable crystalline, by IR (KBr pellet). Available from: URL: NMAM METHOD 7602 (cdc.gov) (Accessed 9 July 2021).

Oberdörster, G, Oberdörster, E, Oberdörster, J. (2005). Nanotoxicology: an emerging discipline evolving from studies of ultrafine particles. Environmental Health Perspectives; 113: 823-839.

Rosental, PA. (2017). Silicosis: a world history. USA: John Hopkins University Press.

Schoeman, JJ, Van den Heever DJ. (2015). Occupational hygiene: the science-volume 1.3rd ed. Bloemfontein, FS: VDH Industrial Hygiene CC.

Sensidyne. (2011). Gilian GilAir Plus air sampling pump — Operation manual. Available from: URL: Gilian GilAir Vision Air Sampling Pump – Operation Manual (sensidyne.com) (accessed 26 May 2021).

Stabile, L, Scungio M, Buonanno, G, Arpino, F, Ficco, G. (2017). Airborne particle emission of a commercial 3D printer: the effect of filament material and printing temperature. Indoor Air; 27: 398-408.

Stefaniak, AB, Johnson, AR., du Preez, S, Hammond, DR, Wells, JR, Ham, JE, LeBouf, RF, Menchaca, KW, Martin, SB, Duling, MG, Bowers, LN, Knepp, AK, Su, FC, de Beer, DJ, Du Plessis JL. (2019). Evaluation of emissions and exposures at workplaces using desktop 3-dimensional printers. Journal of Chemical Health and Safety; 26: 19-30.

Stephen, B, Azimi, P, El, ZB, Ramos, T. (2013). Ultrafine particle emissions from desktop 3D printers. Atmospheric Environment; 1: 334-339.

Sun, C, Shang, G. (2021). On application of metal Additive manufacturing. *World Journal of* Engineering and Technology, 9(1): 194.

Thomas, R.J. (2013). Particle size and pathogenicity in the respiratory tract. Virulence; 4: 847-858.

TWS-ESS-DP-52, R2, (1989). Sample preparation for x-ray Fluorescence analysis: fusing and lapping. Available from: URL: XRF Sample Prep SOP - Example (1).pdf (access: 24 Nov 2022.

TWS-ESS-DP-1 111, R1. (1989). Procedure for X-ray Fluorescence analysed (accessed 14 Nov 2022).

United States Environmental Protection Agency (U.S. EPA). (2009). Integrated Science Assessment for Particulate Matter. Available from: URL: file:///C:/Users/27676/Downloads/PM_ISA_WITHOUT_ANNEXES.PDF (accessed 27 July 2022).

Van der Walt, S, du Preez, S, du Plessis JL. (2022). Particle emissions and respiratory exposure to hazardous chemical substances associated with additive manufacturing utilising polymethyl methacrylate. Hygiene and Environmental Health Advances; 4:1-7.

Voxeljet - Activator VX-2C/8. (2014). Safety data sheet 1907/2006/EC. Available from: URL: MSDS-voxeljet - Activator VX-2C - 8_GB.pdf (accessed 23 Nov 2022).

Voxeljet - Binder VX-2C Type B. (2014). Safety data sheet 1907/2006/EC. Available from: URL: voxeljet - Binder VX-2C Type B_GB (1).pdf (accessed 23 Nov 2022).

Voxeljet - Pre-mixed quarts-sand type. (2014). Safety data sheet 1907/2006/EC. Available from: URL: voxeljet - Premixed Quartz-Sand Type GS14, GS19_GB (1) (1).pdf (accessed 23 Nov 2022).

Zhang, H, LeBlanc, S. (2018). Processing parameters for selective laser sintering or melting of oxide ceramics. In: Zhang, H, LeBlanc, S. Additive Manufacturing of High-performance Metals and Alloys — Modeling and Optimization. Washington: intechopen. pp. 89-118.

Zisook, RE, Simmons, BD, Vater, M, Perez, A, Donovan, EP, Paustenbach, DJ, Cyrs, WD. (2020). Emissions associated with operations of four different additive manufacturing or 3D printing technologies. Journal of Occupational and Environmental Hygiene; 17(10): 464-479.

Supplementary material

Table S1: Description of the activities performed during the AM phases.

Description	Activity	Day			
		1	2	3	4
Pre-processing phase	The software required by the AM machine to produce the part was configured by the AM operator.	Yes	Yes	Yes	No
	The AM operator manually loaded silica sand into the hopper located at the back of the AM research facility	No	Yes	Yes	No
	The AM operator used a rod to level the silica sand in the hopper.	Yes	No	Yes	No
Processing phase	The door of the AM machine was closed during the processing phase. Periodically, the AM operator returned to the AM research facility to check on the progress of the print. Tasks such as office work, operating other AM machines, collecting silica sand outside the AM facility and lunch breaks were performed when the operator left the AM room.	Yes	Yes	Yes	No
	The AM operator manually loaded silica sand into the hopper located at the back of the AM research facility.	No	Yes	Yes	No
	The AM operator used a rod to level the silica sand in the hopper.	No	Yes	No	No
	Upon completion of the processing phase, the part was kept inside the job box of the AM machine for 24 hours to cure.	Yes	Yes	Yes	No
Post-processing phase	The AM operator unlocked the job box platform. The AM machine's door was opened, and the job box was removed using a mobile hydraulic trolley jack. The part was cleaned by wiping the part by hand and using a brush. The cleaned part was placed on a table located in the front of the room. The silica sand on the edges of the job box were brushed into the job box. The AM operator used a ruler to level the sand in the job box.	No	Yes	Yes	Yes
	The inside of the AM machine was cleaned after the processing phase using a Nilfisk Alto Attix 791-2M/B1 vacuum cleaner.	No	Yes	No	Yes
	The job box was placed back in the AM machine using a hydraulic trolley jack. The door of the AM machine was closed.	No	Yes	Yes	Yes
	The AM operator cleaned the speeding station using tissue paper and isopropyl alcohol. Excessive dirt was then scraped off using a Stanley blade.	No	Yes	No	No
	The AM operator levelled silica sand in the hopper.	No	No	No	Yes
Ventilation	During the AM process, the windows and roll-up door were kept closed. When the AM operator opened the door to retrieve buckets of silica sand or to check on the AM machine, natural ventilation was supplied to the AM research facility.	Yes	Yes	Yes	Yes
	The door was left open during the AM phases.	Yes	No	No	No
	The AM research facility had an air conditioner in the back that was set to a constant temperature of 22 °C.	Yes	Yes	Yes	Yes
	Extraction ventilation system directly connected to the AM machine, which ventilated the AM machine's build envelope.	Yes	Yes	Yes	Yes
Personal protective equipment	The operator wore long sleeve T-shirt and long pants.	Yes	Yes	Yes	Yes
	The AM operator wore safety shoes or enclosed shoes.	Yes	No	Yes	Yes
	The AM operator wore latex gloves during the AM phases.	No	Yes	Yes	Yes
	The AM operator wore quality safety assurance European standard 149:2001 filtering face piece (FFP2) half-face disposable respirators during the AM phases.	No	Yes	Yes	Yes

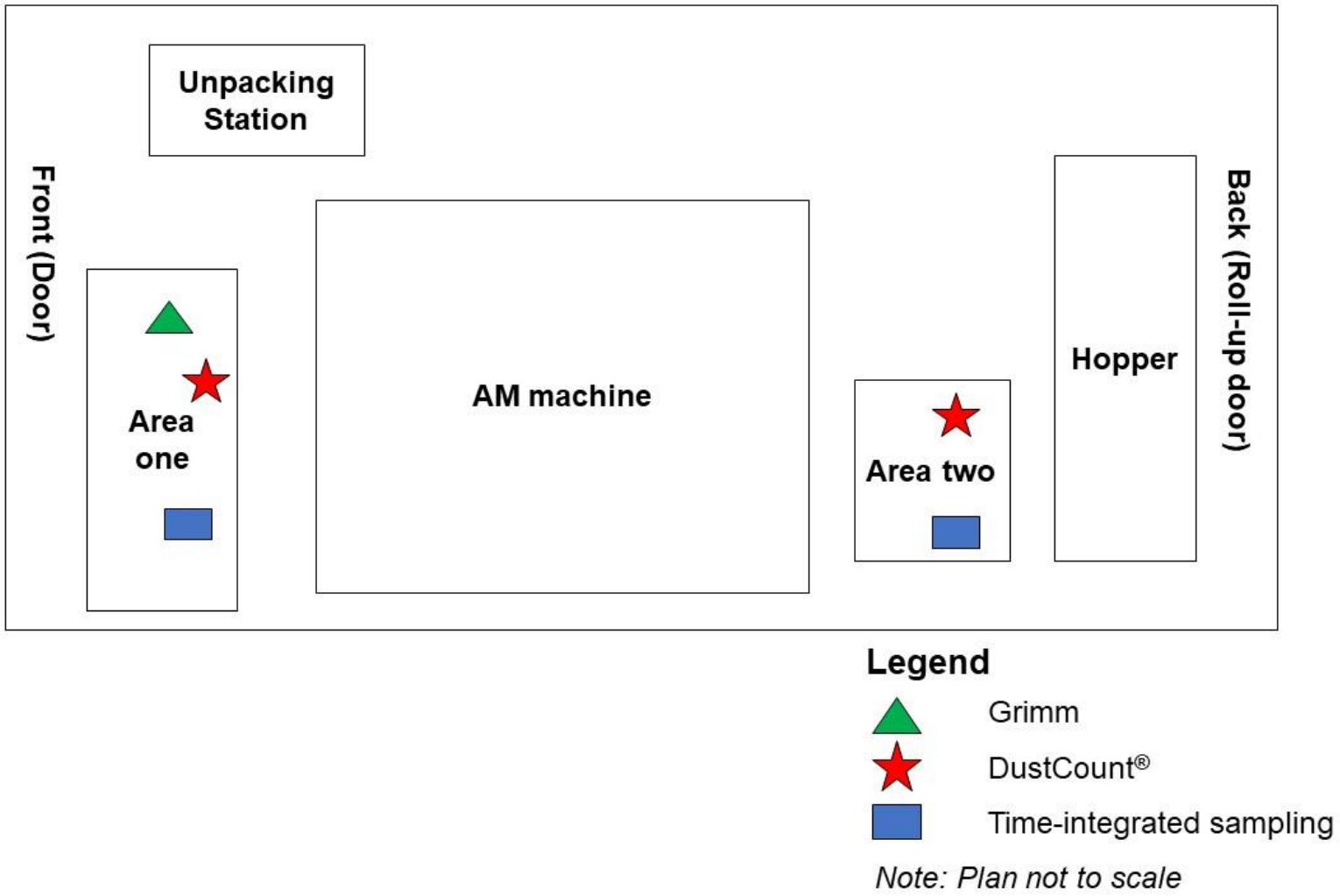

Figure S1: **Floorplan of AM research facility showing the placement of monitoring instruments.**

Table S2: **Average air exchange rate calculations over three repetitions at the AM research facility.**

Repeat	Door open and air conditioner on (air changes/hour)	Door closed and air conditioner on (air changes/hour)
1	3.914	3.363
2	3.611	2.105
3	3.202	3.310
Average	3.575	2.926

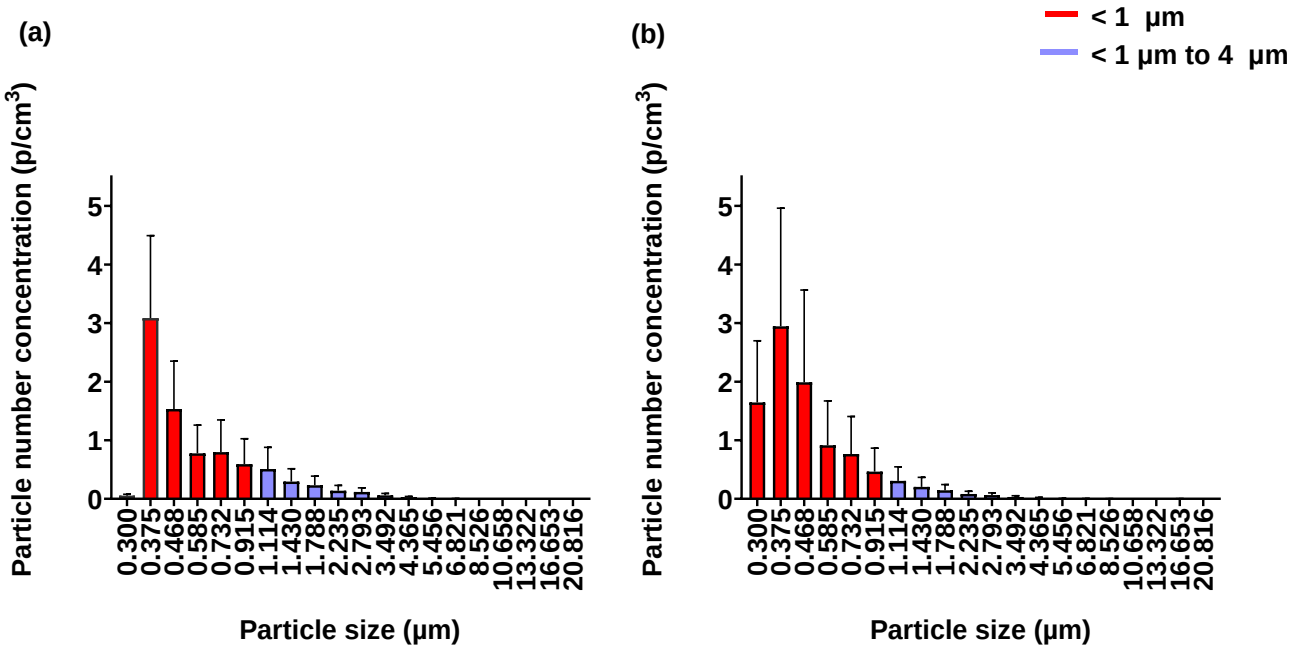

Figure S2: **Illustration of the most prominent particle size fraction during the entire BJ process for day one of printing for a) area two and b) personal exposure monitoring.**

Table S3: Mean and peak particle ERs as measured over four printing days in area one.

Phase		Particle size ranges								
		< 1 µm		**> 1 to < 4 µm**		**> 4 to < 10 µm**		**≥ 10 µm**		***0.01 to 1 µm**
		Grimm	DustCount®	Grimm	DustCount®	Grimm	DustCount®	Grimm	DustCount®	OPC
Pre-processing	Mean p/min	8.74×10^{4}	10.16×10^{0}	2.25×10^{3}	—	1.22×10^{2}	—	5.69×10^{0}	—	1.2×10^{9}
	Peak p/min	1.41×10^{5}	12.09×10^{0}	3.72×10^{3}	—	2.57×10^{2}	—	7.89×10^{0}	—	Not stated
Processing	Mean p/min	1.19×10^{5}	8.23×10^{0}	2.47×10^{3}	1.44×10^{0}	1.34×10^{2}	—	9.67×10^{-1}	—	5.27×10^{8}
	Peak p/min	1.81×10^{5}	11.25×10^{0}	6.13×10^{3}	2.78×10^{0}	3.12×10^{2}	—	1.64×10^{0}	—	Not stated
Post-processing	Mean p/min	2.15×10^{5}	0.33×10^{0}	1.65×10^{3}	1.46×10^{0}	1.89×10^{2}	—	3.53×10^{0}	—	7.74×10^{8}
	Peak p/min	3.06×10^{5}	0.33×10^{0}	2.61×10^{3}	1.46×10^{0}	1.04×10^{2}	—	6.31×10^{0}	—	Not stated

Legend: High background particle number concentration prevented calculation of the mean and peak particle ERs; mean(average): measure central tendency of a probability distribution along median and mode; SD: standard deviation is a measure of how dispersed data is in relation to the mean; peak(maximum): largest value in the data set; *: Mean and peak particle ERs as reported by Matlhatsi (2021:1-133).

CHAPTER 4 CONCLUDING CHAPTER

4.1 Main findings

In this chapter, the conclusion of the main findings of the study are discussed followed by the aims, objectives, and hypotheses. Recommendations based on the findings of this study and recommendations regarding necessary controls are given. Limitations of this study are addressed, and potential future studies are suggested.

4.1.1 Powder characteristics and chemical composition of silica sand

Powder characteristics and chemical composition characteristics of a feedstock material can help identify possible health risks (Happo *et al*., 2014:1-18). A particle's size determines whether it is inhalable, and if so, where it can deposit in the respiratory tract (Maynard and Kuempel, 2005:587-614). The first objective as listed in Chapter 1 of this dissertation was to establish the powder characteristics and chemical composition of uncoated, coated, and used silica sand during BJ. This was evaluated through particle size distribution (PSD) and shape analysis, scanning electron microscopy (SEM), and wavelength dispersive X-ray fluorescence (WD-XRF) of the collected bulk silica sand samples.

PSD analysis of uncoated, coated and used silica sand samples indicated the presence of inhalable sized particles, which was confirmed by SEM images. Mean particle sizes [d (0.5)] were 1.29 ± 0.36 µm, 4.27 ± 0.08 µm and 2.42 ± 0.04 µm, indicating that the AM research facility contained particle sizes that fell within thoracic fraction (< 10 µm), and respirable fraction (< 4 µm) in size. In addition, a statistically significant difference in d(0.5) was found between the particle sizes of used, coated, and uncoated silica sand particles However, 90% of particles [d (0.9)] at the AM research facility for uncoated, coated and used silica sand were smaller than 42.21 ± 29.96 µm, 104.7 ± 23.33 µm and 54.9 ± 49.93 µm, respectively, indicating the presence of inhalable particles.

The SEM images supported the PSD results and showed particles > 100 µm in size. The WD-XRF results indicated that collected silica sand samples (uncoated, coated and used) had a high respirable crystalline silica content of 96.83 to 98.20% crystalline silica, which corresponded with >90% stated in the SDS. Respirable particles present a potential health concern since they can penetrate the alveolar region of the lungs, thoracic particles can deposit beyond the larynx, while inhalable particles can access the nasopharyngeal region (Brown *et al*., 2013:1-12). The high quartz content of uncoated, coated and used silica sand suggests the potential to induce

respiratory health effects such as silicosis, chronic obstructive pulmonary disease and lung cancer (NIOSH: 2002:1-145). The powder characteristics and chemical composition of uncoated, coated, and used silica sands could be determined; thus, the first objective has been achieved.

4.1.2 Particle emissions

The second objective was to quantify particle number concentrations and to determine ERs of particles released during BJ by means of direct-reading instruments during the three phases of AM. Particle number concentrations were monitored over four printing days. This study confirmed the emission of particles < 1 µm to > 10 µm in size, whereby particles were predominantly 0.375 µm in size based on the DustCount®. The mean particle number concentrations ranged between < 0.01 p/cm^3 and 421.44 p/cm^3 for the Grimm, whereas mean particle number concentrations of the DustCount® ranged from < 0.01 p/cm^3 to 23.48 p/cm^3 during the AM phases A peak particle ER of 3.06 × 10^5 p/min occurred during the post-processing phase for the Grimm, while the DustCount® measured peak ER of 12.09 × 10^0 p/m during the pre-processing phase for particles < 1 µm in size. For particles larger than > 1µm in size, the mean particle number concentrations were low, generally marginally above the background concentration. There was a notable difference in the particle number concentrations and particle ERs measured by the real-time instruments, with the DustCount® yielding lower particle number concentrations and particle ERs. Furthermore, higher particle number concentrations were measured in area two by the monitoring equipment. Therefore, the second objective was achieved.

4.1.3 Area monitoring and personal exposure monitoring

The third objective was to assess area concentrations and personal respiratory exposure of the AM operator to respirable crystalline silica and respirable PNOS during BJ utilising silica sand by means of real-time monitoring and time-integrated sampling. Real-time monitoring provided an overview of the AM operator's exposure in addition to time-integrated sampling. DustCount® showed that specific activities during BJ such as software configuration, taking out the job box, loading and levelling silica sand in the hopper, cleaning of the part and AM machine and conducting activities outside the AM research facility led to an increase in particle number concentrations. The particle number concentrations for area monitoring and personal exposure monitoring as measured by the Dustcount® was predominately in the respirable size fraction (0.375 µm). Therefore, the third objective of this study was achieved. The 8-hour TWA personal exposures to respirable crystalline silica and respirable PNOS over four printing days complied with their respective Time-Weighted Average-Occupational Exposure Limit-Maximum

Limits (TWA-OELs). However, time-integrated sampling and real-time monitoring of respirable crystalline silica equaled 10% of the TWA-OEL-ML of 0.1 mg/m^3.

In this study (Meiring, 2024), two hypotheses were formulated. Firstly, that the calculated air exchange rate (AER) is higher than the calculation of Matlhatsi (2021:1-133). The particle ERs of the three AM phases calculated in this study (Meiring, 2024) are lower than the calculated particle ERs of Matlhatsi (2021:1-133) when utilising direct-reading instruments. In this study (Meiring, 2024), the AER was calculated in the AM research facility, rather than using a provided AER. The AER was 2.93 with the door closed and air conditioner on, while it was 3.58 with the door open. The AER was low which indicated a lack of natural and mechanical ventilation. Matlhatsi (2021:1-133), used a much lower AER provided by the AM research facility to calculate emission particle ERs. Matlhatsi (2021:1-133), reported significantly higher mean particle emission rates during the pre-processing (1.2×10^9 p/min), processing (5.27×10^8 p/min) and post-processing phase (7.74×10^8 p/min) for particles 0.01 to 1 µm in size when using an optical particle counter. In this study (Meiring, 2024) the mean ERs was 8.74×10^4 p/min during the pre-processing phase, 1.19×10^5 p/min during the processing phase and 2.15×10^5 p/min during the post-processing phase for particles < 1 µm in size when utilising a Grimm. The hypothesis is therefore accepted.

The second hypothesis was formulated that the AM operator will be exposed to respirable crystalline silica and respirable PNOS at concentrations below the respective South African TWA-OELs in the RHCA for time-integrated sampling. However, peak ERs are anticipated during the full shift of the AM operator for real-time monitoring. Real-time monitoring in area one and area two and personal exposure monitoring, demonstrated that the AM operator was exposed to low particle number concentrations and particle ERs during the BJ process. Real-time monitoring showed that activities carried out during each AM phase influenced exposure to particle number concentration and particle ERs. Both findings from real-time monitoring and time-integrated sampling indicated that the AM operator was exposed to respirable crystalline silica and respirable PNOS TWA concentrations below the TWA-OELs during BJ. However crystalline silica equaled 10% of the TWA-OEL-ML. This hypothesis is therefore accepted.

In this study (Meiring, 2024), personal exposure monitoring was conducted using real-time monitoring and time-integrated sampling, whereas Adams (2016:1-84) and Matlhatsi (2021:1-133), only made use of time-integrated sampling. This study demonstrates that time-integrated monitoring should be used in combination with real-time monitoring for measuring nanoparticle exposure in the workplace. The three objectives were met and the two hypotheses were achieved.

4.2 Recommendations

Based on the guidelines and requirements outlined in the Regulations for Hazardous Chemical Agents (2021), the following recommendations for additional control measures for this AM research facility are proposed for the employer of the AM facility:

I. Local exhaust ventilation (LEV) system with a downdraft hood was present at the unpacking station of the AM research facility, however, it was not in a working order. LEV should be repaired by the management of the AM research facility. LEV would allow the AM operator to remove or capture airborne contaminants at their source before they are released in the working environment during the post-processing phase. As required in terms of Regulation 11 the employees should be encouraged to report to the management whenever equipment such as the AM machine, LEV, or vacuum cleaner appears to liberate more dust than usual, in order to prevent unnecessary respirable crystalline silica and respirable PNOS exposure due to ineffective extraction systems or equipment in poor condition (DoEL, 2021:1-98). As required in terms of Regulation 11, as soon as the LEV have been repaired, its effectiveness to capture airborne contaminants should be tested (DoEL, 2021:1-98).

II. The release of respirable crystalline silica and respirable PNOS during the AM phases may be prevented or controlled by fitting the top of the hopper with a lid that can be opened during the loading and levelling of silica sand and closed afterwards.

III. As required in terms of Regulation 3 the employers should provide employees (AM operators) with suitable and sufficient information, instruction, and training regarding their exposure to understand the potential health risk and the precautions they need to take when working with silica sand. Training should include the following details: (a) Firstly, the source of exposure during the AM phases; (b) Potential health risks involved with the activities conducted during the AM phases, and health effects related to exposure to respirable crystalline silica and respirable PNOS; (c) Measures necessary for protection from exposure to respirable crystalline silica and respirable PNOS, including wearing of respiratory protective equipment (RPE) and personal protective equipment (PPE). Employers are required by Regulation 11 of the RHCA to provide the employee (AM operator) with RPE and PPE that are maintained in good condition and replaced regularly. The management must also strictly enforce the use of RPE and PPE. Employees (AM operators) who are required to wear respirators should be informed, instructed, and trained in the use of RPE. The selection of respirators should include individual fit testing (DoEL, 2021:1-98). During the selection, special attention should be paid to employees who have a wealth of hair, stubble, beards, or glasses that may interfere with

the integrity of the seal around the face. Facial features, such as a particularly large chin, a small face, or an unusually shaped nose bridge may require the provision of an alternative respirator; (d) training on the importance of good housekeeping and personal hygiene practices must be implemented and maintained in the workplace; (e) Finally, the AM operator should be provided with training on the use of extraction ventilation system and control measurements in place at the AM research facility.

IV. Globally Harmonized System (GHS) compliant safety data sheet (SDS) must be available in the AM research facility where the hazardous chemical agents are stored, used or handled (DoEL, 2021:1-98) as required in terms of the Regulation 14A(b) (DoEL, 2021:1-98). However, the physical characteristics of silica sand was not stated on the manufacturer's SDS, as required in terms of Regulation 14A(3)(i) of the Regulations for RHCA (DoEL, 2021:1-98). As required in terms of Regulation 14A(a) a SDS should be reviewed by the importer or manufacturer of the HCA at least once every five years and amended to contain correct and current information (DoEL, 2021:1-98). It is advisable for facilities to maintain an inventory detailing the physical characteristics and chemical composition of the AM feedstock material. This practice enables a precise comparison with the manufacturer's SDS. Utilising this information, AM facilities can pinpoint potential discrepancies in the manufacturer's SDS, as suggested by Du Preez (2018:145).

V. The AM research facility was demarcated as a respirator zone by the posting of South African National Standard (SANS) Dust Mask Mandatory Sign (MV12). As required in terms of Regulation 11, it is recommended that the AM research facility should remain demarcated as respirator zone by a notice that indicates that respiratory protection shall be worn during BJ (DoEL, 2021:1-98).

VI. A box of filtering face piece (FFP) respirators was available on the workbench when entering the AM research facility. It is appropriate to use FFP2 respirators as they filter a minimum of 94% of airborne particles. The practice of issuing the AM operator tasked with activities that may liberate respirable crystalline silica and respirable PNOS into the workroom air with respirators with a FFP2 classification, which provide protection against the inhalation of dust up to ten times the OEL, should be continued. It is, however, recommended that the AM operator wear an FFP3 respirator since they filter at least 99% of airborne particles and provide the highest level of protection against airborne particles (Lee *et al.*, 2016:1-12).

VII. The AM research facility did not have designated containers or storage facilities for RPE and PPE. Clean containers or storage facilities should be provided for RPE and PPE when not in use, as required in terms of Regulation 11(3)(b) of the Regulations for RHCA (DoEL, 2021:1-98). This should be done to avoid contamination of the insides of respirators that would result in contaminant inhalation.

4.3 Study limitations

The following limitations have been identified in this study (Meiring, 2024).

I. Limitation one: The SDS did not state physical characteristics (PSD and shape) of silica sand, as required in terms of Regulation 14A(3)(i) of the Regulations for RHCA (DoEL, 2021:1-98). Therefore, it was not possible to compare the particle size of the silica sand used in this study (Meiring, 2024) with that of the manufacturer.

II. Limitation two: As only one AM operator was performing the AM operations, the number of personal respiratory exposure samples that could be obtained was limited in this study (Meiring, 2024).

III. Limitation three: There are, no studies available on human health risks and exposure during both BJ and PBF-SLS when producing sand moulds under the same manufacturing conditions. Making it difficult to perform comparative studies.

4.4 Future studies

Upon concluding this study and recognising its limitations, the following recommendations for future studies are proposed.

i. Future studies should consider the use of a wider range of BJ machines to produce the exact sand moulds using either the same AM feedstock material or another feedstock material such as chromite sand.

ii. For comprehensive assessments of respiratory exposure among different AM operators performing diverse tasks in the AM process, future studies should involve more than one AM operator. Additionally, investigations should extend to include particle emissions and exposure monitoring across multiple AM facilities employing silica sand during BJ.

iii. To further enhance understanding, it is recommended that upcoming studies delve into particle emissions and exposure monitoring not only during BJ but also during PBF-SLS. This comparative analysis should specifically focus on the production of identical sand moulds using the exact same AM feedstock material.

iv. In order to provide a more holistic view, future studies should also further investigate post-processing activities being performed during BJ such as curing in an oven and densification, which includes processes like sintering and infiltration.

4.5 References

Adams, G.E.M. *Respiratory exposure during the additive manufacturing of sand casting moulds*. Potchefstroom: North-West University (Dissertation – Masters).

Afshar-Mohajer, N., Wu, C. Y., Ladun, T., Rajon, D. A. & Huang. Y. 2015. Characterization of particulate matters and total VOC emissions from a binder jetting 3D printer. *Building and Environment,* 93:293-301.

Alijagic, A., Engwall, M., Särndahl, E., Karlsson, H., Hedbrant, A., Andersson, L., Karlsson, P., Dalemo, M., Scherbak, N., Färnlund, K., Larsson, M. & Persson, A. 2022. Particle Safety Assessment in Additive Manufacturing: From Exposure Risks to Advanced Toxicology Testing. *Toxicology*, 4:1-22.

Brown, J.S., Gordon, T. & Price, O. 2013. 3 and Bahman. Thoracic and respirable particle definitions for human health risk assessment. *Particle and Fibre Toxicology*, 10(12):1-12.

Caiazzo, F., Alfieri, V., Corrado, G. & Argenio, P. 2017. Laser powder-bed fusion of Inconel 718 to manufacture turbine blades. *The International Journal of Advanced Manufacturing Technology*, 93:4023-4031.

Deng, Y., Cao, S.J., Chen, A. & Guo, Y. 2016. The impact of manufacturing parameters on submicron particle emissions from a desktop 3D printer in the perspective of emission reduction. *Building and Environment*, 104:311-319.

Department of Employment and Labour (DoEL). 2021. Regulations for hazardous chemical agents (RHCA), 2021. (Notice 280). *Government Gazette*, 44348:1-67, 29 Mar.2022.

Du Preez, S. *Emissions of and exposure to hazardous chemical substances from selected additive manufacturing technologies*. Potchefstroom: North-West University (Thesis – Doctor).

Gibson, I., Rosen, I.D.W. & Stucker, B. 2015. Additive manufacturing technologies: rapid prototyping to direct digital manufacturing. Cham, Switzerland: Springer. pp. 1-484. Available from Springer eBook Collection: 2010_Book_AdditiveManufacturingTechnolog.pdf (ethernet.edu.et) - Search (bing.com) Date of access: 27 Feb. 2021.

Health and Safety Executive (HSE). 2021. *Controlling airborne contaminants at work A guide to local exhaust ventilation (LEV)* https://www.hse.gov.uk/pubns/priced/hsg258.pdf Date of access: 8 Dec. 2022.

International Organization for Standardizations/American Society of Testing Materials (ISO/ASTM): Additive Manufacturing - General principles – Fundamentals and Vocabulary (ISO/ASTM 52900) [Standard] Geneva, Switzerland: ISO/ASTM, 2021.

Lee, S.A., Hwang, D.C., Li, H.Y., Tsai, C.F., Chen, C.W. & Chen, J.K. 2016. Particle size-selective assessment of production of European standard FFP respirators and surgical masks against particles-tested with human subjects. *Journal of Healthcare Engineering,* 0(0):1-12.

Le Néel T.A., Mognol, P. & Hascoet, J.Y. 2018. A review on additive manufacturing of sand molds by binder jetting and selective laser sintering. *Rapid Prototyping Journal*, 24(8):1325-1336.

Lewinski, N.A., Seconda, L.E. & Ferri, J.K. 2019. On-site three-dimensional printer aerosol hazard assessment: pilot study of a portable in vitro exposure cassette. *Process Safety Progress*, 38(3):1-7.

Matlhatsi, N.L. 2021. *Particulate emissions and respiratory exposure to hazardous chemical substances during additive manufacturing of sand moulds.* Potchefstroom: North-West University. (Masters – Dissertation).

Maynard, A.D., and Kuempe, E.D. 2005. Airborne nanostructured particles and occupational health. *Journal of Nanoparticle Research*, 7:587-614.

National Institute of Occupational Safety and Health (NIOSH). 2002. *Health effects of occupational exposure to respirable crystalline silica.* https://www.cdc.gov/niosh/docs/2002-129/pdfs/2002-129.pdf Date of access: 12 June 2021.

National Institute of Occupational Safety and Health (NIOSH). 2022. Hierarchy of Controls Hierarchy of Controls | NIOSH | CDC Date of access: 2 Dec. 2022.

Occupational Safety and Health Administration. (OSHA). 2023. *Personal sampling for air contaminants*. https://www.osha.gov/otm/section-2-health-hazards/chapter-1#field_blanks Date of access: 08 Feb. 2024.

Sippula, O., Jalava, P.I., Rintala, H., Leskinen, A., Komppula, M., Kuuspalo, K., Mikkonen, S., Lehtinen, K., Jokiniemi, J. & Hirvonen, M.R. 2014. Role of microbial and chemical composition in toxicological properties of indoor and outdoor air particulate matter. *Particle and Fibre Toxicology*, 11:1-18.

Snelling, D., Williams, C.B. & Druschitz, A.P. 2014. *A comparison of binder burnout and mechanical characteristics of printed and chemically bonded sand molds.* 2013-66-Snelling.pdf (utexas.edu) Date of access: 2 Feb. 2022.

Weinberg, J.L., Bunin, L.J. & Das, R. 2009. Application of the industrial hygiene hierarchy of controls to prioritize and promote safer methods of pest control: a case study. *Public Health Reports*, 1(124):53-62.

ANNEXURE A ETHICS APPROVAL LETTER

Private Bag X1290, Potchefstroom
South Africa 2520

Tel: 086 016 9698
Web: http://www.nwu.ac.za/

North-West University Health Research Ethics Committee (NWU-HREC)

Tel: 018 299-1206
Email: Ethics-HRECApply@nwu.ac.za (for human studies)

14 June 2022

ETHICS APPROVAL LETTER OF STUDY

Based on approval by the North-West University Health Research Ethics Committee (NWU-HREC) on 14/06/2022, the NWU-HREC hereby approves your study as indicated below. This implies that the NWU-HREC grants its permission that, provided the general conditions specified below are met and pending any other authorisation that may be necessary, the study may be initiated, using the ethics number below.

Study title: Particle emissions and respiratory exposure to hazardous chemical agents during binder jetting utilising a chromite sand
Principal Investigator/Study Supervisor/Researcher: Dr S du Preez
Student: L Meiring - 28850467

Ethics number:

N	W	U	-	0	0	0	2	7	-	2	2	-	A	1
Institution				Study Number						Year			Status	

Status: S = Submission; R = Re-Submission; P = Provisional Authorisation; A = Authorisation

Application Type: Single study
Commencement date: 14/06/2022
Expiry date: 30/06/2023

Risk: Minimal

Approval of the study is provided for a year, after which continuation of the study is dependent on receipt and review of an annual monitoring report and the concomitant issuing of a letter of continuation. A monitoring report is due at the end of June annually until completion of the study.

General conditions:

While this ethics approval is subject to all declarations, undertakings and agreements incorporated and signed in the application form, the following general terms and conditions will apply:

- *The principal investigator/study supervisor/researcher must report in the prescribed format to the NWU-HREC:*
  - *Annually on the monitoring of the study, whereby a letter of continuation will be provided annually, and upon completion of the study; and*
  - *without any delay in case of any adverse event or incident (or any matter that interrupts sound ethical principles) during the course of the study.*
- *The approval applies strictly to the proposal as stipulated in the application form. Should any amendments to the proposal be deemed necessary during the course of the study, the principal investigator/study supervisor/researcher must apply for approval of these amendments at the NWU-HREC, prior to implementation. Should there be any deviations from the study proposal without the necessary approval of such amendments, the ethics approval is immediately and automatically forfeited.*
- *Annually a number of studies may be randomly selected for active monitoring.*
- *The date of approval indicates the first date that the study may be started.*
- *In the interest of ethical responsibility, the NWU-HREC reserves the right to:*
  - *request access to any information or data at any time during the course or after completion of the study;*
  - *to ask further questions, seek additional information, require further modification or monitor the conduct of your research or the informed consent process;*

- *withdraw or postpone approval if:*
  - *any unethical principles or practices of the study are revealed or suspected;*
  - *it becomes apparent that any relevant information was withheld from the NWU-HREC or that information has been false or misrepresented;*
  - *submission of the annual monitoring report, the required amendments, or reporting of adverse events or incidents was not done in a timely manner and accurately; and/or*
  - *new institutional rules, national legislation or international conventions deem it necessary.*
- *NWU-HREC can be contacted for further information via Ethics-HRECApply@nwu.ac.za or 018 299 1206*

Special conditions of the research approval due to the COVID-19 pandemic:

Please note: Due to the nature of the study i.e. (face-to-face collection of quantitative data via area monitoring and personal exposure monitoring of workers within an additive manufacturing facility at VUT), this study will be able to proceed during the current alert level, following receipt of the approval letter. No additional COVID-19 restrictions have been placed on the study other than that indicated under the COVID-19 risk mitigation strategy as indicated in the application. The researcher must, however, ensure that before proceeding with the study that all research team members have reviewed the North-West University COVID-19 Occupational Health and Safety Standard Operating Procedure.

The NWU-HREC would like to remain at your service and wishes you well with your study. Please do not hesitate to contact the NWU-HREC for any further enquiries or requests for assistance.

Yours sincerely,

Digitally signed by
Prof Petra Bester
Date: 2022.06.14
11:16:09 +02'00'

Chairperson NWU-HREC

Current details:(23239522) G:\My Drive\9. Research and Postgraduate Education\9.1.5.4 Templates\9.1.5.4.2_NWU-HREC_EAL.docm
20 August 2019
File Reference: 9.1.5.4.2

ANNEXURE B DECLARATION OF LANGUAGE EDITING

WOORDE WAT WERK
WORKING WORDS

Venita de Kock
BA HONS. • PEG
084 588 5008
venita.dekock@gmail.com

23 November 2023

LANGUAGE EDITING STATEMENT

I, Jannetje Levina De Kock,
hereby declare that the dissertation submitted in partial fulfilment of the requirements
for the degree Master of Health Sciences in Occupational Hygiene (OHHRI)
at the North-West University
with the title

Particle emissions and exposure to hazardous chemical agents during binder jetting utilising a silica sand

by
Leandra Meiring
28850467

- has been edited for language correctness and spelling.
- has been edited for consistency (repetition, long sentences, logical flow)

No changes have been made to the document's substance and structure (nature of academic content and argument in the discipline, chapter and section structure and headings, order and balance of content, referencing style and quality).

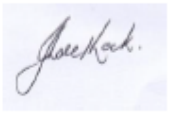

J L DE KOCK